UNIVERSIDADE ESTADUAL PAULISTA “JÚLIO DE MESQUITA FILHO”
FACULDADE DE ENGENHARIA
CÂMPUS DE ILHA SOLTEIRA

SEIFOLLAH ASADPOUR

Planning of the distribution system operation through reconfiguration and optimal placement and sizing of distributed generation using chaotic particle swarm optimization algorithm

Ilha Solteira
2023

UNIVERSIDADE ESTADUAL PAULISTA
"JÚLIO DE MESQUITA FILHO"
Campus de Ilha Solteira

POSTGRADUATE PROGRAM IN ELECTRICAL ENGINEERING

SEIFOLLAH ASADPOUR

Planning of the distribution system operation through reconfiguration and optimal placement and sizing of distributed generation using chaotic particle swarm optimization

The category of the thesis work presented to the Faculty of Engineering, Campus of Ilha Solteira, Sao Paulo State University, as part of the requirements for obtaining the title of doctoral degree (PhD) in Electrical Engineering. Specialty: Automation.

Prof. Dr. Rubén Augusto Romero Lázaro
Advisor

Ilha Solteira

2023

FICHA CATALOGRÁFICA
Desenvolvido pelo Serviço Técnico de Biblioteca e Documentação

A798p

Asadpour, Seifollah.
Planning of the distribution system operation through reconfiguration and optimal placement and sizing of distributed generation using chaotic particle swarm optimization algorithm / Seifollah Asadpour. -- Ilha Solteira: [s.n.], 2023
130 f. : il.

Tese (doutorado) - Universidade Estadual Paulista. Faculdade de Engenharia de Ilha Solteira. Área de conhecimento: Automação, 2023

Orientador: Rubén Augusto Romero Lázaro

Inclui bibliografia

1. Chaotic particle swarm optimization algorithm. 2. Distributed generation. 3. Distribution network reconfiguration. 4. Energy storage system. 5. Photovoltaic system. 6. Power loss.

Amanda Sertori dos Santos
Bibliotecária - CRB/8-9061
Seção Técnica de Referência, Atendimento ao Usuário e Documentação
Diretoria Técnica de Biblioteca e Documentação

UNIVERSIDADE ESTADUAL PAULISTA

Câmpus de Ilha Solteira

CERTIFICADO DE APROVAÇÃO

TÍTULO DA TESE: Planning of the distribution system operation through reconfiguration and optimal placement and sizing of distributed generation using chaotic particle swarm optimization algorithm

AUTOR: SEIFOLLAH ASADPOUR
ORIENTADOR: RUBEN AUGUSTO ROMERO LAZARO

Aprovado como parte das exigências para obtenção do Título de Doutor em Engenharia Elétrica, área: Automação pela Comissão Examinadora:

Prof. Dr. RUBEN AUGUSTO ROMERO LAZARO (Participaçao Presencial)
Departamento de Engenharia Eletrica / Faculdade de Engenharia de Ilha Solteira - UNESP

Prof. Dr. JONATAS BOAS LEITE (Participaçao Presencial)
Departamento de Engenharia Eletrica / Faculdade de Engenharia de Ilha Solteira - UNESP

Prof. Dr. LEONARDO HENRIQUE FARIA MACEDO POSSAGNOLO (Participaçao Presencial)
Departamento de Engenharia de Energia / Faculdade de Engenharia e Ciencias - UNESP

Prof. Dr. LUCAS TELES DE FARIA (Participaçao Presencial)
Departamento de Engenharia de Energia / Faculdade de Engenharia e Ciências - UNESP

Prof. Dr. JUAN MANUEL HOME ORTIZ (Participaçao Virtual)
Faculdade de Engenharia Elétrica e de Computação / Universidade Estadual de Campinas - UNICAMP

Ilha Solteira, 15 de setembro de 2023

DEDICATION

I dedicate this thesis to my dear late father Esmaeil Asadpour Derazcola, who lived all the moments of his life with honesty and courage. Also, I dedicate it to Dr. Elham Mahdavi (Ph.D. in Electrical Engineering from the São Paulo State University (UNESP)) from the province of Razavi Khorasan, Iran, and the land of Fariman, who was always my friend, companion and supporter in achieving this success.

THANKS

To Dr. Elham Mahdavi, for her support, friendship, understanding, and help.

To Professor Dr. Rubén Romero, for his dedication, patience, trust and friendship during the orientation.

To professors Dr. Jonatas Boas Leite (Department of Electrical Engineering / Faculty of Engineering of Ilha Solteira - UNESP), Dr. Leonardo Henrique Faria Macedo Possagnolo (Department of Energy Engineering / Faculty of Engineering and Sciences - UNESP), Dr. Lucas Teles De Faria (Department of Energy Engineering / Faculty of Engineering and Sciences - UNESP), and Dr. Juan Manuel Home Ortiz (Faculty of Electrical and Computer Engineering / State University of Campinas - UNICAMP), as the committee of examiners for their suggestions and friendship during the development of this work.

This work was carried out with the support of the Coordination for the Improvement of Higher Education Personnel - Brazil (CAPES) - Financing Code 001.

“Human beings are members of a whole,
In creation of one essence and soul.
If one member is afflicted with pain,
Other members uneasy will remain.
If you’ve no sympathy for human pain,
The name of human you cannot retain!”. Saadi Shirazi from Iran.

ABSTRACT

Nowadays, due to the increasing consumption of electricity, the need to produce and transmit electrical energy has increased. Therefore, environmental and economic issues have become more important. A lot of different works have been done to optimize the performance of power grids. One of the most important tasks is the use of energy resources in distribution networks. For many years, diesel generators (DG) have been used as auxiliary sources for power plants in the distribution network. However, in recent years, the use of renewable sources such as solar energy production sources or the photovoltaic system (PV) and wind turbines (WT) and energy storage system (ESS) is also increasing in distribution networks. With the emergence of renewable energies and their injection and their impact on distribution networks has expanded to such an extent that the past analysis methods of the power system are not fully responsive to the need for this change and transformation of electric energy distribution. Power changes in a photovoltaic and wind turbine system, which have uncertainty in the production power, cannot be predicted and is a random process. As a result, its effect on the distribution network will be random. With the increase in the number of photovoltaic systems and wind turbines, their adverse effects will also increase in the networks. If these adverse effects caused by the random process are not well controlled, the problem of power quality in the distribution network will increase. The distribution network can be used in a suitable stability mode. In this thesis, our goal is to improve the performance of distribution systems considering renewable energy along with the reconfiguration of the distribution network, which we will concentrate more on the issue of reducing power loss and improving the voltage profile considering the optimal location of distributed generation and related capacities by using MATLAB software and chaotic particle swarm optimization algorithm (CPSO) on IEEE 33, IEEE 69-bus, 136-bus, and 415-bus systems.

Keywords: chaotic particle swarm optimization algorithm; distributed generation; distribution network reconfiguration; energy storage system; photovoltaic system; power loss; wind turbines.

RESUMO

Atualmente, devido ao crescente consumo de energia elétrica, a necessidade de produzir e transmitir energia elétrica aumentou. Portanto, as questões ambientais e econômicas tornaram-se mais importantes. Muitos trabalhos diferentes foram feitos para otimizar o desempenho das redes elétricas. Uma das tarefas mais importantes é a utilização dos recursos energéticos nas redes de distribuição. Por muitos anos, geradores a diesel (GD) têm sido utilizados como fontes auxiliares para usinas de energia na rede de distribuição. No entanto, nos últimos anos, o uso de fontes renováveis como as fontes de produção de energia solar ou o sistema fotovoltaico (FV) e turbinas eólicas (TE) e sistema de armazenamento de energia (SAE) também vêm aumentando nas redes de distribuição. Com o surgimento das energias renováveis e seu impacto nas redes de distribuição se expandiu de tal forma que os métodos anteriores de análise do sistema elétrico não são totalmente adequados à necessidade dessa mudança e transformação da distribuição de energia elétrica. Mudanças de potência em um sistema fotovoltaico e eólico, que possuem incerteza na potência de produção, não podem ser previstas e são um processo aleatório. Como resultado, seu efeito na rede de distribuição será aleatório. Com o aumento do número de sistemas fotovoltaicos e aerogeradores, seus efeitos adversos também aumentarão nas redes. Se esses efeitos adversos causados pelo processo aleatório não forem bem controlados, o problema de qualidade de energia na rede de distribuição aumentará. A rede de distribuição pode ser usada em um modo de estabilidade adequado. Nesta tese, o objetivo é melhorar o desempenho dos sistemas de distribuição com o envolvimento de energia renovável juntamente com a reconfiguração da rede de distribuição, com o objetivo da redução de perdas de energia e melhoria do perfil de tensão considerando a localização ótima de sistemas de geração distribuída. É usado o software MATLAB e algoritmo de otimização de enxame de partículas caóticas (OEPC) em sistemas IEEE 33, IEEE 69, 136 e 415 barras.

Palavras-chave: algoritmo de otimização de enxame de partículas caóticas; geração distribuída; perdas de potência; reconfiguração da rede de distribuição; sistema de armazenamento de energia; sistema fotovoltaico; turbinas eólicas.

LIST OF FIGURES

LIST OF TABLES

LIST OF ABBREVIATIONS

AACO	Adaptive Ant Colony Optimization
ACSA	Adaptive Cuckoo Search Algorithm
ASU	Air Isolation Unit
BCBV	Branch Current to Bus Voltage
BIBC	Bus Injection to Branch Current
CPSO	Chaotic Particle Swarm Optimization
CVaR	Conditional Value-at-Risk
CGA	Continuous Genetic Algorithm
CES	Cryogenic Energy Storage
DG	Distributed Generation
DNO	Distribution Grid Operator
DLF	Distribution Load Forecasting
GA	Genetic Algorithm
HVACs	Heating, Ventilating and Air-Conditioning System
ICA	Imperialist Competitive Algorithm
IEEE	Institute of Electrical and Electronics Engineers
ISO	International Organization for Standardization
KCL	Kirchhoff’s Current Law
KVL	Kirchhoff’s Voltage Law
MCP	Market Clearing Price
MATLAB	MATrix LABoratory
MINP	Mixed-Integer Nonlinear Programming

MPGSA	Modified Plant Growth Simulation Algorithm
MTLBO	Modified Teaching-Learning-Based Optimization Algorithm
OpenDSS	Open Distribution System Simulator
PSO	Particle Swarm Optimization
PV	Photovoltaic
PEMFC-CHP	Proton Exchange Membrane Fuel Cell, Combined Heat and Power
RES	Renewable Energy Sources
SSW	Section Switches
SFS	Stochastic Fractal Search
TSWs	Tie Switches
TOU	Time of Use
UVDA	Uniform Voltage Distribution-Based Constructive Reconfiguration Algorithm
WT	Wind Turbines

LIST OF SYMBOLS

F	Objective function of the problem
P_D	Total active power load
P_G	Active power injection at the substation and DGs
P_{loss}	Total active power losses of the network in kW
N_{bus}	Total number of buses in the network
$P_{DG,i}$	Active power output of the DG unit i
N_{DG}	Number of DG units
C_1	Perceptual parameter
C_2	Social parameter
r_1	Random number in the range of [0,1]
r_2	Random number in the range of [0,1]
$X_i(t)$	Current position of particle
$V_i(t)$	Current velocity of particle
W	Controller of inertial coefficient of particle movement
X_{gbest}	Position of the global best particle
X_i	Initial population
N_p	Number of solutions in the population
N_{Tie}	Number of tie-switches
SW_i	Status of switch i
V	Voltage across an element of circuit in volts
I	Current passing through element in amps

R	Resistance of element in ohms
$I_i^{(k)}$	Nodal current injection
$V_i^{(k-1)}$	Voltage at node i calculated during the (k-1)th iteration
S_i	Specified power injection at node i
Y_i	Sum of all the shunt elements at the node i
$I_{L2}^{(k)}$	Current injection at node L2
$\Delta P_i^{(k)}$	Real power mismatch at bus i
$\Delta Q_i^{(k)}$	Reactive power mismatch at bus i
$P_{DGmin,i}$	Minimum size of the DG unit i
$P_{DGmax,i}$	Maximum size of the DG unit i

SUMMARY

1 INTRODUCTION AND PROBLEM STATEMENT

1.1 INTRODUCTION

The problem of optimization in distribution grid can achieve with goals such as minimizing losses, retrieving service in the grid, minimizing voltage deviation at the consumer power supply point (improving the voltage profile) or increase the level of grid reliability (SHIRMOHAMMADI, 1992). Among the proposed goals, energy losses in power grids waste significant amounts of electrical energy each year, thereby imposing huge sums on electricity companies and their subsidiaries. Meanwhile, a significant share of power grid losses is related to losses in energy distribution grids. The most important reasons for losses in the distribution system are low voltage level and then high current values, reactive power passing along the feeders, radial grid structure, feeder current imbalance, harmonic pollution, equipment wear, and unauthorized branches (this means that people receive energy from the power grid without a license and without privileges, and this type of unauthorized branching occurs mostly in poor areas). There are several ways to reduce losses in distribution grids. These include capacitors, (GRAINGER; LEE, 1981), use of distributed generation sources, (EL-KHATTAM; SALAMA, 2004), transformer load management and grid reconfiguration (KASHEM *et al*., 1998b).

With the increasing use of nonlinear loads including power electronics, home and electromagnetic appliances, a significant amount of harmonic current is transmitted to the grid (TENG; CHANG, 2007). The occurrence of harmonics in electrical systems is the first consequence of nonlinear elements in the grid. Due to the increasing use of nonlinear elements in electrical systems, such as actuators and power converters, the harmonic value of the current waveform and voltage has increased dramatically. So, the importance of the issue is quite clear. The study of harmonic issues led to research that resulted in several points of view on the quality of electricity. According to some researchers, harmonic distortion is the most significant issue in electricity quality (MASOUM *et al*., 2004). Harmonic problems are inconsistent with the most common rules in power system design and performance under the main frequency. Hence the designer encounters unfamiliar phenomena which require sophisticated tools and advanced equipment to solve and analyze problems. Fortunately, in recent years, researchers have realized that if the distribution system is properly designed, it is very unlikely to make a problem caused by harmonics. For example, proper installation of capacitive banks or distributed generation sources can effectively reduce the harmonic value of the grid (distributed generation sources can help in the stability of the distribution network by injecting power and indirectly prevent the weakening of the network against harmonics, but to reduce the effects of harmonics, capacitors are used in the network).

Today, due to the increase in the population in the world and as a result, the urgent need of people for daily life for electric energy on the one hand, on the other hand, the high consumption of electric energy of the subscribers in the distribution system (DN) causes the poor efficiency of the network due to the wastage of energy and weak voltage. Also, the extraction of fossil energy to produce fuel for power plants, which causes destruction of natural resources (or underground), and the consumption of extracted fossil fuels causes environmental pollution (on the ground), which means destruction from two perspectives (underground and on the earth). It has forced the officials of the production, transmission and distribution of electric energy to think of a solution and replacement of this important matter so that they can prevent the destruction of the planet and look for non-polluting, clean and cheaper energy sources, which are renewable solar or photovoltaic (PV) energy sources, wind energy, battery or other cheap energy. This new technology has the ability to eliminate energy losses and restore and improve the voltage profile along with other power and voltage controller equipment and other parameters of the distribution network. Renewable energy is a type of energy that is freely found in nature, and any amount of it we consume will be replaced more quickly in nature, and it is energy that is inexhaustible, these resources never run out, and are naturally capable of supplying any amount of consumption such as sunlight, wind speed, water, geothermal, and environmental fuels, which are at the center of the transition to a low-carbon and sustainable energy system. Its intensity and decrease in any part of the world depends on the nature of that area and it depends on the wind blowing, raining, intensity of sunlight, movement of waves and tides of the sea and oceans and other related environmental factors. Renewable energy sources are used to reduce power losses and improve voltage profile, efficiency, grid stability and protection systems, which will result in greater reliability and power quality.

Among the other features and operating parameters that increase efficiency and stability to DN is the use of distribution network reconfiguration operations, that is, choosing an optimal combined process of open and closed switches in order to optimize a certain goal and its main focus is to minimize power losses, improve voltage profile in buses, implement without violating the limits defined in the initial design of the network, find a new radial structure, and reduce technical losses, which is the most common method to reduce losses and improve the voltage profile of distribution networks, buses and feeders, which is one of the important goals of the operator in every network. The choice of reconfiguration is a complex compound problem and many switches and configurations are involved, which increases the complexity and volume of the distribution system and requires effective methods to solve the problem in reconfiguring the distribution network. Although in this case, many meta-heuristic algorithms have been used in solving the optimization of the global problem, but searching for an optimal solution close to the optimal response in a reasonable time is still a research challenge for the reconfiguration of distribution networks.

The advantages of switches that are opened and closed in the reconfiguration of the distribution network are: recovery of the distribution network and power sources, line isolation, reduction of power losses, improvement of the voltage profile, optimal utilization of production generators, coordination of distributed resources, creation of load balancing, improvement of stability, reliability, and power quality in the distribution system, etc.

1.2 STATEMENT OF THE PROBLEM

The use of distributed generation is increasing rapidly in electricity generation for various reasons such as reducing environmental pollution, improving power quality indicators, reducing losses, and grid stability. As distributed generation role in the electricity industry has been expanding in recent years, this role will be significant and decisive shortly. By definition, distributed generation is the generation of electricity-producing units with a capacity of less than 10 MW that connects to the grid at substations, distribution feeders, or customer levels. Distributed generations include different types such as combustion gas turbines, small turbines, energy storage devices, wind turbines, biomass energy, fuel cells, and solar cells (ZANGENEH; JADID, 2010).

These resources include the latest technologies, reliability, high efficiency, and easy operation that increase their ability to compete with the power system. In some cases, distributed generations offer the customer a lower price and higher reliability than the power grid. Sometimes they help with improving the grid performance by connecting to the power grid (EL-KHATTAM; SALAMA, 2004).

Connecting distributed generation to the power grid can have a positive or negative effect on grid performance. One of the positive effects of connecting distributed generation to the grid is to reduce distribution system losses, which depend on the amount and location of distributed generation. Determining the optimal size and location of distributed generation, grid losses number can be minimized (YASIN; RAHMAN, 2006). But in addition to the positive effects, improper use of distributed generation resources may cause environmental pollution or be installed and operated in a way that is not economically viable (CELLI *et al*., 2005). Therefore, in the location of DGs, we need to consider the other goals including, the cost-reducing investment and the amount of pollution associated with the establishment of distributed generation units.

Another way to reduce losses at the distribution level is to reconfiguration the distribution grid. Reconfiguration is the change of grid arrangement to achieve a specific goal such as greater reliability, lower losses, better voltage profile, etc. When changing the layout, note that the new grid maintains its radial structure includes all the buses, and at the same time, all the constraints in the grid design are observed, for example, voltage and line current. And other grid equipment within the permitted range. Performing the reconfiguration process by considering the limitations and conditions in the grid is a complex optimization problem that requires an optimization solution algorithm such as a genetic algorithm and PSO, etc. Since the lines used in the grid can change by reconfiguring the grid structure through changing and closing the same number of switches that are closed normally, therefore by reconfiguring, the power distribution path and the bus connection method can be different in the grid.

Concerns about global warming (greenhouse gas emissions), fossil fuel reserves, and primary energy independence in countries have led to a dramatic increase in the influence of renewable energy sources (RES), mainly wind and solar, on electric power systems (LAMONT; OBESSIS, 1995). Increasing penetration of renewable energy sources in microgrids and the random nature of the market clearing price (MCP) in the environment, the electricity market has been deregulated, which caused a drastic change in electricity prices. The distribution grid operator (DNO) is responsible for the optimal operation of microgrids needs to manage the intermittent behavior of RERs to maintain a balance of power between supply and demand (NIKMEHR; RAVADANEGH, 2015). One of the most necessary and practical solutions to increase the efficiency and performance of microgrids is the reconfiguration problem, which is the process of changing the topology of microgrids using some section switches (SSW) so that all operational constraints and structures achieve simultaneously. In addition, to enhance the usefulness and effectiveness of the proposed reconfiguration problem, some tie switches (TSWs) in the grid have been used to increase the flexibility and resilience of microgrids in the face of various exploits of uncertainty. These added switches can change the microgrid connections to effectively increase under different operating conditions, which has significantly improved the performance of the proposed method (RADHA *et al.*, 2003).

Distributed generation units are applied to provide local power in the power system and achieve the allowable voltage range. In addition, proper DG placement will improve the power factor, reduce losses and improve the harmonic status of the grid. Therefore, correct use of distributed generation leads to reduced losses and improved grid voltage profile. The question here is what effects, the changes of the layout of a grid in distributed generation, have on the power losses and voltage profile of the grid, and if the connection of distributed generation to the grid is optimal, how much reconfiguration will help to reduce grid loss, or if the siting and sizing of distributed generation and reconfiguration are determined simultaneously, how much improvement will be made in grid conditions?

The significance of obtaining high-quality electricity to customers and environmental considerations has driven electricity companies to improve the quality of system power and reduce pollution caused by distributed generation and energy storage. Using optimization with multiple criteria makes it possible for the views of the designer to create an interaction between the objectives of the problem. This thesis presents a new method to express and implement the problem of optimal location of distributed generation units with the multi-objective method. In the proposed method, reducing the losses and improving the voltage profile have been considered as the objectives of locating the distributed generation units in the distribution grid. The first different models are presented for distributed generation. The optimal location is then calculated to gain the minimum losses and increase the voltage profile for these models. Once the optimal location for distributed generation have been achieved, the grid will be reconfigured in the presence of these units. The objective in both cases is the optimal location of the distributed generation and also the reconfiguration in the presence of the distributed generation to minimize losses and improve the voltage profile. We examine the effect of optimal location and size of distributed generation on reducing losses and improving the voltage profile resulting from the reconfiguration in this thesis. The problem of reconfiguration will be expanded as an optimization problem due to technical and physical constraints. Finally, the proposed integrated model is solved with one of the metaheuristic optimization algorithms and the simulation results on one or more test sample distribution systems will be analyzed and compared during a certain period of time.

1.3 RESEARCH OBJECTIVES

1- Planning of the distribution systems operation through reconfiguration and optimal placement and sizing of distributed generation using CPSO.
2- Reduction of power loss in distribution systems through reconfiguration and optimal placement and sizing of distributed generation using CPSO.
3- Improvement of voltage profile in distribution systems through reconfiguration and optimal placement and sizing of distributed generation using CPSO.

1.4 ASSUMPTIONS

1- Considering generation management, load management, and generation and load management simultaneously to establish a balance between production and demand.
2- It is required to recreate the model used in the arrangement of distributed generations to use them in the best way during each reconfiguration of the grid.

2 THEORETICAL FOUNDATIONS AND RESEARCH BACKGROUND

2.1 INTRODUCTION

Power system stability has been introduced since 1920 as an influential and fundamental issue for the reliable operation of the system. We can realize the significance of this issue because most serious outages occur due to the instability of the power system (TIRANUCHIT; THOMAS, 1988). Various types of voltage instability have been developed by expanding power systems through interconnection, using new technology and controllers, and increasing performance in high-stress conditions.

It is possible to consider the stability of the power system as a feature of the power system that is in equilibrium in normal conditions and will retrieve a different acceptable mode if it is influenced by turbulence.

2.2 LOAD FLOW

The analysis of a power grid includes its study in normal and stable operating conditions (load flow analysis) and also its study in short circuit conditions (short circuit analysis). Load flow is an essential tool to analyze the steady-state of any power system. The main purpose of load flow is to find the voltage of different buses so that the flow of active and reactive powers in different lines can be obtained for a specific loading condition. In power systems, load flow is highly important because it determines the two main quantities of these grids, which means voltage and current (GHATAK; MUKHERJEE, 2017).

Power systems include three parts: generation, transmission, and distribution. The generation sector will be modeled as the sources of the transmission part in the load flow, but there are differences in structure and topology of the transmission and distribution grid that have made, the proposed methods for load flow of the two parts, different. The structure of the transmission is meshed, but the structure of the distribution grid is radial.

This radial grid includes distribution substations that each one feeds several low-voltage feeders. Each low-voltage feeder also feeds a part of a town or village. According to the simple and radial structure of these feeders, their load flow is much simpler than transmission grids. Normally, it is possible to solve independently the load flow issue of each feeder assuming the distribution bus as the reference bus.

Load flow analysis of a feeder can provide the following parameters:

1- Magnitude and angle of voltage in all buses
2- Current flow in each of the lines
3- Losses in each line
4- Total feeder losses

2.3 KIRCHHOFF'S LAW IN ELECTRICAL CIRCUIT

Ohm's law, Kirchhoff's Voltage Law, and Kirchhoff's Current Law are essential in the circuit analysis. Kirchhoff's laws deal with the voltage and current in the circuit. Ohm's law relates voltage, current and resistance to one another. These three laws apply to resistive circuits where the only elements are voltage and/or current sources and resistors. Using the three laws any resistance of, current through or voltage across a resistor can be found if any two are already known. The purpose of this research is to provide verification of these laws. In the year 1845, Gustav Kirchhoff (German physicist) introduces a set of laws which deal with current and voltage in the electrical circuits. The Kirchhoff's Laws are generally named as KCL (Kirchhoff's Current Law) and KVL (Kirchhoff's Voltage Law). The KVL states that the algebraic sum of the voltage at node in a closed circuit is equal to zero. The KCL law states that, in a closed circuit, the entering current at node is equal to the current leaving at the node. A single equivalent resistance, (RT) can be found when multiple resistors are connected in series or parallel, these circuits obey Ohm's law. But, in complex electrical circuits, we cannot use this law to calculate the voltage and current. For these kinds of calculations, we can use KVL and KCL.

2.3.1 Circuit analysis techniques

The following sections describe the three basic laws that are used in analyzing linear circuits.

2.3.1.1 Ohm's law

Ohm's law is used to relate voltage to current and resistance. It states that voltage is directly proportional to current and resistance. This is stated mathematically as equation (1).

$$V = IR \tag{1}$$

Where V is the voltage across an element of the circuit in volts, I is the current passing through the element in amps and R is the resistance of the element in ohms. Given any two of these quantities Ohm's law can be used to solve for the third.

2.3.1.2 Kirchhoff's voltage law

Kirchhoff's Voltage Law (KVL) states that the sum of all voltages in a closed loop must be zero. A closed loop is a path in a circuit that doesn't contain any other closed loops. Loops 1 and 2 in Figure 1 are examples of closed loops.

Figure 1 – An example of KVL

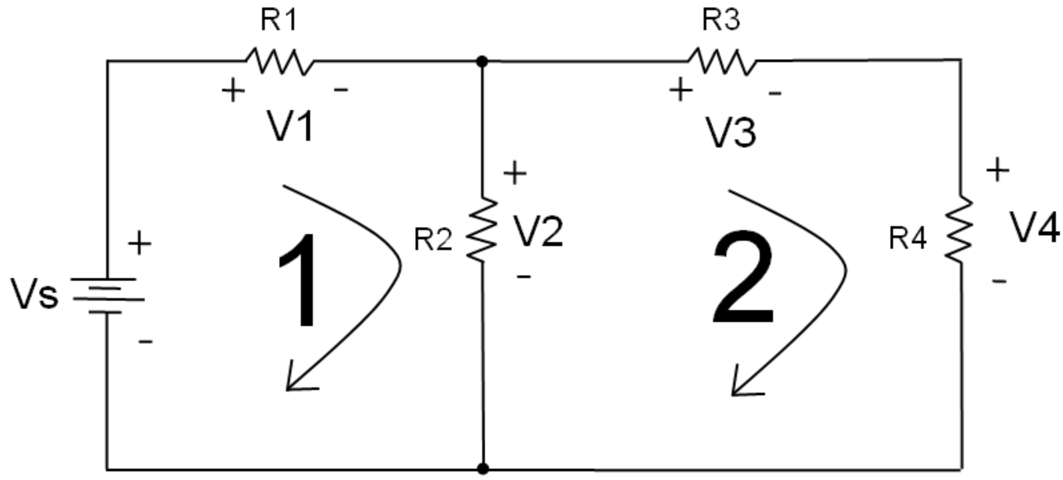

Source: Raj *et al*. (2017).

The perimeter of the circuit is also a closed loop, but since it includes loops 1 and 2 it would be repetitive to include a KVL equation for it. If loop 1 is followed clockwise, the KVL is equation (2).

$$V_1 + V_2 - V_S = 0 \quad (2)$$

This equation holds true only if the passive sign convention is satisfied. In the case of KVL the passive sign convention states that when a positive node is encountered while following a loop the voltage across the element is positive. If a negative node is encountered the corresponding element voltage is negative. In order to simplify the KVL equations, the polarities should be assigned to satisfy the passive sign convention whenever possible.

2.3.1.3 Kirchhoff's current law

Kirchhoff's Current Law (KCL) deals with the currents flowing into and out of a given node. KCL states that the sum of all currents at a node must equal zero. This is illustrated in Figure 2.

Figure 2 – An example of KCL

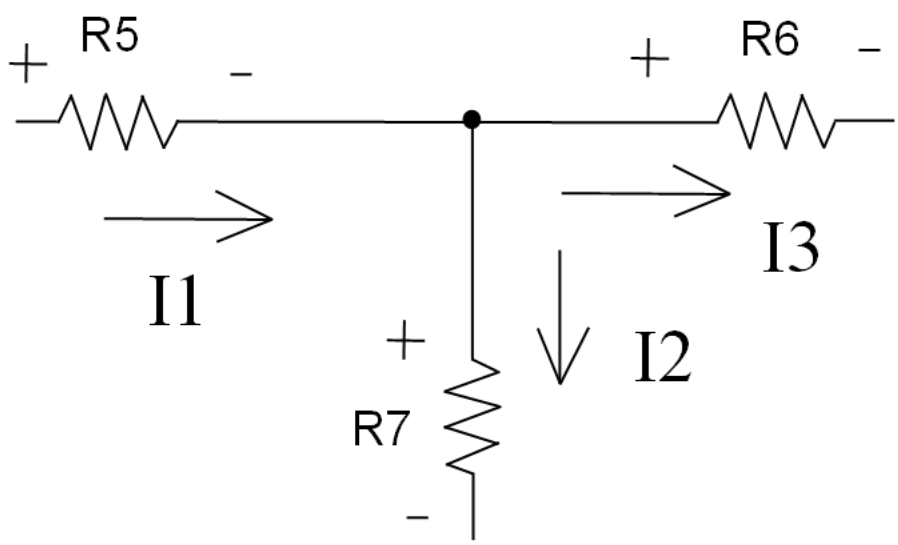

Source: Raj *et al*. (2017).

The equation obtained by KCL for the node shown in Figure 2 is.

$$I_1 - I_2 - I_3 = 0 \quad (3)$$

In the case of KCL the passive sign convention deals with the direction of currents with respect to the node. Currents entering the node must have opposite signs as those exiting the node. The passive sign convention with respect to KVL can also be applied to KCL. On many schematics the polarities of resistors are already assigned, so the directions of the currents should be assigned such that the current is entering the positive terminal.

2.4 DIFFERENT METHODS OF LOAD FLOW IN DISTRIBUTION SYSTEMS

Various methods have been suggested for load flow of distribution systems. Some of these methods are (HAMOUDA; ZEHAR, 2011):

1- Newton-Raphson (NR)
2- Backward - Forward Sweep Power Flow

Backward-forward methods have been extensively used in load flow calculations due to their high speed, low computational memory requirements, and good convergence properties.

The general algorithm of this load flow includes two basic backward and forward stages. These two steps can be simply described as follows:

Backward step: The feeder is swept in this step from the end of the feeder to its origin, and one of the parameters related to the leading sweep parameter is regularly updated in this step, of course if the bus voltage is updated in the forward sweep. The branches flow is updated from the end of the feeder in this step using the bus voltage acquired from the previous sweep.

Forward step: In this step, the complete length of the grid is swept from the reference bus, which is the distribution post, to the end of the feeder, and one of the grid parameters, such as bus voltage is usually updated at this stage. In other words, it is possible to update bus voltages at this stage by having the branch flow from the previous iteration and using the radial structure of the grid. In general, a parameter is updated which the nature of its changes is from the origin of the feeder to its end in this step.

The matrices of bus injection to branch flow and the matrix of branch current to bus voltage have been applied to calculate the voltage and flow in the backward-forward load flow. This algorithm is repeated until convergence is realized. The flowchart of the above load flow has been shown in Figure 3.

Figure 3 – Flowchart of backward-forward load flow

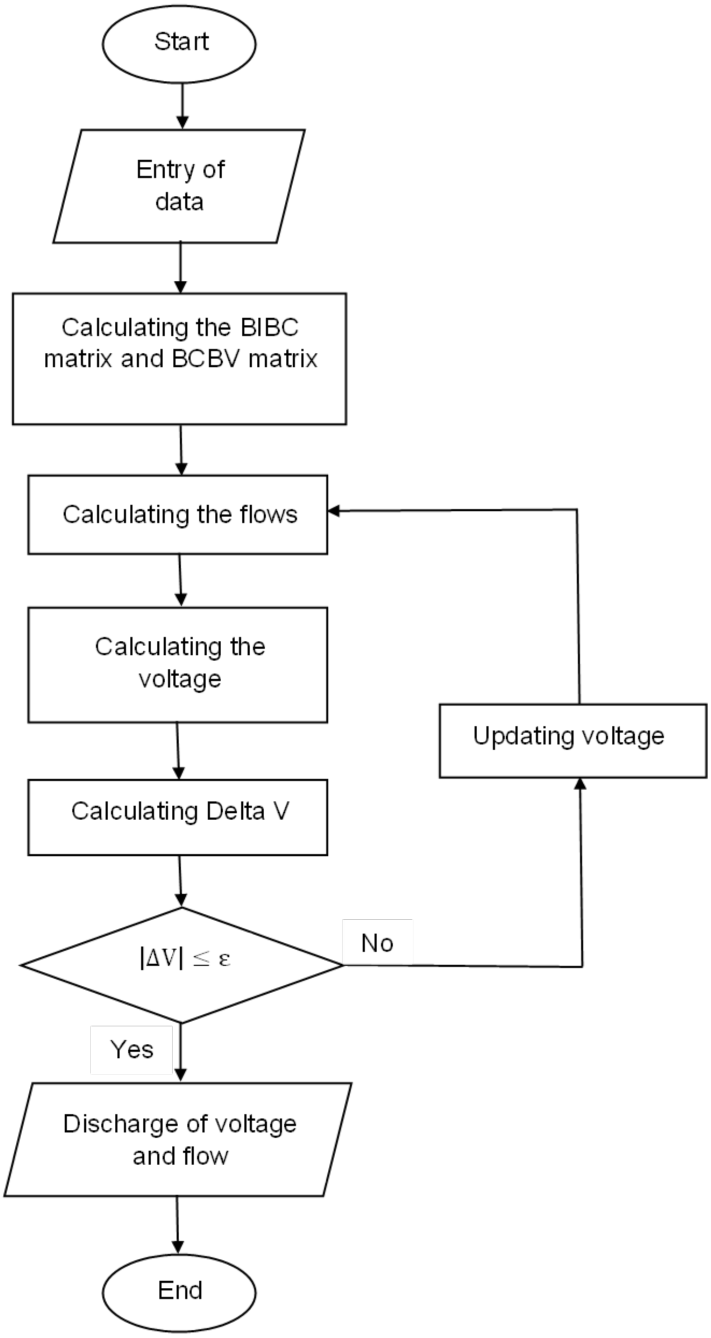

Source: Author's elaboration.

2.5 SOLUTION OF A RADIAL DISTRIBUTION NETWORK

In algorithm that is described by Shirmohammadi *et al*. (1988), regardless of its original topology, the distribution network is first converted to a radial network. Hence, an efficient algorithm for the solution of radial networks is crucial to the viability of the overall solution method.

The solution method used for radial distribution networks is based on the direct application of the KVL and KCL. For our implementation, we developed a branch-oriented approach using an efficient branch numbering scheme to enhance the numerical performance of the solution method. We first describe this branch numbering scheme.

2.5.1 Branch numbering

In contrast to all classical power flow techniques which use nodal solution methods for the network, this algorithm is branch-oriented. Figure 4 shows a typical radial distribution network with n nodes, b(=n-1) branches and a single voltage source at the root node. In this tree structure, the node of a branch L closest to the root note is denoted by L1 and the other node by L2. We number the branches in layers away from the root node as shown in Figure 5. The numbering of branches in one layer starts only after all the branches in the previous layer have been numbered. This numbering scheme is very simple and straightforward, and has been implemented in our power flow program.

Figure 4 – A typical radial distribution network

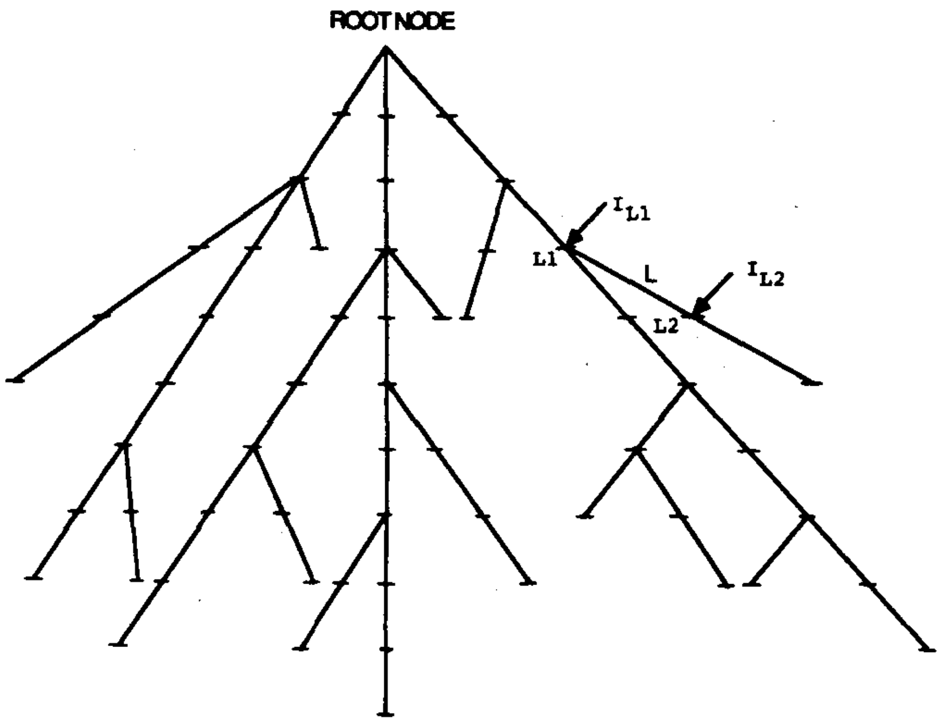

Source: Shirmohammadi *et al*. (1988).

Figure 5 – Branch numbering of the radial distribution network

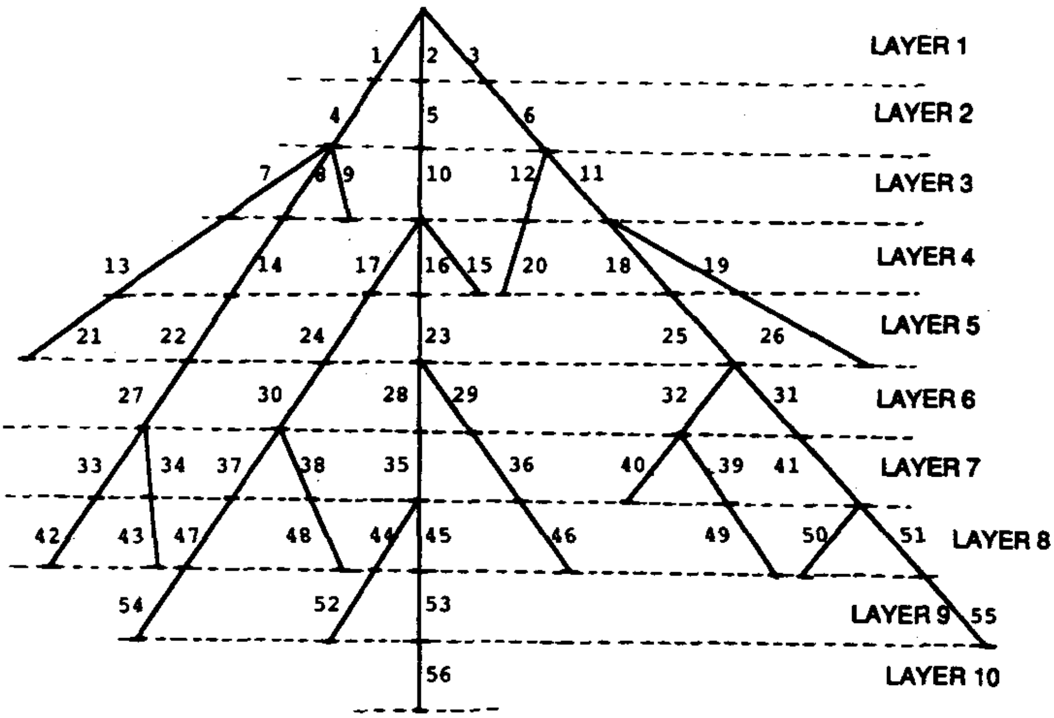

Source: Shirmohammadi *et al*. (1988).

2.5.2 Solution method

Given the voltage at the root node and assuming a flat profile for the initial voltages at all other nodes, the iterative solution algorithm consists of three steps:

1- Nodal current calculation: At iteration k, the nodal current injection, $I_i^{(k)}$, at network node i is calculated as,

$$I_i^{(k)} = \left(\frac{S_i}{V_i^{(k-1)}}\right)^* - Y_i V_i^{(k-1)} \qquad i = 1,2,\dots,n \tag{4}$$

Where $V_i^{(k-1)}$ is the voltage at node i calculated during the $(k-1)^{th}$ iteration and S_i is the specified power injection at node i. Y_i is the sum of all the shunt elements at the node i.

2- Backward sweep: At iteration k, starting from the branches in the last layer and moving towards the branches connected to the root node the current in branch L, J_L, is calculated as:

$$J_L^{(k)} = -I_{L2}^{(k)} + \sum_{from\ node\ L_2}^{currents\ in} (branches\ emanating) \qquad L = b, b-1, \dots, 1 \tag{5}$$

Where $I_{L2}^{(k)}$ is the current injection at node L2. This is the direct application of the KCL.

3- Forward sweep: Nodal voltages are updated in a forward sweep starting from branches in the first layer toward those in the last. For each branch, L, the voltage at node L2 is calculated using the updated voltage at node L1 and the branch current calculated in the preceding backward sweep:

$$V_{L2}^{(k)} = V_{L1}^{(k)} - Z_L J_L^{(k)} \qquad L = 1, 2, \dots, b \tag{6}$$

Where Z_L is the series impedance of branch L. This is the direct application of the KVL.

Steps 1, 2 and 3 are repeated until convergence is achieved.

2.5.3 Convergence criterion

We used the maximum real and reactive power mismatches at the network nodes as our convergence criterion. As described in the solution algorithm, the nodal current injections, at iteration k, are calculated using the scheduled nodal power injections and node voltages from the previous iteration (Equation (4)). The node voltages at the same iteration are then calculated using these nodal current injections (Equations (5) and (6)). Hence, the power injection for node i at kth iteration, $S_i^{(k)}$, is calculated as:

$$S_i^{(k)} = V_i^{(k)} (I_i^{(k)})^* - Y_i \left| V_i^{(k)} \right|^2 \tag{7}$$

The real and reactive power mismatches at bus i are then calculated as:

$$\Delta P_i^{(k)} = \left|Re[S_i^{(k)} - S_i]\right|$$

i=1,2,...,n (8)

$$\Delta Q_i^{(k)} = \left|Im[S_i^{(k)} - S_i]\right|$$

Figure 6 shows the flow chart of the overall power flow solution method for radial networks.

Figure 6 – Power flow solution algorithm for the radial networks

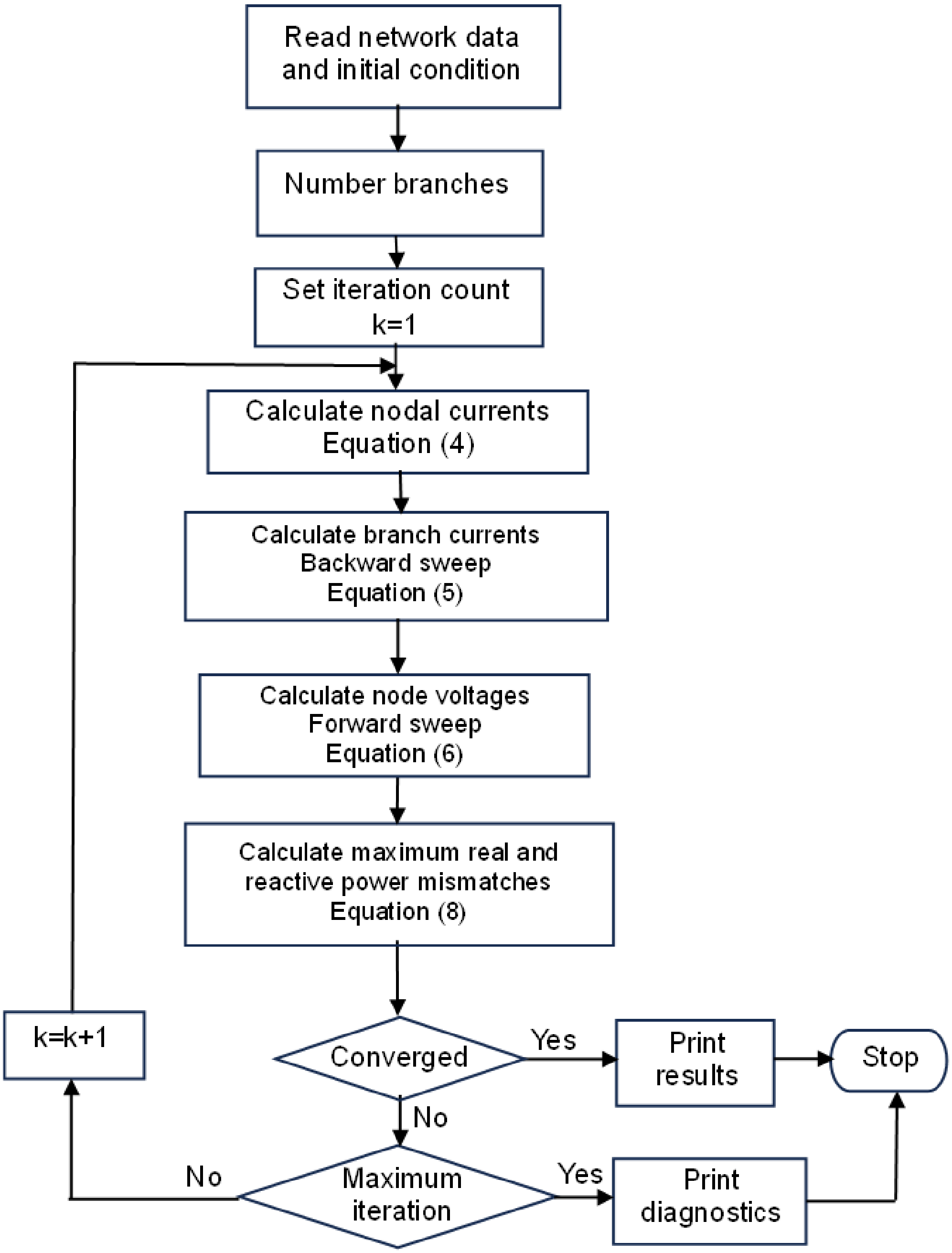

Source: Shirmohammadi *et al.* (1988).

2.6 LITERATURE REVIEW

The issue of installation and adjustment of distributed generation units in distribution systems has been one of the important research priorities in the decade. A lot of work has been done on it in the past and there are several techniques to solve this issue. Significant research has been conducted to find the optimal location and other DG parameters. The reduction of grid losses, of course, without considering the pollution caused by the installation of these devices or the way to change the harmonic rate of the grid in the presence of these resources has been highly important in most of these studies. Optimal location of distributed generation in the distribution grid is an optimization problem with discrete and continuous variables.

Zangeneh and Jadid (2010) and El-Khattam and Salama (2004) have presented an analytical method to determine the optimal location of distributed generation units. The main drawback of the analytical method is that it is time consuming and these important drawbacks make this method inefficient against large grids. Moreover, increasing the number of DGs also enhances the computation time. In recent years, with the development of intelligent search algorithms, this problem has been solved quiet well.

Devaraj and Roselyn (2010) has used a method based on a genetic algorithm to determine the location and capacity of distributed generation sources. Some research has used intelligent and evolutionary methods to find the optimal location of DGs. The fuzzy-genetic algorithm has been used in Kim *et al*. (2002) and the tabu search algorithm has been used in Nara *et al*. (2001) and the bee algorithm has been used in Niknam (2011). Also, Niknam (2008) has used the ant-colony algorithm and in El-Zonkoly (2011), the PSO algorithm. But the installation of DGs is usually sought with a single objective in most of the conducted studies. For example, in Choudhry and Khan (2010) aim only to minimize the amount of grid losses. But other parameters are also required to be considered in designing a grid. In Biswas *et al*. (2012) has examined distribution generation to reduce voltage drop.

In Mithulananthan and Than (2006) have employed distributed generation to improve the load capacity limit in the grid and in Borges and Falcão (2006) have determined the parameters of distributed generation that define the objective function based on increasing the reliability and improving the voltage profile.

Since the reconfiguration of feeders has been widely used as a quick and inexpensive method among other available methods to reduce losses, so far different methods have been used to solve the problem. Reconfiguration is provided in distribution grids. Although methods such as branch change method and optimal power flow are simple and effective, they may not produce the overall optimal point and it is possible to be inaccurate. Recent methods such as genetic algorithm and tabu search, unlike the suggested methods, determine the optimal solution in a more trustworthy way.

In the meantime, less research has been done on the simultaneous installation and adjustment of distributed generation units and reconfiguration. In some of these studies, DGs have been modeled first and then reconfiguration has been used to improve the situation in Wu *et al*. (2010) and Olamaei *et al*. (2008).

What is further studied in this thesis is the reconfiguration and allocation of DG with the aim of improving the voltage profile and reducing power losses.

Simultaneous load response scheduling and reconfiguration programming have been analyzed to reduce operating costs and also strengthen the reliability and flexibility of microgrids in experiencing uncertainties applying the Hong point analysis method in Aghajani and Ghadimi (2018).

Singh *et al*. (2016) provides a comparative and critical analysis of decision strategies and solution methods for microgrid energy management systems. Also, different methods of measuring uncertainty have been investigated to manage the fluctuation and intermittent renewable energy sources and load demand.

Xiang *et al*. (2016) examines multi-network architectures to form a microgrids. The microgrids has been examined as a single entity and its possible interactions with external networks have been initially examined. Microgrids architectures have been then defined in terms of design, line technology, and communication technology. Finally, different architectures have been compared in terms of cost, scalability, protection, reliability, stability, communications, and business models.

Trifunovic *et al*. (2011) presents an approach to reduce peak loads using home area network (HAN) systems in residential units. The HAN system algorithm, which is run by the HAN controller, is modeled employing the Integrated Modeling Language (UML).

Eddahech *et al*. (2013) has proposed a method to divide the distribution system into functional blocks of the network along with a method to predict the electrical values of the distribution. Applied blocks allow the assets to be organized in such a way to provide detailed information for advanced analysis of a geoelectric zone. Active decisions in network performance blocks have been made using highly short-term forcasts of variables (voltage, current, active power, and reactive power). These forecasts are performed based on a creative method in order to select forecast techniques based on online and historical information to rank the performance of forecast techniques. Authors develop methods to increase the flexibility of smart grids in relation to dynamic changes in distribution networks in the presence of distributed flexible sources, demand management, VAR voltage optimization, protection voltage reduction, self-repair, storage, and electric vehicles.

Niknam *et al*. (2010) has examined risk-based energy management based on the CVaR index for optimal flexibility and to reduce operating costs in the commercial building of microgrids when severe weather conditions such as storms, tsunamis, and similar events occur that result in the islanding of the microgrid from the main network.

Bornapour *et al*. (2019) has proposed a stochastic model for coordinated programming of renewable and thermal units. The studied units include fuel cell units with proton exchange membrane, combined heat and power generation (PEMFC-CHP), wind turbines, and photovoltaic. Also, a hydrogen storage strategy has been considered for PEMFC-CHP units. Uncertainty of wind speed, solar radiation, and electricity market price has been considered using the scenario-based method. The hydrogen storage strategy is considered with a mixed-integer (MINP) nonlinear programming problem in the proposed stochastic programming problem. Finally, modified teaching–learning-based optimization algorithm (MTLBO) has been used to solve this problem.

Ramadan and Helmi (2021) has provided a risk-based optimal daily programming for smart grids under intelligent reconfiguration in the presence of wind turbines in order to maximize the operation of microgrids.

Kusakana (2020) has been provided to examine the cost-based demand response and photovoltaic as DG to develop an approach modeling them as energy sources for the sustainable programming of power equipment. This method includes a case study based on the IEEE test system with 8500 nodes of feeder and 1177 low voltage consumers using the Open Distribution System Simulator (OpenDSS). This method uses the Time of Use (TOU) tariffs for the household consumer load response program and measurements for roof photovoltaic systems.

Santos *et al*. (2017) provides a randomized method for optimally combining wind energy and large-scale energy storage according to the load response program in the electricity market. It has also provided a method for integrating the Air Isolation Unit (ASU) and Cryogenic energy storage (CES) to store energy in liquid form during outage periods and to regenerate electricity during peak hours.

Abdi *et al*. (2016) has modeled different types of demand response programs based on the cost elasticity of demand and has presented the concept of customer profit. On the other hand, the effect of running the demand response programs on the operation of microgrids connected to the main network has been analyzed, and several scenarios have been examined to model the uncertainty of the operation of microgrids during the error of generation units and the outage of transmission and upstream lines.

Amin *et al*. (2020) has studied machine learning algorithms for demand response application in smart grids which uses various energy systems such as electric vehicles, heating and cooling systems (HVACs), and batteries. This paper has considered the welfare related to consumers during the implementation of demand response programs.

Thakar *et al*. (2019) is a review paper on studies conducted on microgrid reconfiguration that has examined and categorized these studies. Classifications are based on the used objective functions, the considered constraints, the optimization techniques, the methods of combining uncertainty in using renewable resources. This paper has also presented research gaps and future challenges.

Zakariazadeh *et al*. (2014) has presented energy management of microgrid in the presence of renewable and fossil energy sources to supply thermal and electrical loads. Additionally, the influence of both incentive-based and cost-based demand response programs, both in the island mode and in the grid-connected mode in the presence of uncertainties has been studied to achieve the best demand-side management.

3 METHODOLOGY

3.1 RESEARCH METHODOLOGY

The distribution system obtains a connection among the customer and the network where it applies different switches such as disconnector, circuit breakers, etc. It is applied to protect and manage network makeup. The network can have higher efficiency when changing the load by altering its makeup. Recent researches indicate that nearly 12% of total power generation is wasted as line losses in the distribution system. Thus, determining methods for grid reconfiguration is very beneficial. The objective of grid reconfiguration is to decrease power losses. In this chapter, the concepts of grid reconfiguration are provided.

3.2 GRID RECONFIGURATION

Under normal working conditions, by switching, they change the grid to reduce the losses of lines and improve the voltage profile while obtaining the load and adjusting the grid requirements, enhancing the voltage profile of the grid.

In this case, the constraints of the network and load are as follows**:**

1- Radiality of the new grid.
2- The new grid covers all the bus.
3- The network load is within the permissible limits.
4- The voltage of bus and grid equipment is within the permissible limits.
5- The flow of lines and grid equipment is within the permissible limits.

Regarding all these issues makes network reconfiguration a complex and nonlinear optimizing problem. The exact solution to this problem is only possible with the large volume of calculations and the investigation of all of the switches, which will be very time-taking for real grids with a large number of switches. Several algorithms were applied to solve the reconfiguration problem, each of which has faced problems such as the following problems:

1- Too much computing time for medium and large grids.
2- They are based on intelligent methods, thus, the solutions are not optimum.
3- Difficulty in providing possible solutions

One of the works in this field that leads to the reduction of losses in the distribution grid can be seen in Choudhry and Khan (2010). The authors present a linear programming model that is solved by discrete branch and bound method. The solution method is that the meshed network starts with the closure of all its switches. Switches are opened one by one to achieve a new radial grid. Due to the nature of the problem, it is required to test a large number of grid configuration for a real system.

In Das (2006), first all the switches are closed and then they open the switches one by one by distributing the load to reach the radial structure.

Intelligent switch replacement method is suggested in Tabanjat *et al*. (2015) which a computational formula is proposed to determine the rate of loss change in exchange of switches. In Naveen *et al*. (2015) and Tabanjat *et al*. (2015), the method presented is expanded and at each stage the operation limits the change of switch in a loop. This method of single meshed optimizing is superior to other algorithms because this method provides easy implementation, effective calculations and possible and optimal solutions.

In Pegado *et al*. (2019), to decrease losses, the grid configuration problem becomes an optimalization problem with quadratic objective function with state variables 0 and 1. This resulted in applying simplex method and indicated that the single meshed method originates from the same technical principles of the simplex method. Besides, a simple and effective design is used for distributing the load and calculating the change of losses when changing the switches. Then, a smart method for switch program is provided which achieves optimal makeup with the least change operation. This optimal switch program is achieved by eliminating unnecessary switch operations during repeated problem-solving operations.

In Bompard *et al*. (2000), the search method is completed based on the idea of branch change for rearranging a balanced distribution system. To aid the search method, two methods are proposed to compute the load flow of radial networks: approximate load flow and forward-back load flow method. Furthermore, an algebraic expression is presented that estimates the reduction of losses and the balance index of loads to change the structure of grid. As a solution to this problem, a non-repetitive and simple computational method was suggested that can calculate the load and voltage of the bus with acceptable accuracy and greatly reduce the computational volume.

A more effective solution to the reconfiguration problem in Savier and Das (2011) was suggested. In Savier and Das (2011), a method in order to reduce losses is presented based on a comprehensive search. This method uses graph theory to increase speed. This algorithm can be applied for medium-sized grids. The advantage of this algorithm compared to other algorithms is that it finds the overall optimal point under assumed conditions.

In Fathabadi (2016) and Kashem *et al*. (1998a) new methods based on artificial intelligence are applied to reconfiguration the distribution grid. In Kashem *et al*. (1998a), simulated annealing optimizing method was applied to solve the reconfiguration problem, which is very time consuming. To apply this method, it should be modified to increase its speed.

One of the first cases where intelligent algorithm was used to find optimal solution to reconfiguration problem is discussed in Fathabadi (2016). It is indicated that intelligent algorithm has better performance than simulated annealing.

3.3 OBJECTIVE FUNCTION

One of the main benefits of network reconfiguration with the simultaneous allocation of DGs is to minimize the power losses in the distribution network.

Equation (9) defines the total network power losses.

$$P_{loss} = P_G - P_D \tag{9}$$

Where P_{loss} is the total power losses of the network; P_G is the total active power injection at the substation and DGs; P_D is the total active power load.

In addition, bus voltage and voltage stability are increased by installing DGs in the distribution network.

The objective function (F) of the problem is to minimize the active power losses, which is presented in (10).

$$\text{minimize } F = P_{loss} \qquad (10)$$

3.4 PARTICLE SWARM OPTIMIZATION (PSO) ALGORITHM

This algorithm is the analysis method of the multiple goals of this research. This algorithm was first proposed by Kennedy and Eberhart in 1995. PSO is an evolutionary computational algorithm inspired by nature and based on iteration. The inspiration source of this algorithm was the social behavior of animals such as the collective movement of birds and fish. As PSO also starts with an initial random population matrix, it is similar to many other evolutionary algorithms such as Continuous Genetic Algorithm (CGA) and Imperialist Competitive Algorithm (ICA). Unlike genetic algorithm, PSO does not have any evolution operators such as mutation and mating. For this reason, it can be said that the imperialist competitive algorithm is more similar to PSO than to GA. Each element of the population is called a particle (which is equivalent to a chromosome or a country in the imperialist competitive algorithm). In fact, the PSO algorithm consists of a certain number of particles that randomly take an initial value. For each particle, two position and velocity values are defined, which are modeled with a location vector and a velocity vector, respectively. These particles move iteratively in the n-dimensional space of the problem to search for new possible options by calculating the optimality value as an evaluation criterion. The dimension of the problem space is equal to the available number of parameters in the desired function for optimization. One memory is dedicated to storing the best position of each particle in the past and one memory is dedicated to storing the best position among all particles. With the experience of these memories, the particles decide how to move in the next turn. Every time the particles repetition, they update their velocities and positions according to the absolute and local solutions. The PSO algorithm updates the velocity vector of each particle and then adds the new velocity value to the position or value of the particle. Velocity updates are affected by both the value of the local best solution and the absolute best solution. The best local solution and the best absolute solution are the best solutions that have been obtained by a single particle and in the whole population, respectively, until the current moment of the algorithm execution. The constants are called perceptual parameter and social parameter, respectively. The main advantage of PSO is that the implementation of this algorithm is simple and requires the determination of few parameters. According to the values of pbest (the best position of the particle or personal best) and gbest (the position of the best particle among all particles or global best position), each particle uses the following equations to determine the next position.

$$V_i(t+1) = WV_i(t) + C_1 r_1 \left(X_{ipbest}(t) - X_i(t)\right) + C_2 r_2 \left(X_{igbest}(t) - X_i(t)\right) \quad (11)$$

$$X_i(t+1) = X_i(t) + V_i(t+1) \quad (12)$$

In the above equations, C_1 and C_2 are perceptual and social parameters, respectively. r_1 and r_2 are random numbers in the range of [0,1]. $X_i(t)$ is the current position of the particle. $V_i(t)$ is the current velocity of the particle. W is the controller of the inertial coefficient of the particle movement.

Performance of each particle is calculated using fitness function of its position. Each particle compares the fitness value of its new position with the fitness value of its historical best position according to the following rule in Hefny and Azab (2010):

If fitness (current position) < fitness (best position)
Then Best position = current position

Compare fitness value of the global best position with current particle position to get the new global best position using the following rule:

If fitness (current position) < fitness (gbest position)
Then gbest index = current particle index

Those steps are repeated until a stopping criterion is met. The stopping criteria of the PSO algorithm can be one, or more, of the following conditions in Nedjah and Mourelle (2006):

1- Fixed number of iterations.
2- Fixed value of the fitness function.
3- Fixed number of iterations without improvement: If the velocity changes are close to zero for all the particles, it is likely means that there will be no further improvements can be achieved.

4- An accepted threshold error value for the fitness function is reached: If the error between the obtained objectives function value and the best fitness value is less than a predefined value.
5- An upper limit of CPU usage has been reached.

Figure 7 illustrates the flowchart of the PSO algorithm.

Figure 7 – Flow Chart of PSO

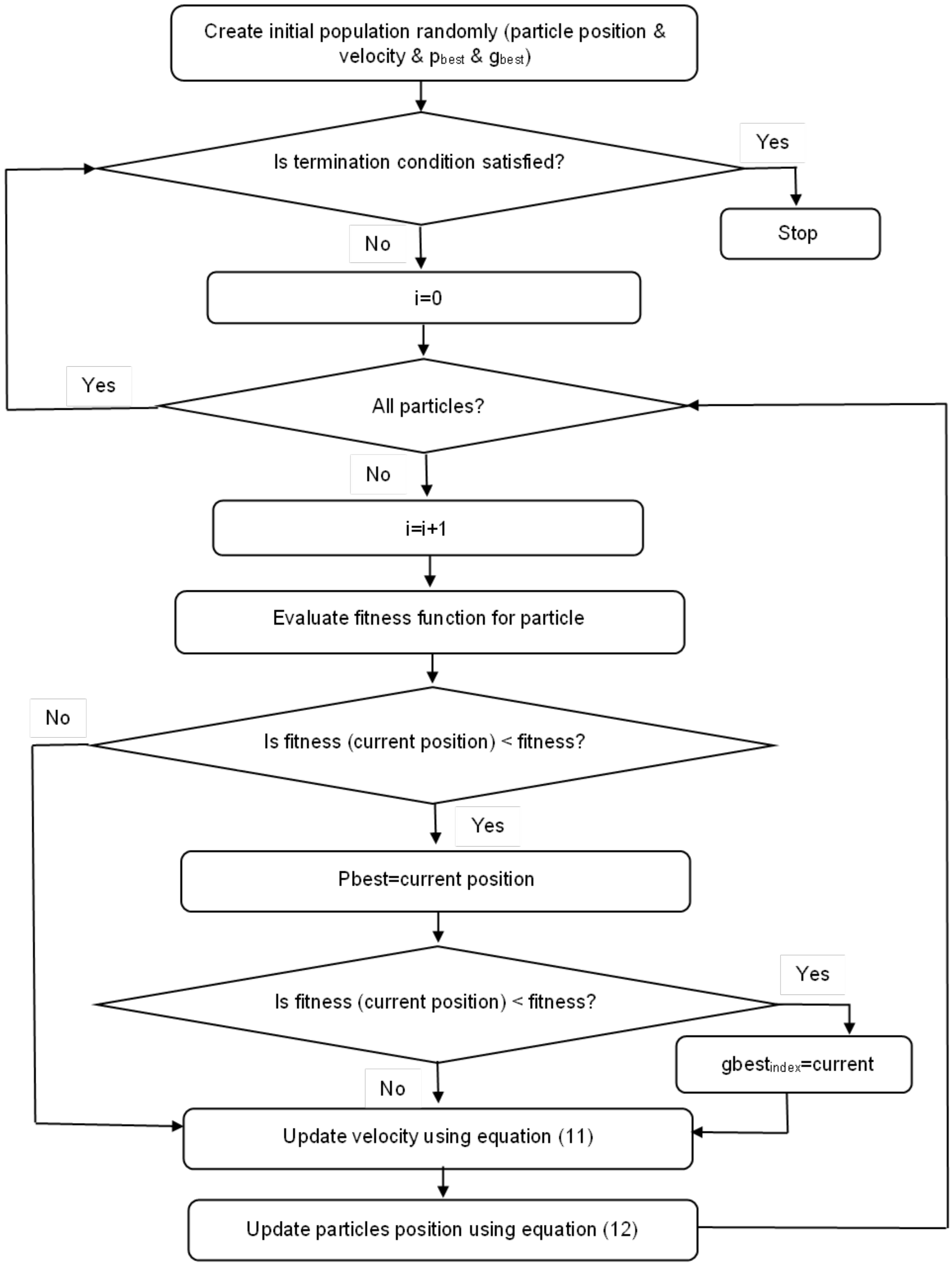

Source: Hefny and Azab (2010).

3.5 CHAOTIC PARTICLE SWARM OPTIMIZATION (CPSO) ALGORITHM

Particle Swarm Optimization (PSO) is an efficient, simple and fertile Optimization Algorithm. However, it suffers from premature convergence; moreover, the performance of PSO depends significantly on its parameter's settings. PSO attracts attention from researchers; they try to improve algorithm performance and avoid its weakness. Hefny and Azab (2010) propose a new methodology that uses chaotic agents to search in promising areas that are explored by PSO. The results proved that this method enhances the search efficiency significantly and improve the search quality.

3.5.1 Chaos behavior

Chaos in the dictionary means "a state of complete disorder and confusion". In science, there is no standard definition of chaos. But it is widely accepted that chaos is a "phenomenon that has deterministic underlying rules behind irregular appearances", which can be called "order in disorder" in Gries and Schneider (2008).

Chaos is deterministic and it can be generated using fixed rules or equations. In chaos, the future is completely determined by the past. However, actually, a very small change can lead to a very different result, which is called: "Butterfly effect". As for example, the “logistic equation” which is one of the most famous chaos equations, is given in (13):

$$X_{t+1} = \mu X_t(1 - X_t) \qquad (13)$$

The most common characteristics of chaos are in Gries and Schneider (2008):

1- Deterministic: the system follows deterministic rule.
2- Nonlinear: The underlying rules are nonlinear.
3- Irregular: The behaviour of the system shows sustained irregularity.
4- Sensitive to initial conditions means small changes in the initial state of chaotic systems can lead to a great change. This is called "Butterfly Effect"; perturbation of a butterfly lapping its wings can affect whether sunny or cloudy skies will dominate days later.

A chaotic motion can traverse every state in a certain search region, while every state is visited only once. Chaos search has a very special ability to avoid being trapped in local optima. However, chaotic motion often needs a large number of iterations to reach global optima and it is not effective in large searching space (SONG *et al.*, 2007).

3.6 PSO AND CHAOS

PSO can converge quickly to a good solution. In fact, the chaotic behaviour enables the searching particles to get very close to the global optima. However, it can easily trap in a local optimum. On the other hand, Chaos search can without difficulty escape from suboptimal solution. However, Chaos search need a long time to reach a global solution. The CPSO algorithm is shown as follows (LIU *et al.*, 2005):

- *Step 1* – Initialization as standard PSO.
- *Step 2* – Repeat until a stopping criterion is satisfied.
- *Step 3* – Update particle velocity using (11).
- *Step 4* – Update particle position using (12).
- *Step 5* – Evaluate performance of particle (using fitness function).
- *Step 6* – If current position is less than best position, let X_{pbest} be equal to current position.
- *Step 7* – If current position is less than gbest, let gbest be equal to current particle index.
- *Step 8* – Keep the top $\frac{n}{5}$ particles.
- *Step 9* – Perform chaotic local search (CLS) for global best particle.
- *Step 10* – Mapping decision variables X_i into chaotic variables cX_i using (14).

$$cX_i = \frac{X_i - X_{min}}{X_{max} - X_{min}} \quad (14)$$

- *Step 11* – Determine chaotic variable in next iteration using (13).

$$cX_i(t+1) = \mu cX_t\big(1 - cX_i(t)\big) \quad (15)$$

- *Step 12* – Convert chaotic variables cX_i into decision variables X_i using (16).

$$X_i = X_{min} + cX_i(X_{max} - X_{min}) \tag{16}$$

- *Step 13* – Evaluate the new solution.
- *Step 14* – If the new solution is better than already found gbest or maximum iteration number is reached exit chaotic local search; otherwise go to step 2.
- *Step 15* – Decrease search space using (17) and (18).

$$X_{min} = max\left(X_{min}, X_{gbest} - rand \times (X_{min} - X_{max})\right) \tag{17}$$

$$X_{max} = min\left(X_{max}, X_{gbest} - rand \times (X_{min} - X_{max})\right) \tag{18}$$

Where $rand \in [0,1]$ and X_{gbest} is the position of the global best particle.

- *Step 16* – Randomly generate $\frac{4n}{5}$ new particles within decreased search space and evaluate them.
- *Step 17* – Construct the new population consisting of the $\frac{4n}{5}$ new particles and the old top $\frac{n}{5}$ particles in which the best particle is replaced by the result of CLS.
- *Step 18* – Let $k \leftarrow k + 1$ and go back to step 2.

3.7 IMPLEMENTATION OF THE CPSO FOR DISTRIBUTION NETWORK RECONFIGURATION CONSIDERING THE ALLOCATION OF DG

3.7.1 Initialization

The element i, X_i, of the population represents a solution vector with three parts. The numbers of the open switches (SW_i) is considered the first part considering the fundamental loop lists. The numbers of determined buses ($x_{DG,i}$) to which the DGs are connected are represented in the second part. The third part shows the capacity of DGs ($P_{DG,i}$). The number of elements in the first and second parts are integer values. Therefore, these parts form the structure to specify the open switches, the locations of DGs, and the capacities of DGs, as shown in (19).

$$X_i = [SW_1, \dots, SW_{N_{Tie}}, x_{DG,1}, \dots, x_{DG,N_{DG}}, P_{DG,1}, \dots, P_{DG,N_{DG}}] \quad (19)$$

In the CPSO, the solutions are randomly generated within the specified ranges. Thus, the variables of the initial solution proposals are generated as shown in (20)–(22).

$$SW_i = \text{round}\left[SW_{min,i} + \text{rand}(0,1) \cdot \left(SW_{max,i} - SW_{min,i}\right)\right] \quad (20)$$
$$i = 1, \dots, N_{Tie}$$

$$x_{DG,i} = \text{round}\left[x_{DGmin,i} + \text{rand}(0,1) \cdot \left(x_{DGmax,i} - x_{DGmin,i}\right)\right] \quad (21)$$
$$i = 1, \dots, N_{DG}$$

$$P_{DG,i} = P_{DGmin,i} + \text{rand}(0,1) \cdot \left(P_{DGmax,i} - P_{DGmin,i}\right) \quad (22)$$
$$i = 1, \dots, N_{DG}$$

Where $SW_{min,i}$ and $SW_{max,i}$ equals to the i^{th} fundamental loop vector length. SW_i is the sequential number of each switch in the i^{th} fundamental loop. N_{Tie} and N_{DG} are the number of open switches and the number of DGs, respectively.

3.7.2 Fundamental loop

The proposal of fundamental loops (FLs) allows for building an array of matrix forms, and the branches belonging to each fundamental loop appear in each row of the matrix. The number of rows of this matrix is equal to the number of fundamental loops, i.e., it is equal to the number of open branches to generate a radial topology (see illustrative examples presented in Table 1 according to Figure 10). This matrix allows the generation of radial topologies simply and efficiently.

Table 1 – Fundamental loops of the IEEE 33-bus network

FL	Switches	Length of the FL
1	2, 3, 4, 5, 6, 7, 18, 19, 20, 33	10
2	9, 10, 11, 12, 13, 14, 34	7
3	8, 9, 10, 11, 21, 33, 35	7
4	6, 7, 8, 9, 10, 11, 12, 13, 14, 15, 16, 17, 25, 26, 27, 28, 29, 30, 31, 32, 36	21
5	3, 4, 5, 22, 23, 24, 25, 26, 27, 28, 37	11

Source: Author’s elaboration.

3.7.3 Radiality constraint checking

The radial topology of the distribution network must be checked after determining the FLs. The radial structure of the network configuration is checked by the incidence matrix A. First, the reference bus and the tie-switches, which in matrix A include the first column and rows related to those switches, respectively, are removed. The network configuration is a radial topology when the rest of the matrix A is square, and its determinant is 1 or –1.

3.7.4 Overall procedure

The distribution network reconfiguration with the simultaneous allocation of DGs is implemented using the CPSO as follows:

- *Step 1* – Initialize population size (N_p) and the maximum number of iterations ($itmax$).
- *Step 2* – Specify the fundamental loops of the distribution network (see Section 3.7.2). Determine the lower and upper limits for each loop.
- *Step 3* – Check the radiality condition of the solution (see Section 3.7.3) and if it is not radial, find another solution until the radial condition is met.
- *Step 4* – Calculate the fitness function (9) by performing power flow calculations and determine the minimum power losses. Start the iteration counter from $t \leftarrow 1$.
- *Step 5* – Update the position of the particles using (11)–(13).
- *Step 6* – Check the radiality condition (see Section 3.7.3) and if the solution is not radial, find another solution until the radial condition is met, determine the fitness function by performing power flow calculations according to (9), and determine the minimum power losses.
- *Step 7* – If the obtained fitness function is lower, replace the best solution with the previous best solution.
- *Step 8* – Let $t \leftarrow t + 1$. If $t < itmax$, increase the number of iterations and return to Step 5. If $t \geq itmax$, print the results and stop the algorithm.

The flowchart of the CPSO for the distribution network reconfiguration problem with simultaneous DG allocation is illustrated in Figure 8.

Figure 8 – Flowchart of the proposed CPSO for distribution network reconfiguration with simultaneous allocation of DGs

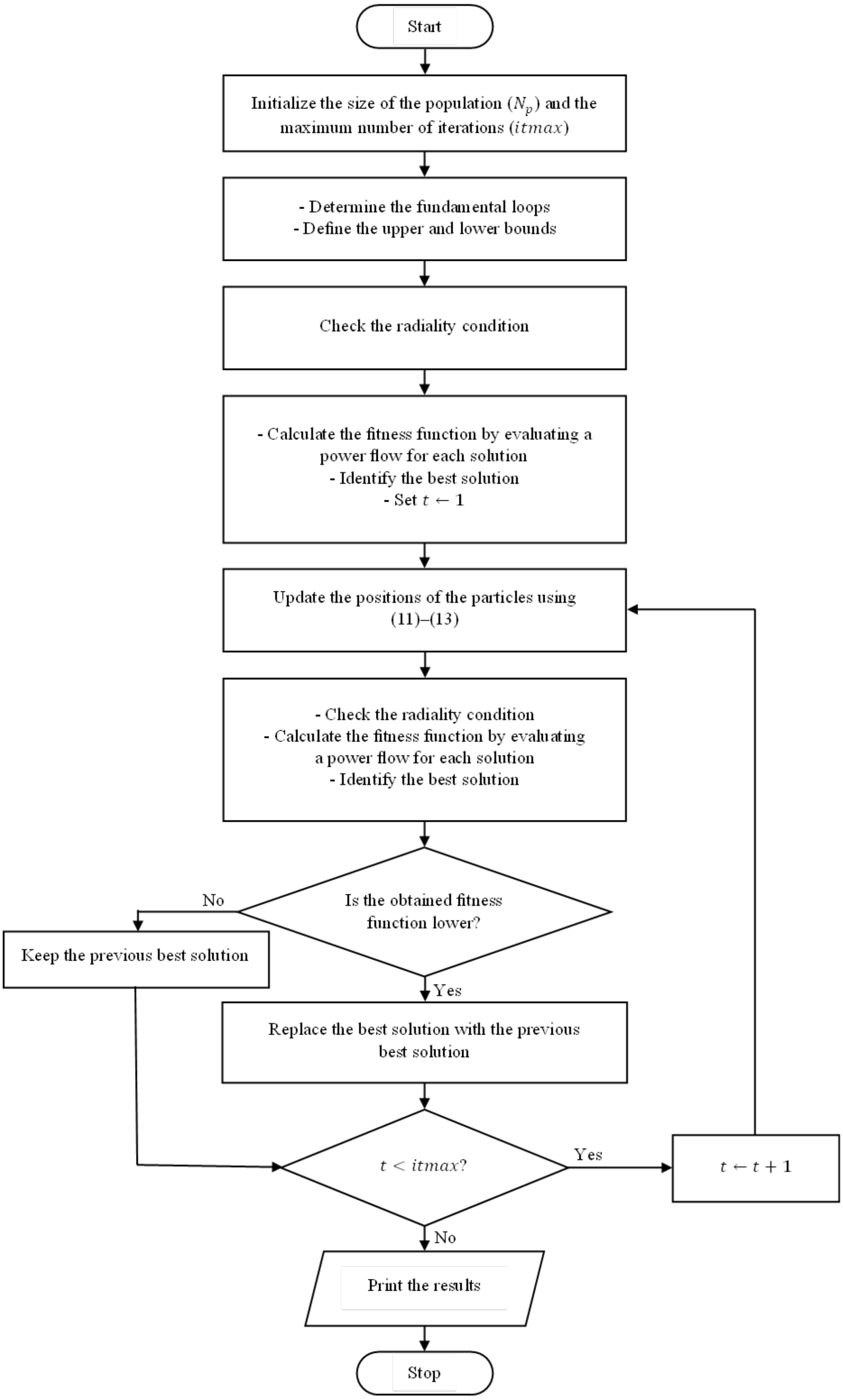

Source: Author's elaboration.

3.8 MODELING

The problem must be transformed into a mathematical form. The objective of this thesis is to reconfiguration distribution grid by considering distributed generations and reducing the power loss and improving the voltage profile. The variables that need to be achieved with the help of the optimization problem are:

1- Switches to be opened and closed
2- Siting and sizing of DGs

To model the reconfiguration problem, the following assumptions are considered:

1- The grid is in a steady state and error-free.
2- All grid switches can be remotely controlled.
3- The amount of load per period is constant.

- Constraints:

The constraints are as follows:

i. The obtained voltage magnitudes must not exceed the permissible limits, as presented in (23).

$$V_{min} \leq V_i \leq V_{max}; \quad i = 1, 2, \dots, N_{bus} \qquad (23)$$

Where V_i is the voltage magnitude at bus i; V_{min} is the minimum acceptable bus voltage magnitude; V_{max} is the maximum acceptable bus voltage magnitude; and N_{bus} is the total number of buses in the network.

ii. The distribution network must maintain its radial topology and, after reconfiguration, must supply all loads.

iii. The amount of power produced by the DGs must be within the permissible limits, as shown in (24).

$$P_{DGmin,i} \leq P_{DG,i} \leq P_{DGmax,i}; \quad i = 1, 2, \dots, N_{DG} \qquad (24)$$

Where $P_{DG,i}$ is the active power output of the DG unit at node i; $P_{DGmin,i}$ is the minimum size of the DG unit at node i; $P_{DGmax,i}$ is the maximum size of the DG unit at node i; and N_{DG} is the number of DG units that can be installed in the system.

iv. The nonlinear equations that represent Kirchhoff's current and voltage laws, i.e., the equations of the power flow problem. The power flow analysis calculates the power losses on the network branches for each topology with DGs.

The optimal reconfiguration of radial grid is done with the objective of decreasing power loss and improving the voltage profile by meta-heuristic algorithm such as chaotic particle swarm optimization (CPSO) algorithm using MATLAB m-file. The main objective of this function is to define two objective functions to renew the system reconfiguration by regarding distributed generations (DGs). The load flow that is implemented in this research, is the Forward-Backward Sweep method. Also, we test on IEEE 33-bus, IEEE 69-bus, 136-bus, and 415-bus systems.

Figure 9 depicts the schematic representation of the proposed method.

Figure 9 – Schematic representation of proposed method

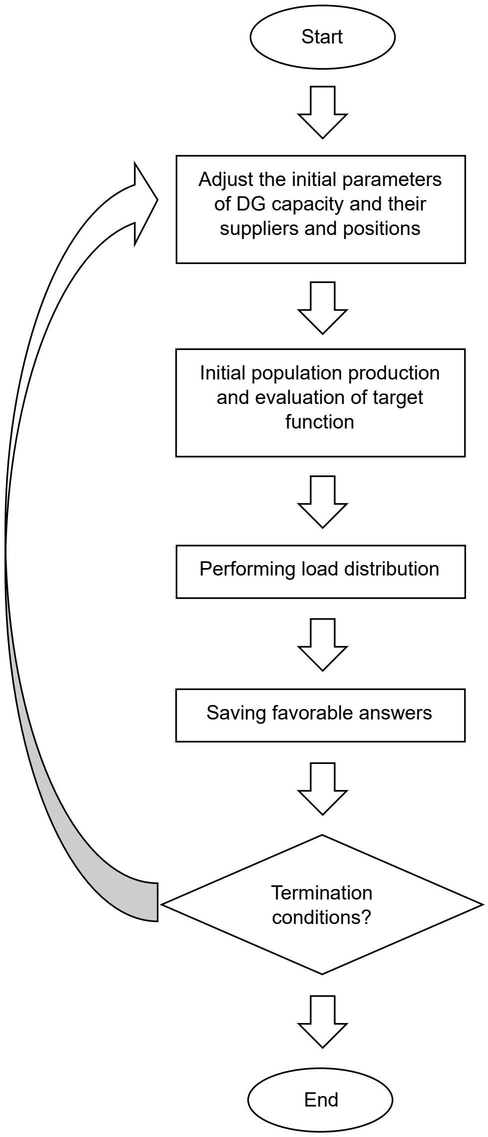

Source: Author's elaboration.

4 CASE STUDY

Applying the CPSO on 33, 69, 136, and 415-bus systems for reconfiguration and distributed generation (DG) problem using MATLAB R2018a executed on processor core i7-8565U @1.80 GHz with 16 GB RAM. Forward-Backward Sweep power flow algorithm is used in power flow analysis during reconfiguration process and optimal placement and sizing of DGs to get power loss and minimum voltage of the system. The objective functions are to find the optimal placement and sizing of DGs, minimize the power loss, and improve the voltage profile. The population sizes for the 33-bus, 69-bus, 136-bus, and 415-bus systems were 50, 50, 100, and 100, respectively and the maximum number of iterations for the 33-bus, 69-bus, 136-bus, and 415-bus networks were equal to 300, 400, 1000, and 500, respectively. The C_1 and C_2 are constants that equal to 2. The W is calculated by equation (25). The data of four test systems are available in Appendix A, B, C, and D, respectively.

$$W = W_{max} - \frac{W_{max} - W_{min}}{iter_{max}} \times k \qquad k = 1,2, \dots , iter_{max} \tag{25}$$

Where W is inertia weight; W_{max} is equal to 0.9; W_{min} is equal to 0.4; $iter_{max}$ is the maximum number of iterations; and k is iteration counter.

In this research, four scenarios were considered, which are:

1- Base case (without distribution network reconfiguration and DGs).
2- Distribution network reconfiguration using chaotic particle swarm optimization (CPSO) algorithm.
3- The optimal location and size of 3 DGs after distribution network reconfiguration (according to the result of Case 2) using chaotic particle swarm optimization (CPSO) algorithm.
4- The simultaneous distribution network reconfiguration and the optimal location and size of 3 DGs using chaotic particle swarm optimization (CPSO) algorithm.

In addition, the voltage magnitudes at buses were limited as presented in (26).

$$0.93 \le V_i \le 1.05; \qquad i = 1,2, \dots , N_{bus} \tag{26}$$

Where the limits are in p.u.; V_i is the value of the voltage magnitude at bus i; and N_{bus} is the total number of buses.

For the optimal location and size of DGs, three DGs were considered, and the capacity range of each DG are shown in (27).

$$10 \leq P_{DG,i} \leq \frac{P_D}{6}; \qquad i = 1,2,3 \tag{27}$$

Where $P_{DG,i}$ is the active power size of the i^{th} DG (kW) and P_D is the total active power demand of the system (kW).

4.1 33-BUS TEST SYSTEM

The 33-bus system is presented in Soliman *et al*. (2020). It has 32 load buses, one substation bus and 37 feeders. The voltage at the substation bus is 12.66 kV and the base power of the system is 100 MVA. The total active and reactive power demands are 3715 kW and 2300 kVAr, respectively. The maximum size of each DG unit is 619.17 kW.

Figure 10 illustrates the 33-bus system with five tie switches 33, 34, 35, 36 and 37 that are initially open and illustrated by dashed lines. The complete data of this system are presented in Appendix A.

Figure 10 – Schematic of the studied network of 33-bus

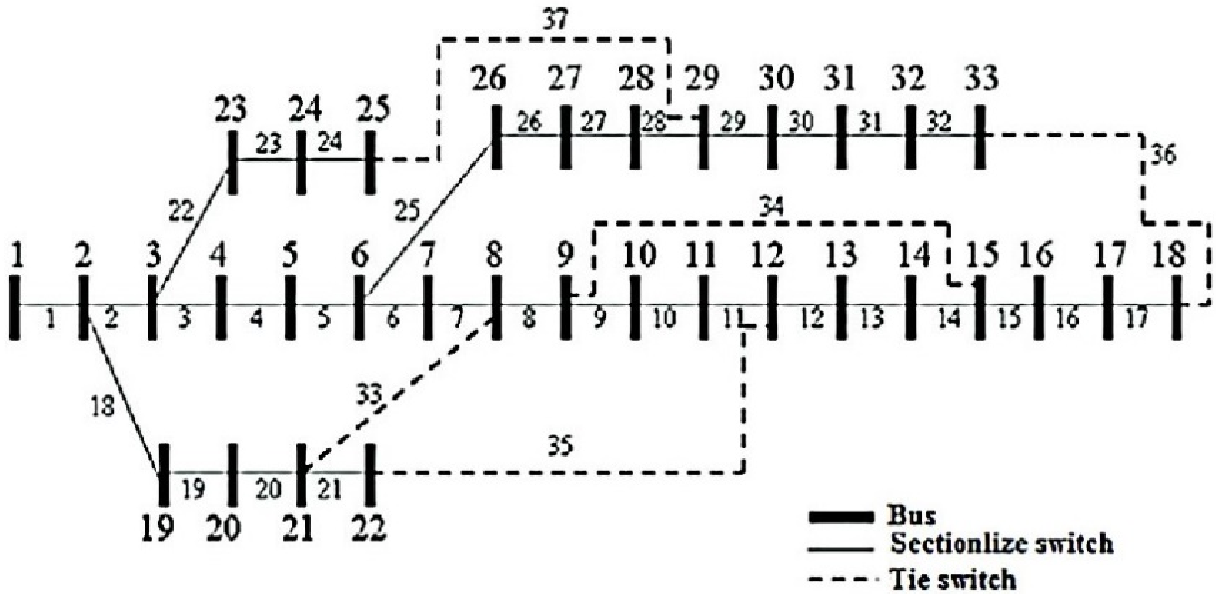

Source: Soliman *et al*. (2020).

4.1.1 Distribution network reconfiguration using chaotic particle swarm optimization (CPSO) algorithm

Figure 11 illustrates voltage profile variations before and after network reconfiguration on a 33-bus system. As shown in Figure 11 and Table 2, the power loss was 202.68 kW and minimum voltage was 0.9131 per-unit in base case. The power loss was reduced to 141.63 kW, thus having a reduction of 30.12 % compared to the base case. The minimum voltage was improved to 0.9413 per-unit after network reconfiguration. The tie switches which were opened after network reconfiguration, were 7, 11, 14, 28, and 32.

Figure 11 – Voltage profile variations before and after network reconfiguration

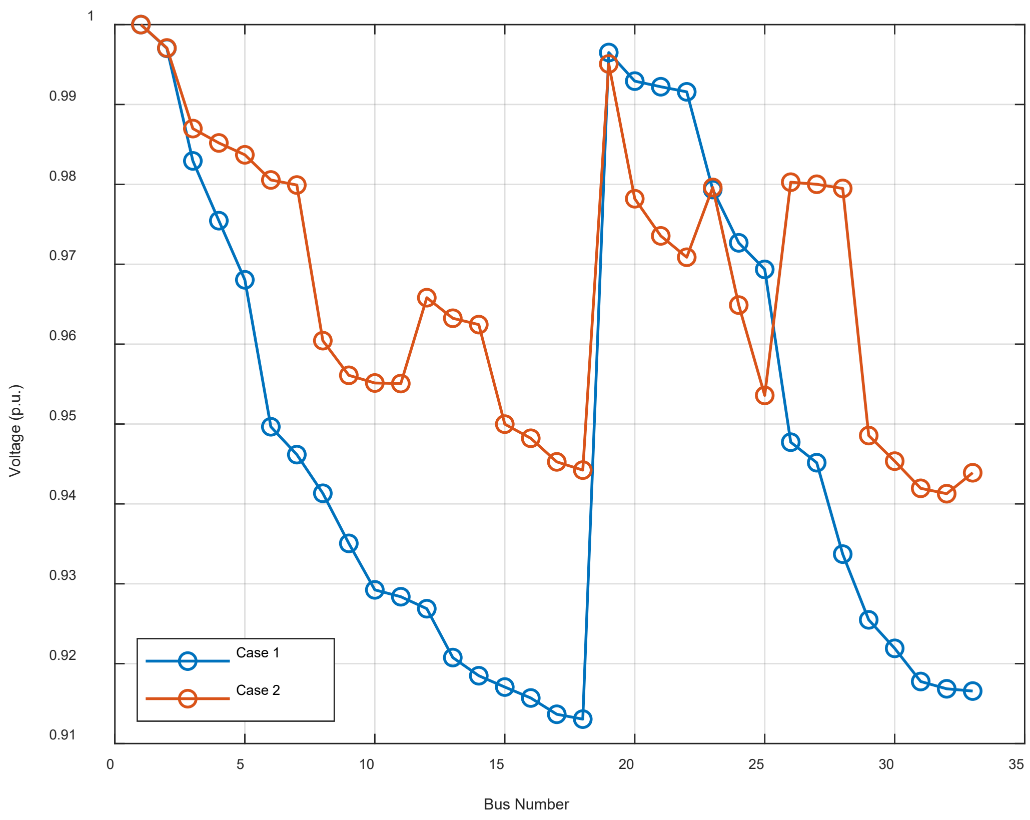

Source: Author's elaboration.

Table 2 – Simulation results before and after network reconfiguration using CPSO

Simulation results of 33-bus distribution network		
	Base Case	Network Reconfiguration
Active power loss:	202.68 kW	141.63 kW
Reactive power loss:	135.14 kVAr	106.15 kVAr
Active power loss reduction:	–	30.12 %
Tie switches:	33, 34, 35, 36, 37	7, 11, 14, 28, 32
Minimum voltage/(Bus):	0.9131 p.u./(18)	0.9413 p.u./(32)

Source: Author's elaboration.

Figure 12 illustrates the convergence of the CPSO after network reconfiguration along the iterations on a 33-bus system. In Figure 12, the fitness (optimal solution) was found in about 23 iterations.

Figure 12 – Convergence of CPSO after network reconfiguration

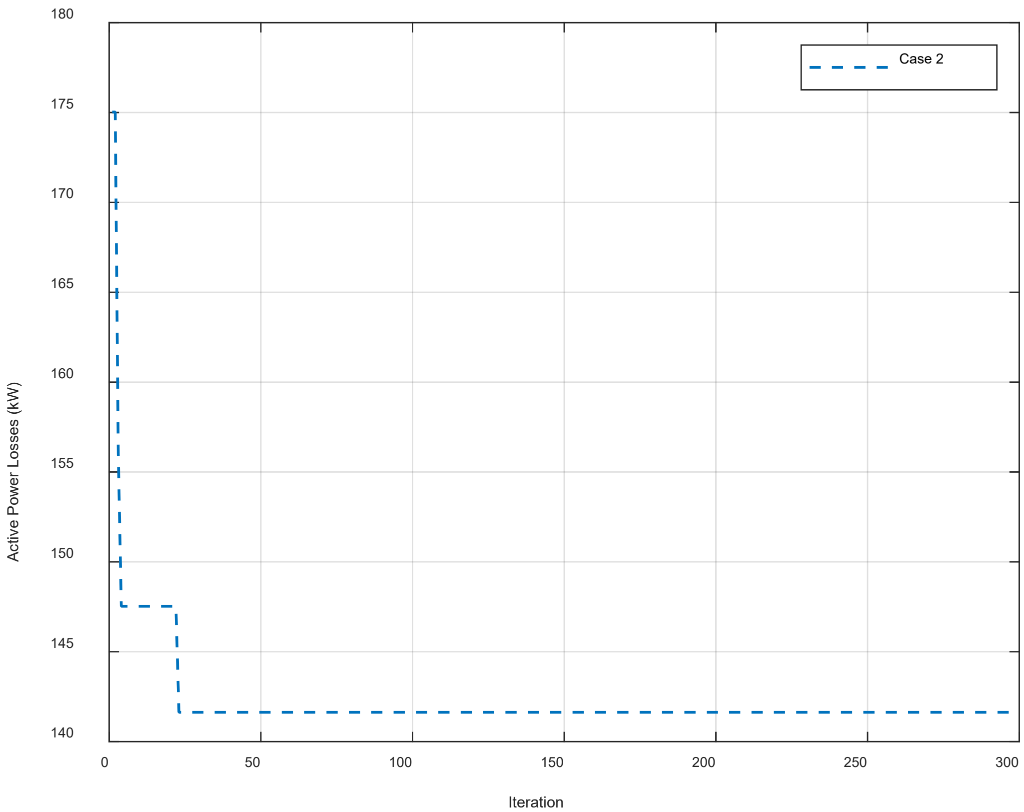

Source: Author's elaboration.

4.1.2 The optimal location and size of 3 distributed generations (DGs) after distribution network reconfiguration (according to the result of Case 2) using chaotic particle swarm optimization (CPSO) algorithm

The tie switches were determined after network reconfiguration in scenario 2 and the opened tie switches were 7, 11, 14, 28, and 32. We assumed that these switches were open and then the optimal location and size of DG units were specified by CPSO algorithm. We installed 3 DG units in this scenario after network reconfiguration.

Figure 13 illustrates voltage profile variations before and after network reconfiguration and installing 3 DG units on a 33-bus system. As shown in Figure 13 and Table 3, the power loss was 202.68 kW and minimum voltage was 0.9131 per-unit in base case. The power loss was reduced to 40.68 kW, thus having a reduction of 79.93 % compared to the base case. The minimum voltage was improved to 0.9737 per-unit after network reconfiguration and installing 3 DG units. Also, the optimal location and size of DGs were obtained by the CPSO algorithm and 3 DG units with the capacity of 487.0, 460.0, and 617.0 kW were allocated in buses 18, 25, and 32.

Figure 13 – Voltage profile variations before and after network reconfiguration and installing 3 DG units

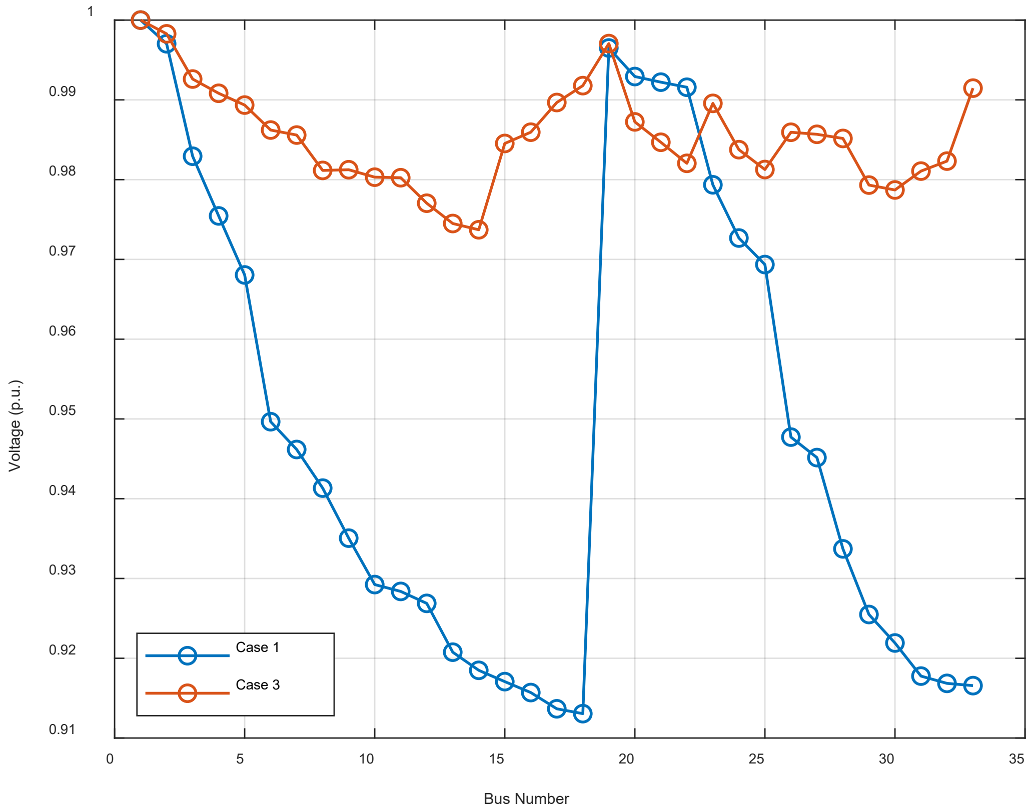

Source: Author's elaboration.

Table 3 – Simulation results before and after network reconfiguration and installing 3 DG units using CPSO

Simulation results of 33-bus distribution network		
	Base Case	3 DGs After Network Reconfiguration
Active power loss:	202.68 kW	40.68 kW
Reactive power loss:	135.14 kVAr	30.70 kVAr
Active power loss reduction:	_	79.93 %
Tie switches:	33, 34, 35, 36, 37	7, 11, 14, 28, 32
Optimal DG location	_	18, 25, 32
Optimal DG size P	_	487.0, 460.0, 617.0 kW
Minimum voltage/(Bus):	0.9131 p.u./(18)	0.9737 p.u./(14)

Source: Author's elaboration.

Figure 14 illustrates the convergence of the CPSO after network reconfiguration and installing 3 DG units along the iterations on a 33-bus system. In Figure 14, the fitness (optimal solution) was found in 50 iterations.

Figure 14 – Convergence of CPSO after network reconfiguration and installing 3 DG units

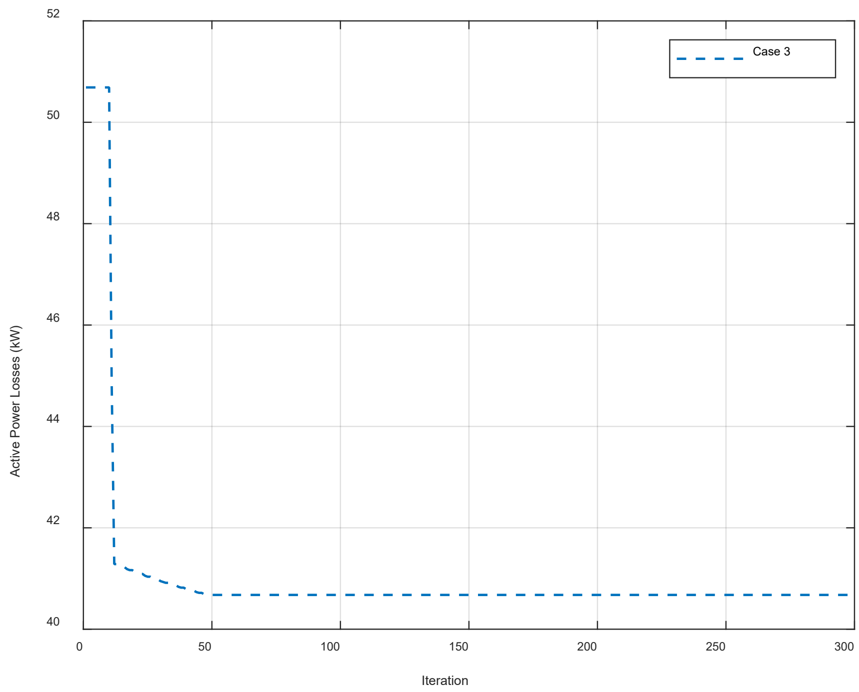

Source: Author's elaboration.

4.1.3 The simultaneous distribution network reconfiguration and the optimal location and size of 3 distributed generations (DGs) using chaotic particle swarm optimization (CPSO) algorithm

Figure 15 illustrates voltage profile variations before and after simultaneous network reconfiguration and installing 3 DG units on a 33-bus system. As shown in Figure 15 and Table 4, the power loss was 202.68 kW and minimum voltage was 0.9131 per-unit in base case. The power loss was reduced to 58.46 kW, thus having a reduction of 71.16 % compared to the base case. The minimum voltage was improved to 0.9628 per-unit after simultaneous network reconfiguration and installing 3 DG units. Also, the optimal location and size of DGs were obtained by the CPSO algorithm and 3 DG units with the capacity of 615.0, 342.0, and 445.0 kW were allocated in buses 15, 22, and 29. The tie switches which were opened after simultaneous network reconfiguration and installing 3 DG units, were 6, 8, 9, 27, and 31.

Figure 15 – Voltage profile variations before and after simultaneous network reconfiguration and installing 3 DG units

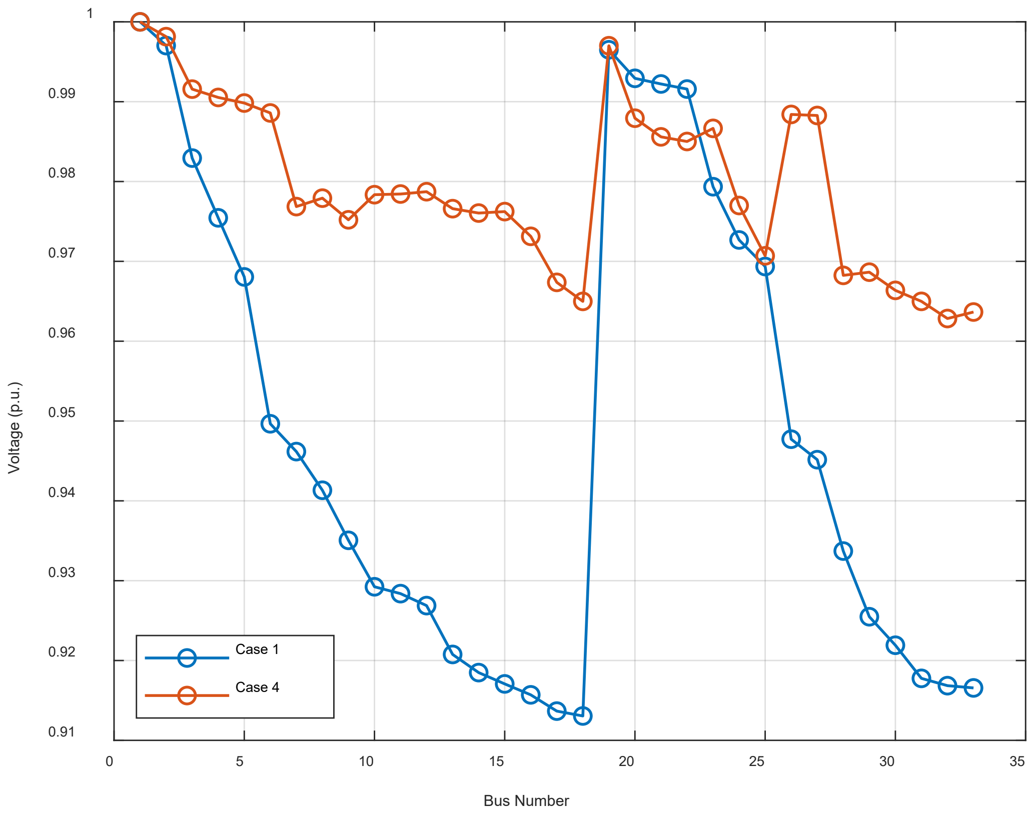

Source: Author's elaboration.

Table 4 – Simulation results before and after simultaneous network reconfiguration and installing 3 DG units using CPSO

Simulation results of 33-bus distribution network		
	Base Case	Simultaneous network reconfiguration and 3 DGs
Active power loss:	202.68 kW	58.46 kW
Reactive power loss:	135.14 kVAr	43.48 kVAr
Active power loss reduction:	_	71.16 %
Tie switches:	33, 34, 35, 36, 37	6, 8, 9, 27, 31
Optimal DG location	_	15, 22, 29
Optimal DG size P	_	615.0, 342.0, 445.0 kW
Minimum voltage/(Bus):	0.9131 p.u./(18)	0.9628 p.u./(32)

Source: Author's elaboration.

Figure 16 illustrates the convergence of the CPSO after simultaneous network reconfiguration and installing 3 DG units along the iterations on a 33-bus system. In Figure 16, the fitness (optimal solution) was found in about 75 iterations.

Figure 16 – Convergence of CPSO after simultaneous network reconfiguration and installing 3 DG units

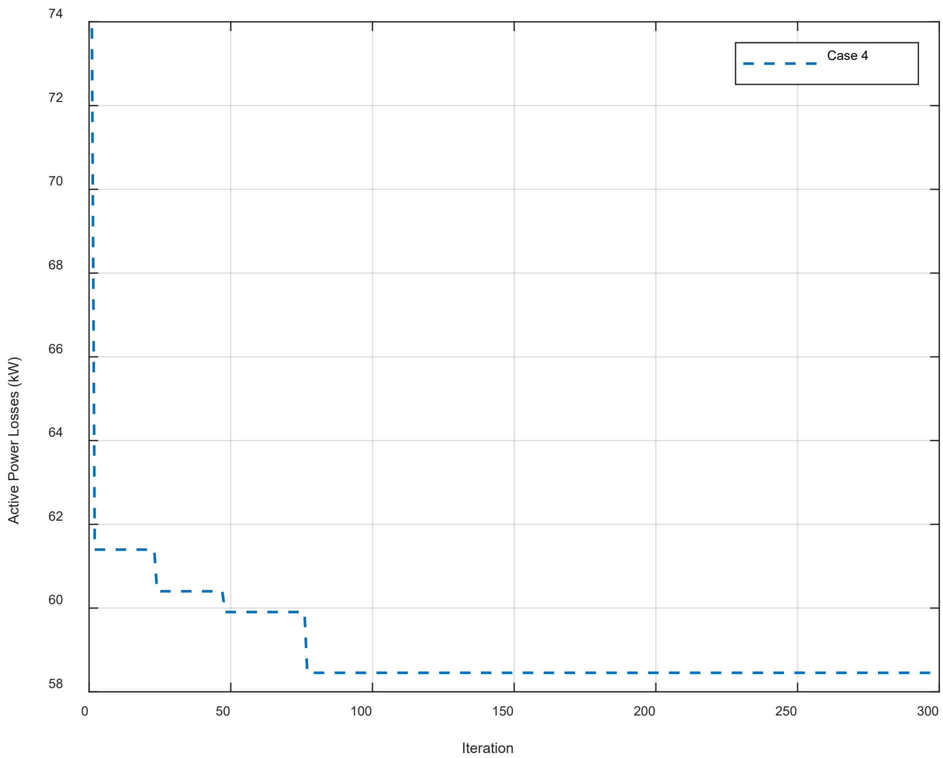

Source: Author's elaboration.

As shown in Figure 17, a comparison was made between 4 scenarios in voltage profile variations on a 33-bus system. A comparison of convergence between 3 scenarios in a 33-bus system is shown in Figure 18. For comparing the performance of the CPSO method with other methods, adaptive cuckoo search algorithm (ACSA) in Nguyen *et al*. (2016), uniform voltage distribution-based constructive reconfiguration algorithm (UVDA) in Bayat *et al*. (2016), modified plant growth simulation algorithm (MPGSA) in Rajaram *et al*. (2015), and stochastic fractal search (SFS) in Tran *et al*. (2020) methods are considered (see Table 5). As you can see in Table 5, the power loss and minimum voltage of Cases 2 and 4 in CPSO and other methods are almost the same. In Case 3, CPSO performed much better than other methods in terms of power loss.

Figure 17 – Comparison of voltage profile variations in 4 scenarios

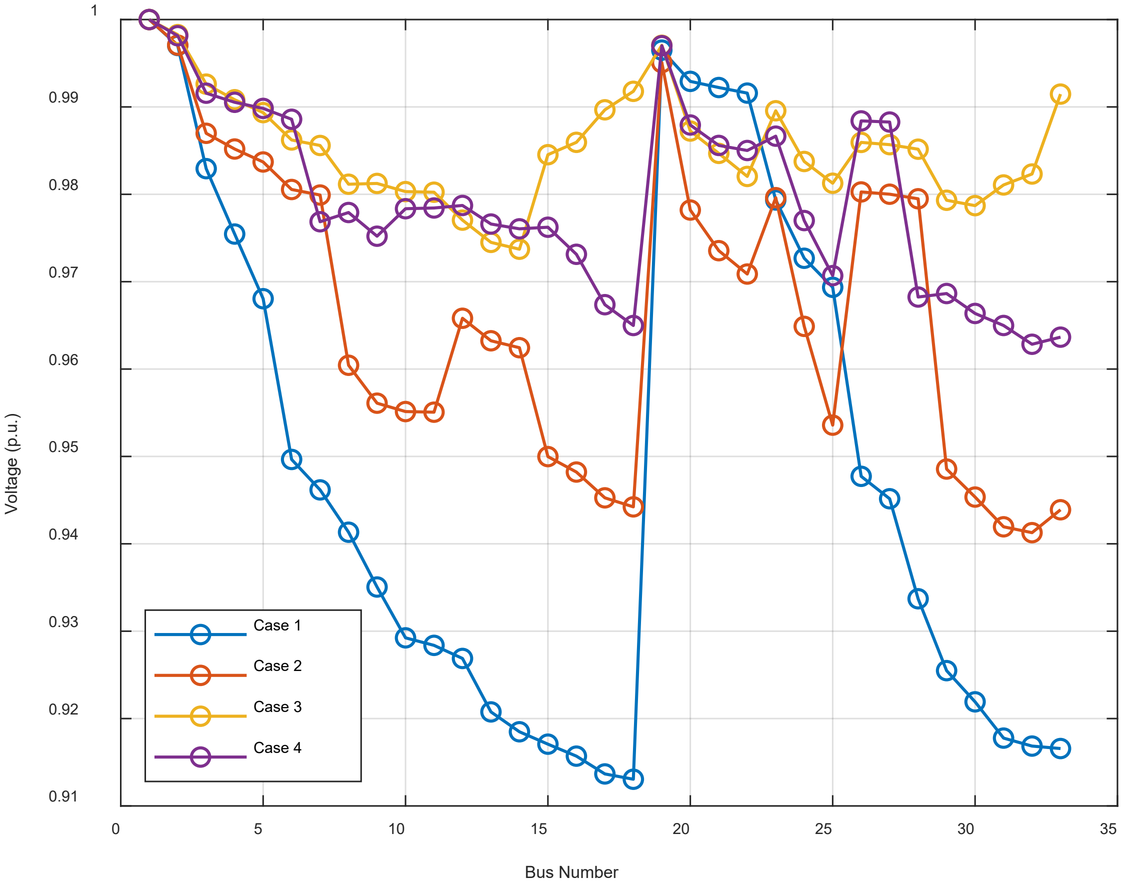

Source: Author's elaboration.

Figure 18 – Comparison of convergence in 3 scenarios

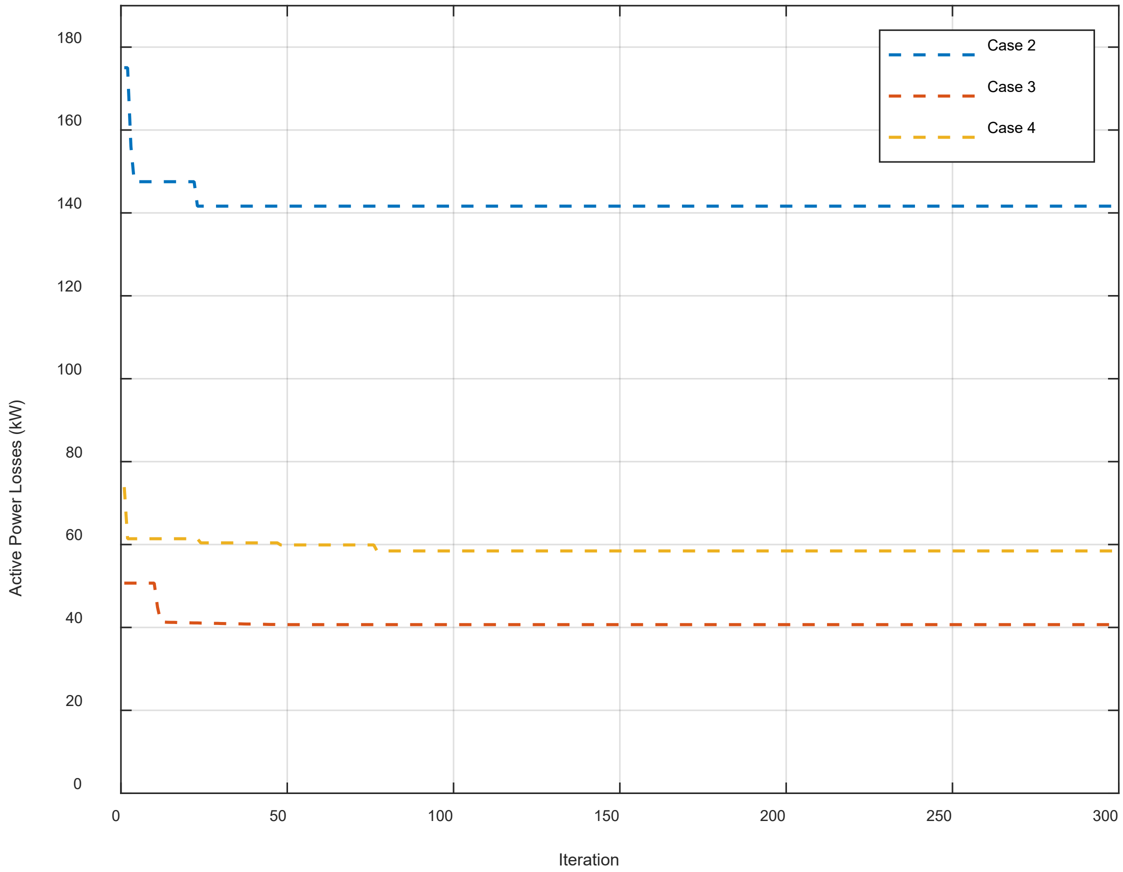

Source: Author's elaboration.

Table 5 – Summary of the results for the 33-bus network

Case	Item	ACSA (NGUYEN *et al.*, 2016)	UVDA (BAYAT *et al.*, 2016)	MPGSA (RAJARAM *et al.*, 2015)	SFS (TRAN *et al.*, 2020)	CPSO
1	Tie switches	–	–	–	–	33-34-35-36-37
	P_L (kW)	–	–	–	–	202.68
	Q_L (kVAr)	–	–	–	–	135.14
	$V_{\min}$ (p.u.)	–	–	–	–	0.9131
	Time (s)	–	–	–	–	1.1
2	Tie switches	7-9-14-28-32	7-9-14-32-37	7-9-14-32-37	7-9-14-32-37	7-11-14-28-32
	P_L (kW)	139.98	139.55	139.55	139.55	141.63
	Q_L (kVAr)	–	–	–	–	106.15

	P_L **reduction (%)**	30.93	31.15	31.15	31.15	30.12
	$V_{\min}$ **(p.u.)**	0.9413	0.9378	0.9378	0.9378	0.9413
	Time (s)	–	–	–	–	9356.5
3	**Tie switches**	7-9-14-28-32	7-9-14-32-37	7-9-14-32-37	7-9-14-32-37	7-11-14-28-32
	P_{DG} **(kW)/(Bus)**	539.7/(12) 504.5/(16) 1753.6/(29)	526.0/(12) 592.0/(15) 1125.0/(30)	246.9/(31) 179.5/(32) 664.5/(33)	931.7/(8) 1068.2/(24) 950.3/(30)	487.0/(18) 460.0/(25) 617.0/(32)
	P_L **(kW)**	58.79	66.60	92.87	58.88	40.68
	Q_L **(kVAr)**	–	–	–	–	30.70
	P_L **reduction (%)**	71.00	67.14	54.17	70.95	79.93
	$V_{\min}$ **(p.u.)**	0.9802	0.9758	0.9482	0.9741	0.9737
	Time (s)	–	–	–	–	2803.6
4	**Tie switches**	11-28-31-33-34	–	–	7-9-14-27-30	6-8-9-27-31
	P_{DG} **(kW)/(Bus)**	964.6/(7) 896.8/(18) 1438.1/(25)	– – –	– – –	775.3/(22) 1285.8/(25) 735.6/(33)	615.0/(15) 342.0/(22) 445.0/(29)
	P_L **(kW)**	53.21	–	–	53.01	58.46
	Q_L **(kVAr)**	–	–	–	–	43.48
	P_L **reduction (%)**	73.75	–	–	73.85	71.16
	$V_{\min}$ **(p.u.)**	0.9806	–	–	0.9720	0.9628
	Time (s)	–	–	–	–	8805.3

Source: Author's elaboration.

4.2 69-BUS TEST SYSTEM

The 69-bus system is presented in Soliman *et al*. (2020). It has 68 load buses, one substation bus and 73 feeders. The voltage at the substation bus is 12.66 kV and the base power of the system is 100 MVA. The total active and reactive power demands are 3801.9 kW and 2694.1 kVAr, respectively. The maximum size of each DG unit is 633.7 kW.

Figure 19 illustrates the 69-bus system with five tie switches 69, 70, 71, 72 and 73 that are initially open and illustrated by dashed lines. The complete data of this system are presented in Appendix B.

Figure 19 – Schematic of the studied network of 69-bus

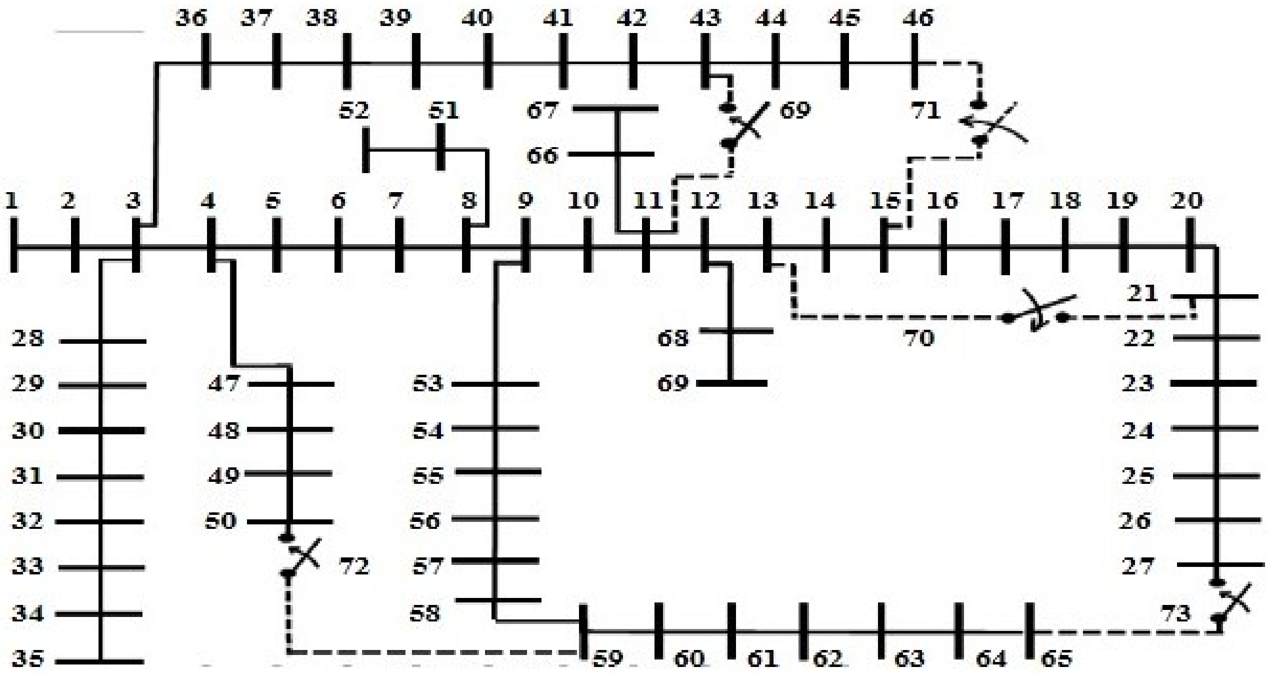

Source: Soliman *et al*. (2020).

4.2.1 Distribution network reconfiguration using chaotic particle swarm optimization (CPSO) algorithm

Figure 20 illustrates voltage profile variations before and after network reconfiguration on a 69-bus system. As shown in Figure 20 and Table 6, the power loss was 224.96 kW and minimum voltage was 0.9090 per-unit in base case. The power loss was reduced to 100.67 kW, thus having a reduction of 55.25 % compared to the base case. The minimum voltage was improved to 0.9413 per-unit after network reconfiguration. The tie switches which were opened after network reconfiguration, were 14, 58, 63, 69, and 70.

Figure 20 – Voltage profile variations before and after network reconfiguration

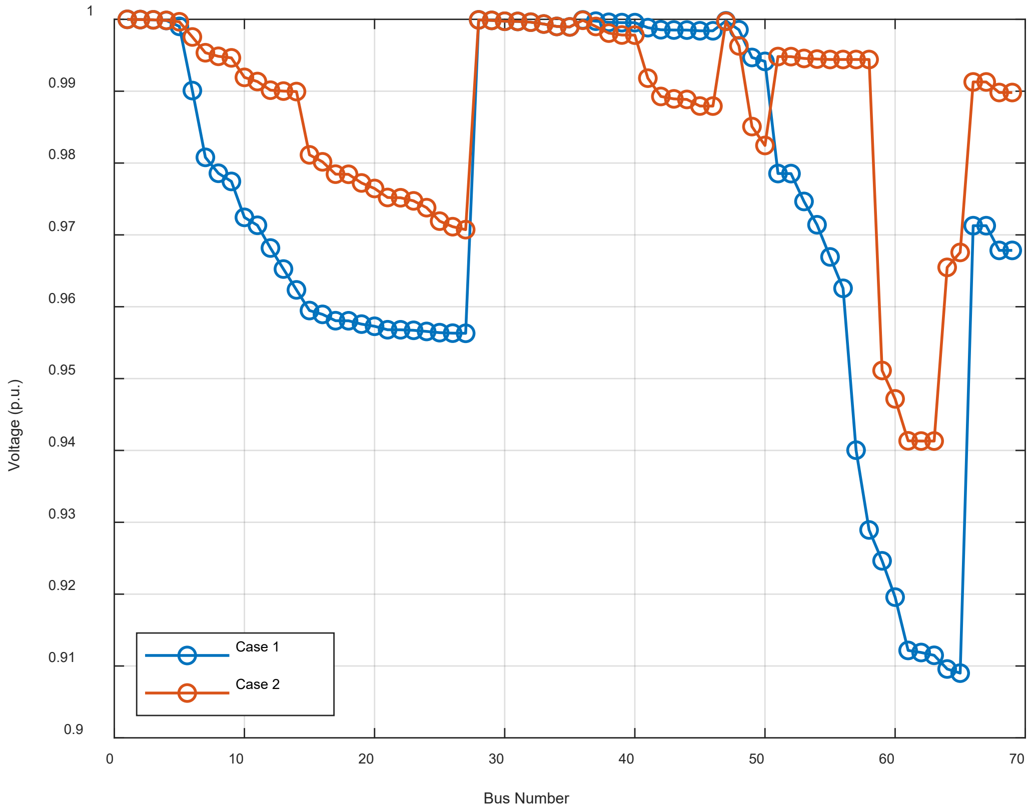

Source: Author's elaboration.

Table 6 – Simulation results before and after network reconfiguration using CPSO

Simulation results of 69-bus distribution network		
	Base Case	Network Reconfiguration
Active power loss:	224.96 kW	100.67 kW
Reactive power loss:	102.15 kVAr	116.78 kVAr
Active power loss reduction:	–	55.25 %
Tie switches:	69, 70, 71, 72, 73	14, 58, 63, 69, 70
Minimum voltage/(Bus):	0.9090 p.u./(65)	0.9413 p.u./(62, 63)

Source: Author's elaboration.

Figure 21 illustrates the convergence of the CPSO after network reconfiguration along the iterations on a 69-bus system. In Figure 21, the fitness (optimal solution) was found in about 240 iterations.

Figure 21 – Convergence of CPSO after network reconfiguration

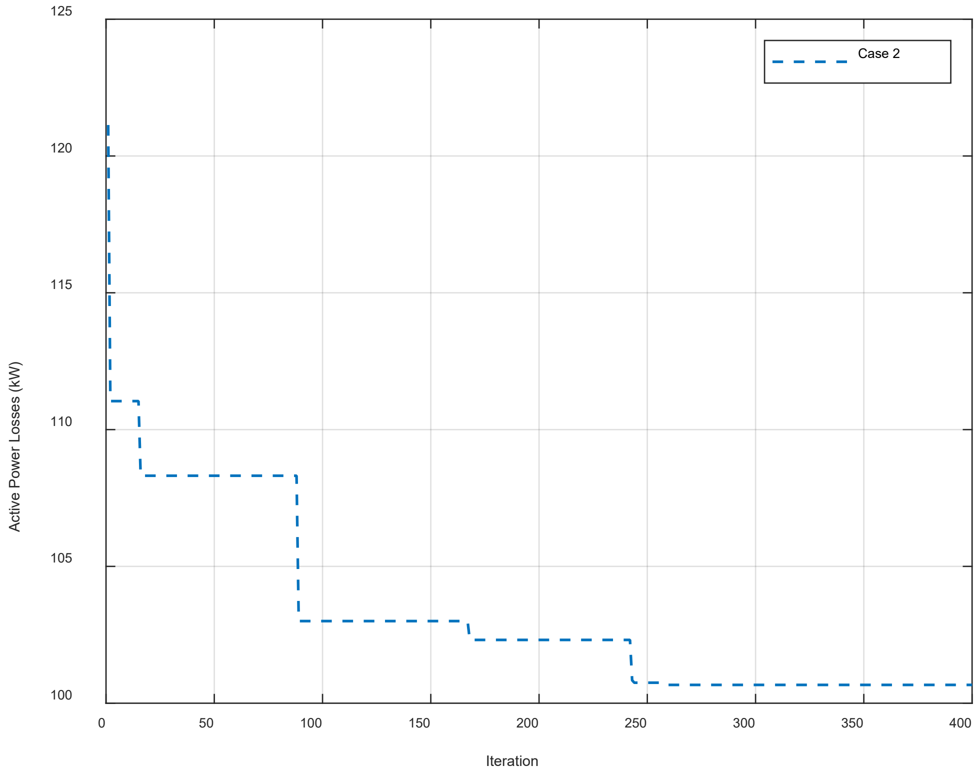

Source: Author's elaboration.

4.2.2 The optimal location and size of 3 distributed generations (DGs) after distribution network reconfiguration (according to the result of Case 2) using chaotic particle swarm optimization (CPSO) algorithm

The tie switches were determined after network reconfiguration in scenario 2 and the opened tie switches were 14, 58, 63, 69, and 70. We assumed that these switches were open and then the optimal location and size of DG units were specified by CPSO algorithm. We installed 3 DG units in this scenario after network reconfiguration.

Figure 22 illustrates voltage profile variations before and after network reconfiguration and installing 3 DG units on a 69-bus system. As shown in Figure 22 and Table 7, the power loss was 224.96 kW and minimum voltage was 0.9090 per-unit in base case. The power loss was reduced to 42.27 kW, thus having a reduction of 81.21 % compared to the base case. The minimum voltage was improved to 0.9628 per-unit after network reconfiguration and installing 3 DG units. Also, the optimal location and size of DGs were obtained by the CPSO algorithm and 3 DG units with the capacity of 415.0, 585.0, and 157.0 kW were allocated in buses 26, 59, and 61.

Figure 22 – Voltage profile variations before and after network reconfiguration and installing 3 DG units

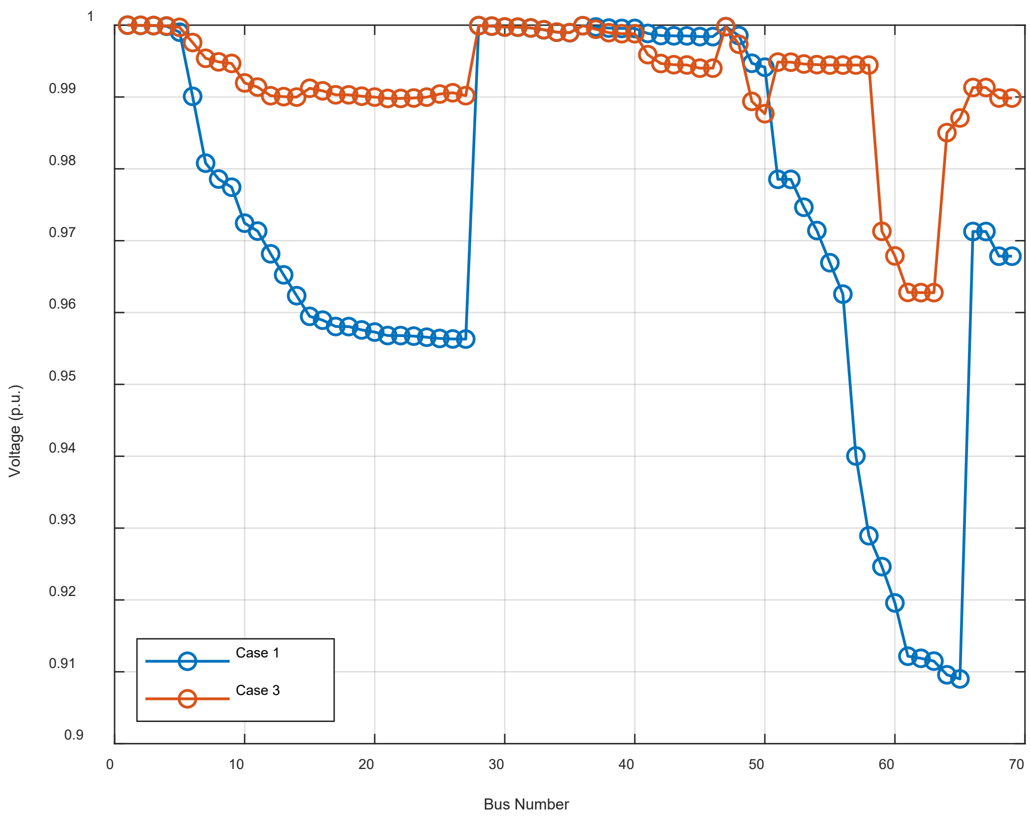

Source: Author's elaboration.

Table 7 – Simulation results before and after network reconfiguration and installing 3 DG units using CPSO

Simulation results of 69-bus distribution network		
	Base Case	3 DGs After Network Reconfiguration
Active power loss:	224.96 kW	42.27 kW
Reactive power loss:	102.15 kVAr	46.03 kVAr
Active power loss reduction:	_	81.21 %
Tie switches:	69, 70, 71, 72, 73	14, 58, 63, 69, 70
Optimal DG location	_	26, 59, 61
Optimal DG size P	_	415.0, 585.0, 157.0 kW
Minimum voltage/(Bus):	0.9090 p.u./(65)	0.9628 p.u./(62, 63)

Source: Author's elaboration.

Figure 23 illustrates the convergence of the CPSO after network reconfiguration and installing 3 DG units along the iterations on a 69-bus system. In Figure 23, the fitness (optimal solution) was found in about 10 iterations.

Figure 23 – Convergence of CPSO after network reconfiguration and installing 3 DG units

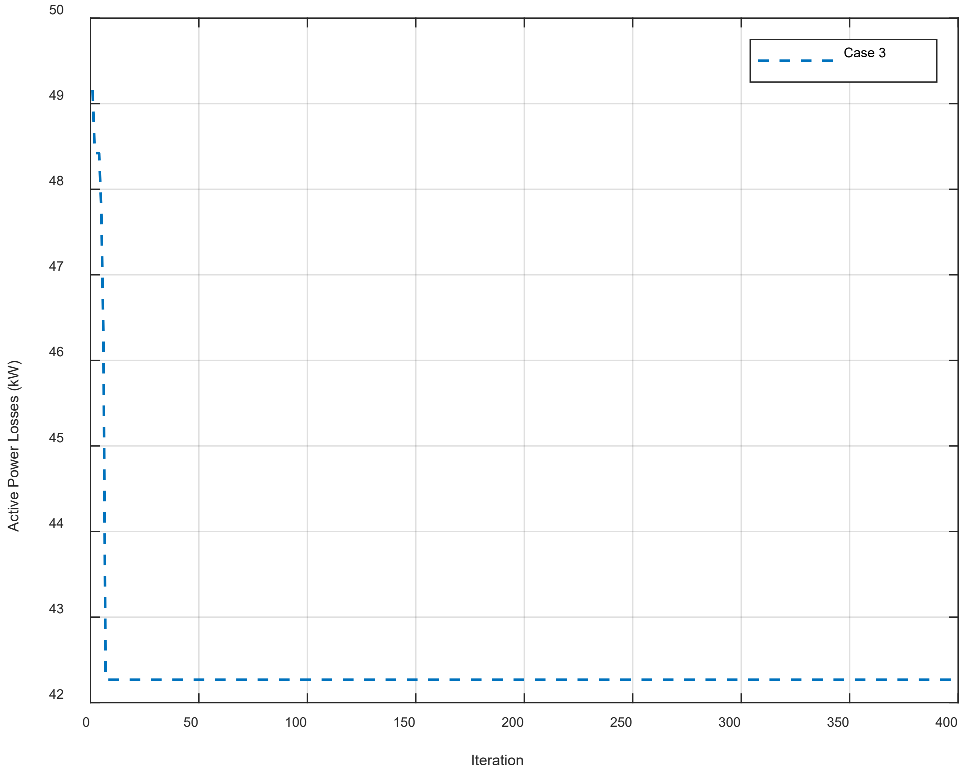

Source: Author's elaboration.

4.2.3 The simultaneous distribution network reconfiguration and the optimal location and size of 3 distributed generations (DGs) using chaotic particle swarm optimization (CPSO) algorithm

Figure 24 illustrates voltage profile variations before and after simultaneous network reconfiguration and installing 3 DG units on a 69-bus system. As shown in Figure 24 and Table 8, the power loss was 224.96 kW and minimum voltage was 0.9090 per-unit in base case. The power loss was reduced to 37.78 kW, thus having a reduction of 83.21 % compared to the base case. The minimum voltage was improved to 0.9700 per-unit after simultaneous network reconfiguration and installing 3 DG units. Also, the optimal location and size of DGs were obtained by the CPSO algorithm and 3 DG units with the capacity of 479.0, 593.0, and 617.0 kW were allocated in buses

26, 54, and 60. The tie switches which were opened after simultaneous network reconfiguration and installing 3 DG units, were 6, 10, 13, 19, and 23.

Figure 24 – Voltage profile variations before and after simultaneous network reconfiguration and installing 3 DG units

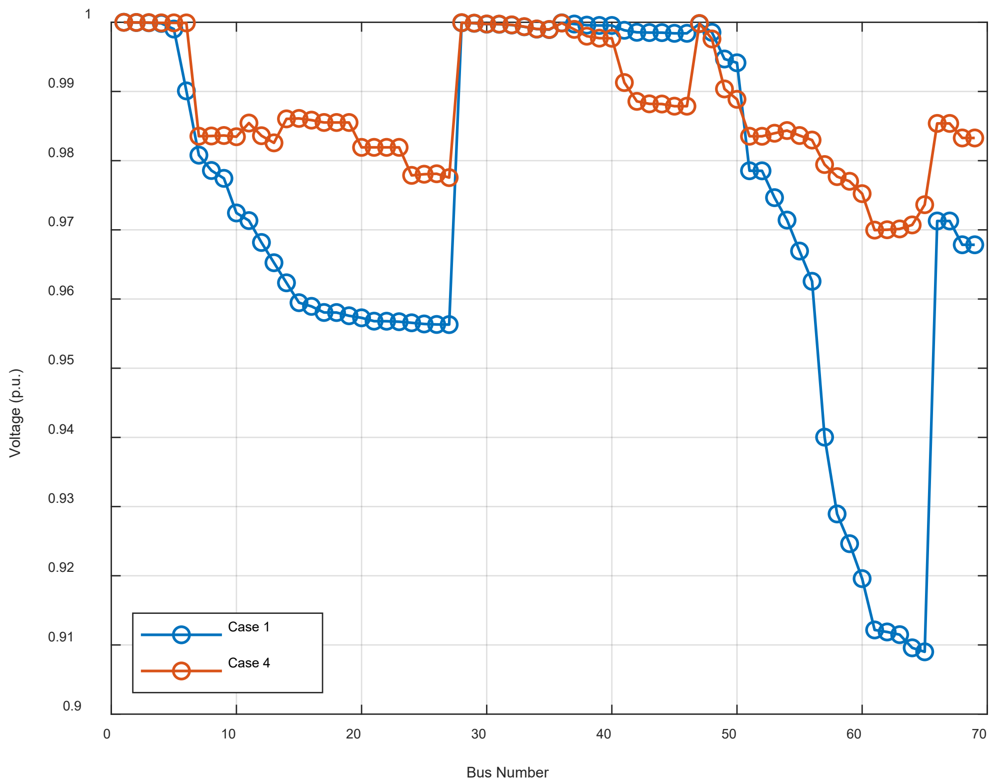

Source: Author's elaboration.

Table 8 – Simulation results before and after simultaneous network reconfiguration and installing 3 DG units using CPSO

Simulation results of 69-bus distribution network		
	Base Case	Simultaneous network reconfiguration and 3 DGs
Active power loss:	224.96 kW	37.78 kW
Reactive power loss:	102.15 kVAr	42.07 kVAr
Active power loss reduction:	_	83.21 %
Tie switches:	69, 70, 71, 72, 73	6, 10, 13, 19, 23
Optimal DG location	_	26, 54, 60
Optimal DG size P	_	479.0, 593.0, 617.0 kW
Minimum voltage/(Bus):	0.9090 p.u./(65)	0.9700 p.u./(61)

Source: Author's elaboration.

Figure 25 illustrates the convergence of the CPSO after simultaneous network reconfiguration and installing 3 DG units along the iterations on a 69-bus system. In Figure 25, the fitness (optimal solution) was found in about 30 iterations.

Figure 25 – Convergence of CPSO after simultaneous network reconfiguration and installing 3 DG units

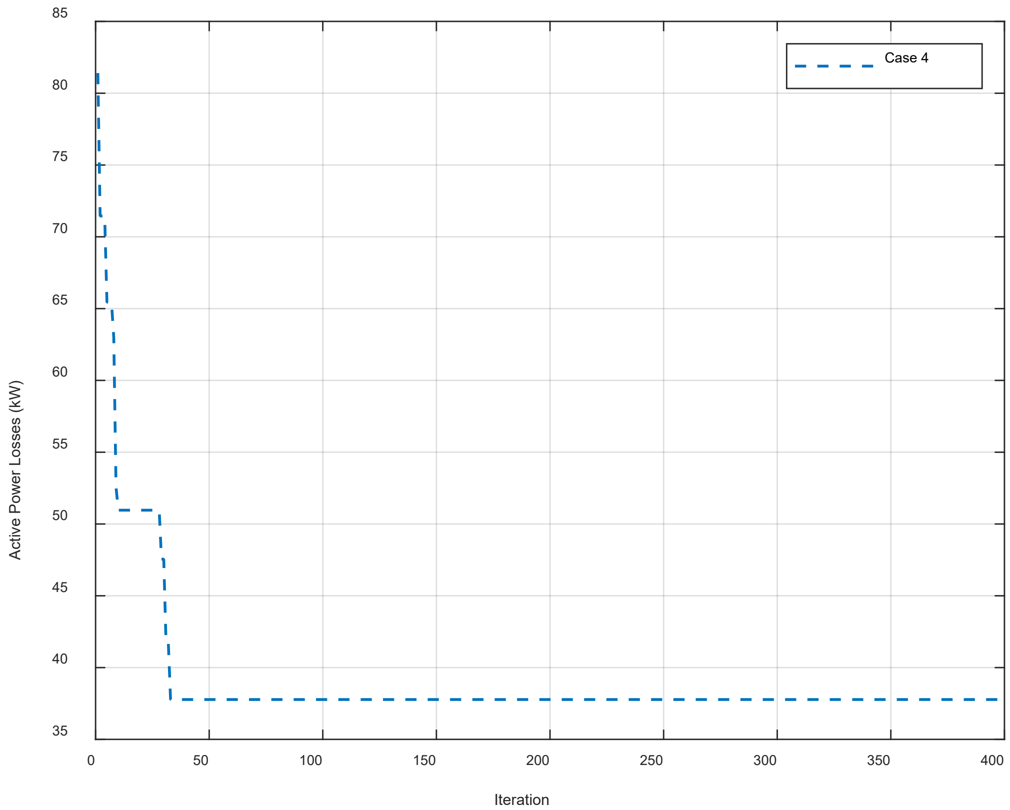

Source: Author's elaboration.

As shown in Figure 26, a comparison was made between 4 scenarios in voltage profile variations on a 69-bus system. A comparison of convergence between 3 scenarios in a 69-bus system is shown in Figure 27. For comparing the performance of the CPSO method with other methods, ACSA in Nguyen *et al*. (2016), UVDA in Bayat *et al*. (2016), and SFS in Tran *et al*. (2020) methods are considered (see Table 9). As you can see in Table 9, the power loss and minimum voltage of Cases 2, 3, and 4 in CPSO and other methods are almost the same.

Figure 26 – Comparison of voltage profile variations in 4 scenarios

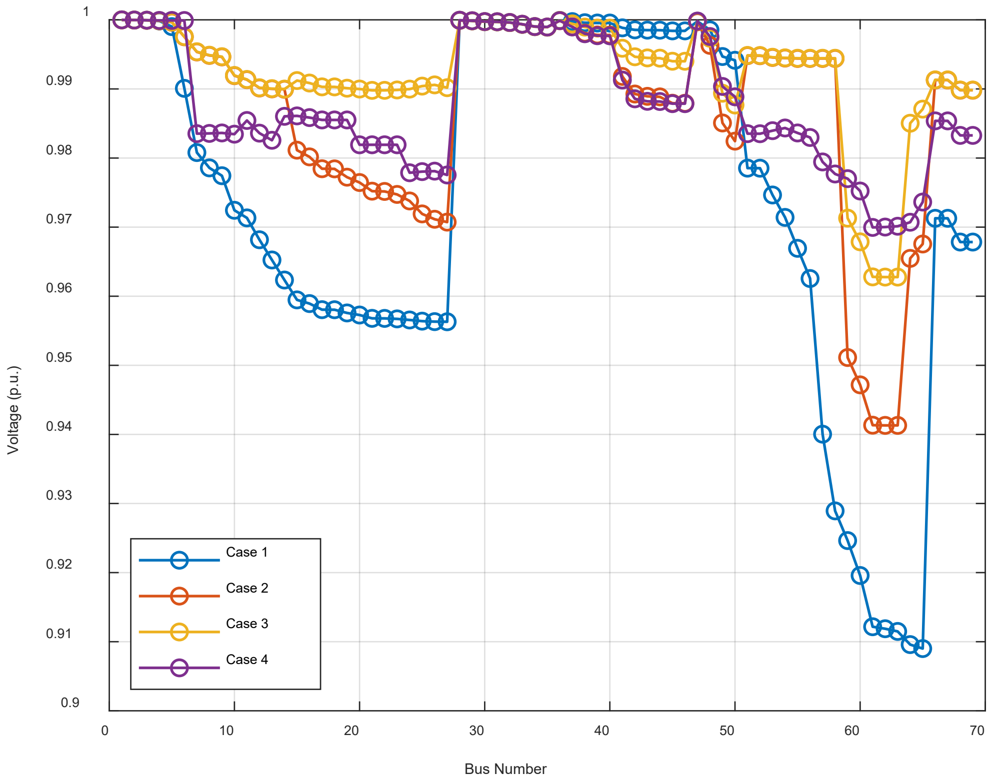

Source: Author's elaboration.

Figure 27 – Comparison of convergence in 3 scenarios

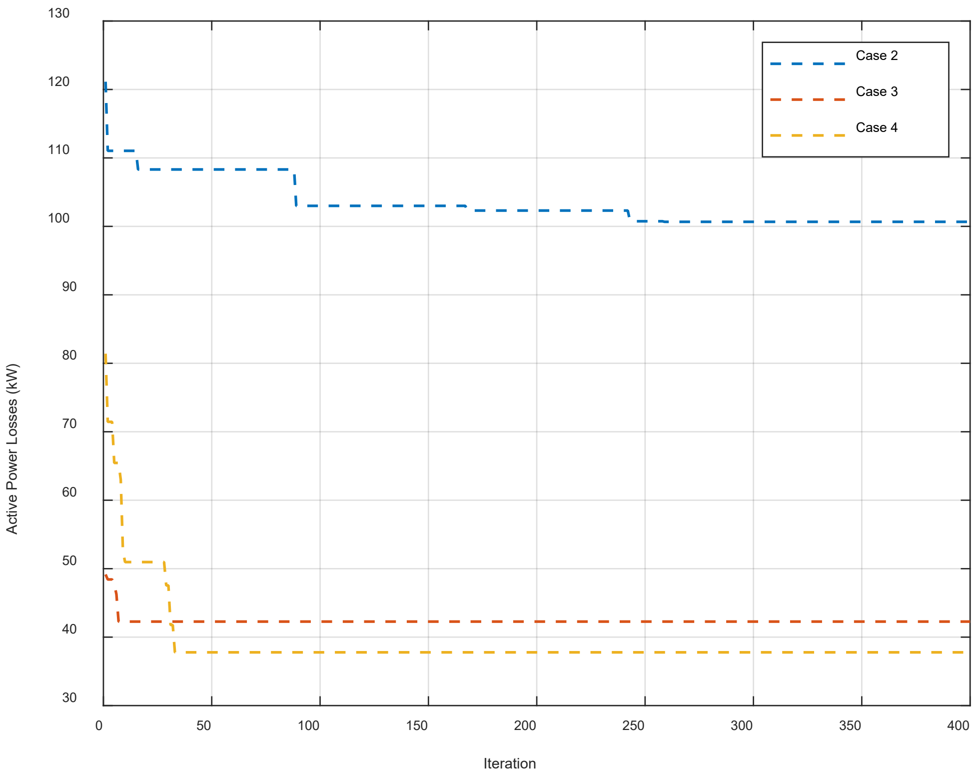

Source: Author's elaboration.

Table 9 – Summary of the results for the 69-bus network

Case	Item	ACSA (NGUYEN *et al.*, 2016)	UVDA (BAYAT *et al.*, 2016)	SFS (TRAN *et al.*, 2020)	CPSO
1	Tie switches	–	–	–	69-70-71-72-73
	P_L (kW)	–	–	–	224.96
	Q_L (kVAr)	–	–	–	102.15
	$V_{\min}$ (p.u.)	–	–	–	0.9090
	Time (s)	–	–	–	1.1
2	Tie switches	14-57-61-69-70	14-58-61-69-70	14-55-61-69-70	14-58-63-69-70
	P_L (kW)	98.59	98.58	98.62	100.67
	Q_L (kVAr)	–	–	–	116.78
	P_L reduction (%)	56.16	56.19	56.17	55.25
	$V_{\min}$ (p.u.)	0.9495	0.9495	0.9495	0.9413
	Time (s)	–	–	–	41464.6
3	Tie switches	14-57-61-69-70	14-58-61-69-70	14-55-61-69-70	14-58-63-69-70
	P_{DG} (kW)/(Bus)	368.6/(12) 1725.4/(61) 466.6/(64)	620.0/(11) 1378.0/(61) 722.0/(64)	537.6/(11) 1434.0/(61) 490.3/(64)	415.0/(26) 585.0/(59) 157.0/(61)
	P_L (kW)	37.23	37.84	35.17	42.27
	Q_L (kVAr)	–	–	–	46.0306
	P_L reduction (%)	83.45	83.18	84.37	81.21
	$V_{\min}$ (p.u.)	0.9870	0.9801	0.9813	0.9628
	Time (s)	–	–	–	12822.4
4	Tie switches	14-58-61-69-70	–	14-56-61-69-70	6-10-13-19-23
	P_{DG} (kW)/(Bus)	541.3/(11) 1724.0/(61) 553.6/(65)	– – –	537.6/(11) 1434.0/(61) 490.3/(64)	479.0/(26) 593.0/(54) 617.0/(60)
	P_L (kW)	37.02	–	35.16	37.78
	Q_L (kVAr)	–	–	–	42.07
	P_L reduction (%)	83.54	–	84.37	83.21
	$V_{\min}$ (p.u.)	0.9869	–	0.9810	0.9700
	Time (s)	–	–	–	43294.3

Source: Author's elaboration.

4.3 136-BUS TEST SYSTEM

The 136-bus system is presented in Mantovani *et al*. (2000). It has 135 load buses, one substation bus and 156 feeders. The voltage at the substation bus is 13.80 kV and the base power of the system is 100 MVA. The total active and reactive power demands are 18313.810 kW and 7932.534 kVAr, respectively. The maximum size of each DG unit is 3052.3015 kW.

Figure 28 illustrates the 136-bus system with 21 tie switches 136, 137, 138, 139, 140, 141, 142, 143, 144, 145, 146, 147, 148, 149, 150, 151, 152, 153, 154, 155, and 156 that are initially open and illustrated by dashed lines. The complete data of this system are presented in Appendix C.

Figure 28 – Schematic of the studied network of 136-bus

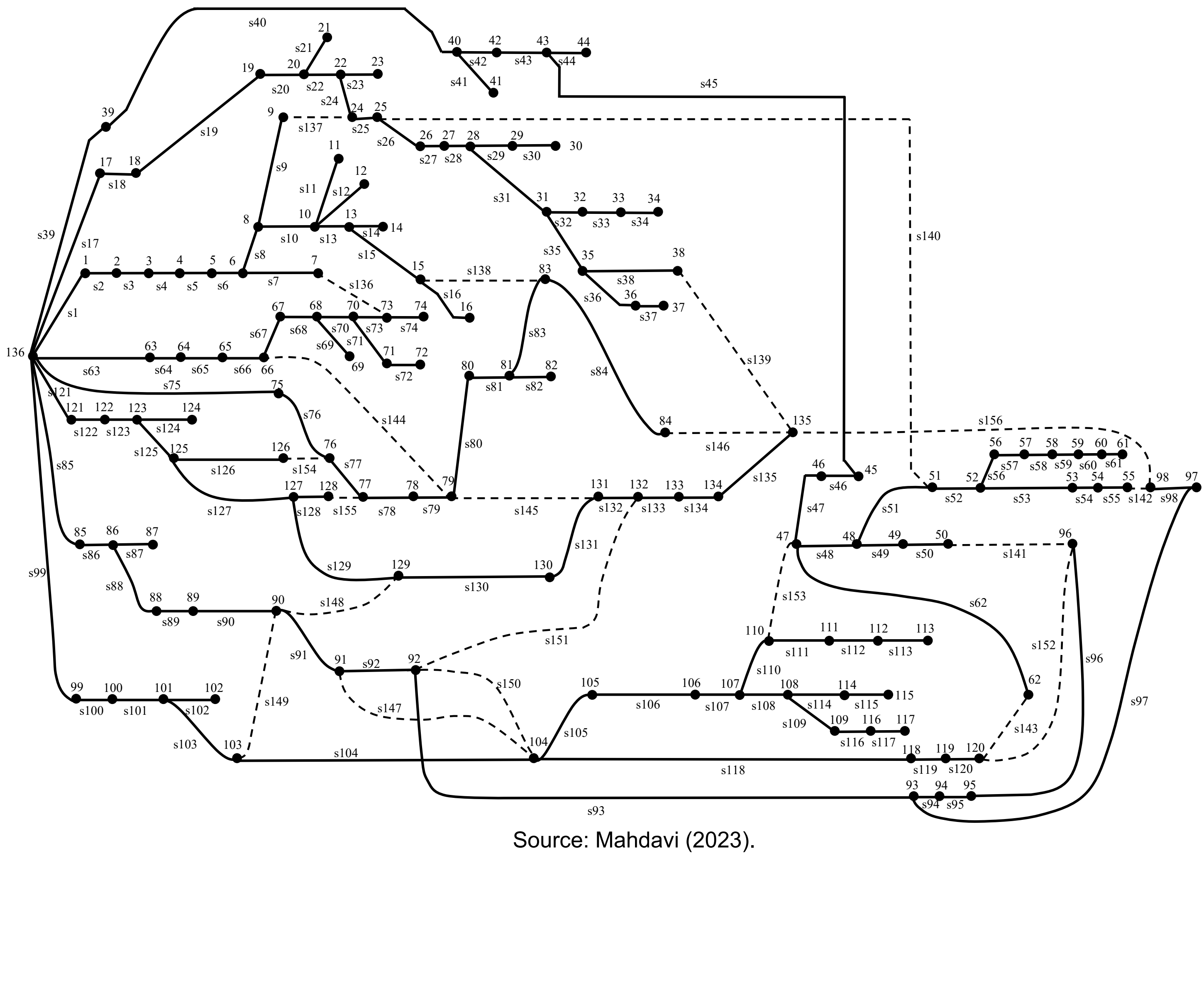

Source: Mahdavi (2023).

4.3.1 Distribution network reconfiguration using chaotic particle swarm optimization (CPSO) algorithm

Figure 29 illustrates voltage profile variations before and after network reconfiguration on a 136-bus system. As shown in Figure 29 and Table 10, the power loss was 320.37 kW and minimum voltage was 0.9290 per-unit in base case. The power loss was reduced to 285.34 kW, thus having a reduction of 10.93 % compared to the base case. The minimum voltage was improved to 0.9635 per-unit after network reconfiguration. The tie switches which were opened after network reconfiguration, were 7, 9, 83, 38, 51, 95, 53, 119, 144, 145, 146, 147, 148, 149, 150, 151, 152, 106, 126, 128, and 156.

Figure 29 – Voltage profile variations before and after network reconfiguration

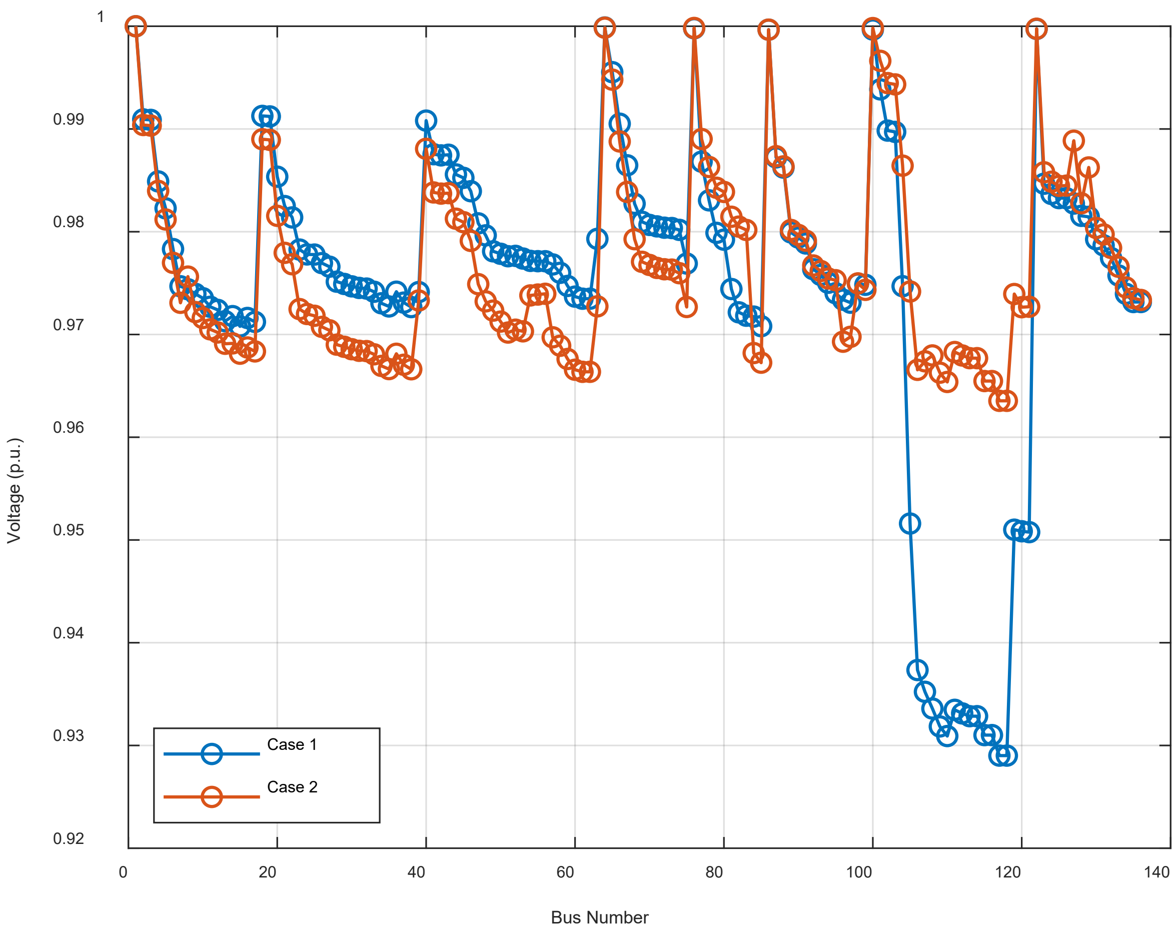

Source: Author's elaboration.

Table 10 – Simulation results before and after network reconfiguration using CPSO

Simulation results of 136-bus distribution network		
	Base Case	Network Reconfiguration
Active power loss:	320.37 kW	285.34 kW
Reactive power loss:	702.95 kVAr	621.55 kVAr
Active power loss reduction:	–	10.93 %
Tie switches:	136, 137, 138, 139, 140, 141, 142, 143, 144, 145, 146, 147, 148, 149, 150, 151, 152, 153, 154, 155, 156	7, 9, 83, 38, 51, 95, 53, 119, 144, 145, 146, 147, 148, 149, 150, 151, 152, 106, 126, 128, 156
Minimum voltage/(Bus):	0.9290 p.u./(117, 118)	0.9635 p.u./(117, 118)

Source: Author's elaboration.

Figure 30 illustrates the convergence of the CPSO after network reconfiguration along the iterations on a 136-bus system. In Figure 30, the fitness (optimal solution) was found in about 500 iterations.

Figure 30 – Convergence of CPSO after network reconfiguration

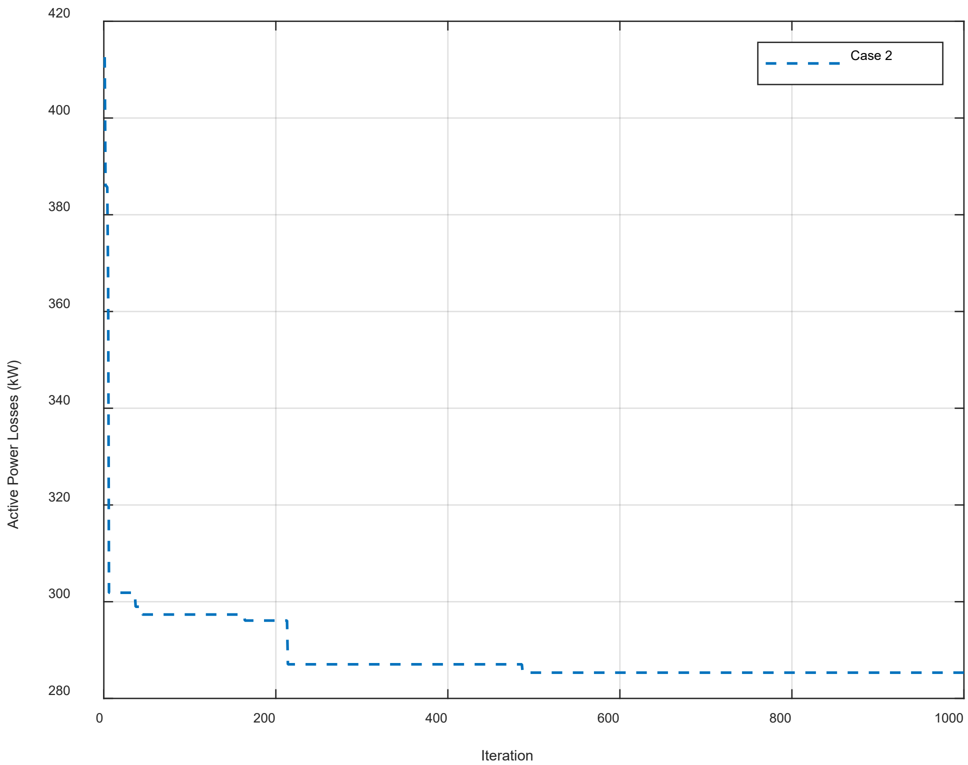

Source: Author's elaboration.

4.3.2 The optimal location and size of 3 distributed generations (DGs) after distribution network reconfiguration (according to the result of Case 2) using chaotic particle swarm optimization (CPSO) algorithm

The tie switches were determined after network reconfiguration in scenario 2 and the opened tie switches were 7, 9, 83, 38, 51, 95, 53, 119, 144, 145, 146, 147, 148, 149, 150, 151, 152, 106, 126, 128, and 156. We assumed that these switches were open and then the optimal location and size of DG units were specified by CPSO algorithm. We installed 3 DG units in this scenario after network reconfiguration.

Figure 31 illustrates voltage profile variations before and after network reconfiguration and installing 3 DG units on a 136-bus system. As shown in Figure 31 and Table 11, the power loss was 320.37 kW and minimum voltage was 0.9290 per-unit in base case. The power loss was reduced to 144.23 kW, thus having a reduction of 54.98 % compared to the base case. The minimum voltage was improved to 0.9666 per-unit after network reconfiguration and installing 3 DG units. Also, the optimal location and size of DGs were obtained by the CPSO algorithm and 3 DG units with the capacity of 2505.0, 2494.0, and 2516.0 kW were allocated in buses 10, 31, and 110.

Figure 31 – Voltage profile variations before and after network reconfiguration and installing 3 DG units

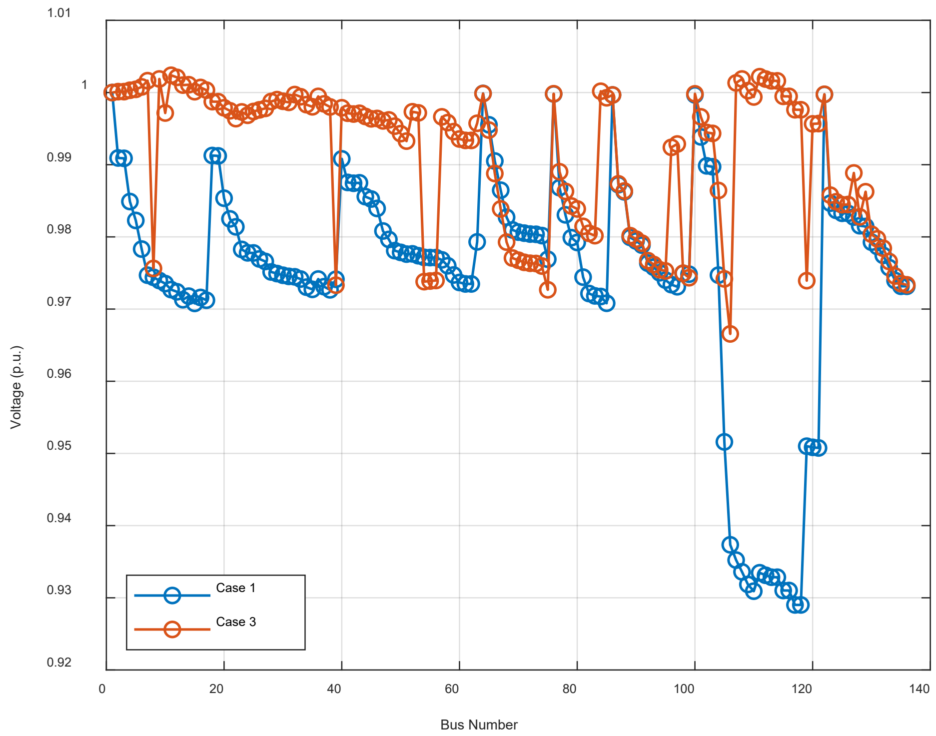

Source: Author's elaboration.

Table 11 – Simulation results before and after network reconfiguration and installing 3 DG units using CPSO

Simulation results of 136-bus distribution network		
	Base Case	3 DGs After Network Reconfiguration
Active power loss:	320.37 kW	144.23 kW
Reactive power loss:	702.95 kVAr	300.62 kVAr
Active power loss reduction:	_	54.98 %
Tie switches:	136, 137, 138, 139, 140, 141, 142, 143, 144, 145, 146, 147, 148, 149, 150, 151, 152, 153, 154, 155, 156	7, 9, 83, 38, 51, 95, 53, 119, 144, 145, 146, 147, 148, 149, 150, 151, 152, 106, 126, 128, 156
Optimal DG location	_	10, 31, 110
Optimal DG size P	_	2505.0, 2494.0, 2516.0 kW
Minimum voltage/(Bus):	0.9290 p.u./(117, 118)	0.9666 p.u./(106)

Source: Author's elaboration.

Figure 32 illustrates the convergence of the CPSO after network reconfiguration and installing 3 DG units along the iterations on a 136-bus system. In Figure 32, the fitness (optimal solution) was found in about 40 iterations.

Figure 32 – Convergence of CPSO after network reconfiguration and installing 3 DG units

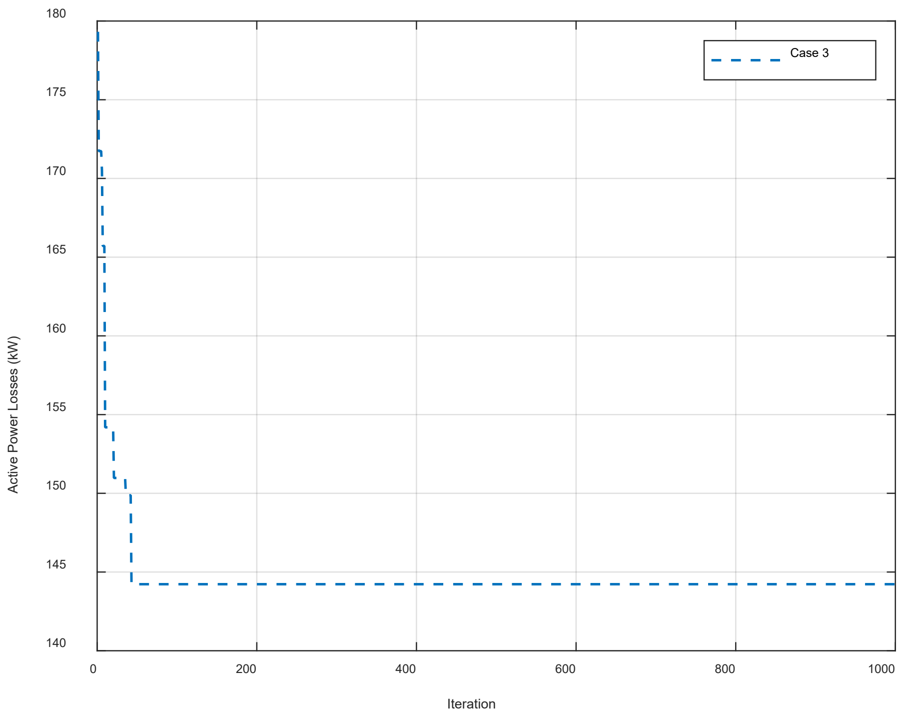

Source: Author's elaboration.

4.3.3 The simultaneous distribution network reconfiguration and the optimal location and size of 3 distributed generations (DGs) using chaotic particle swarm optimization (CPSO) algorithm

Figure 33 illustrates voltage profile variations before and after simultaneous network reconfiguration and installing 3 DG units on a 136-bus system. As shown in Figure 33 and Table 12, the power loss was 320.37 kW and minimum voltage was 0.9290 per-unit in base case. The power loss was reduced to 163.28 kW, thus having a reduction of 49.03 % compared to the base case. The minimum voltage was improved to 0.9584 per-unit after simultaneous network reconfiguration and installing 3 DG units. Also, the optimal location and size of DGs were obtained by the CPSO algorithm and 3 DG units with the capacity of 2751.0, 1873.0, 2678.0 kW were allocated in buses 52, 57, and 83. The tie switches which were opened after simultaneous network reconfiguration and installing 3 DG units, were 66, 18, 78, 135, 48, 93, 98, 120, 144, 145, 84, 147, 148, 149, 150, 151, 152, 107, 154, 128, and 156.

Figure 33 – Voltage profile variations before and after simultaneous network reconfiguration and installing 3 DG units

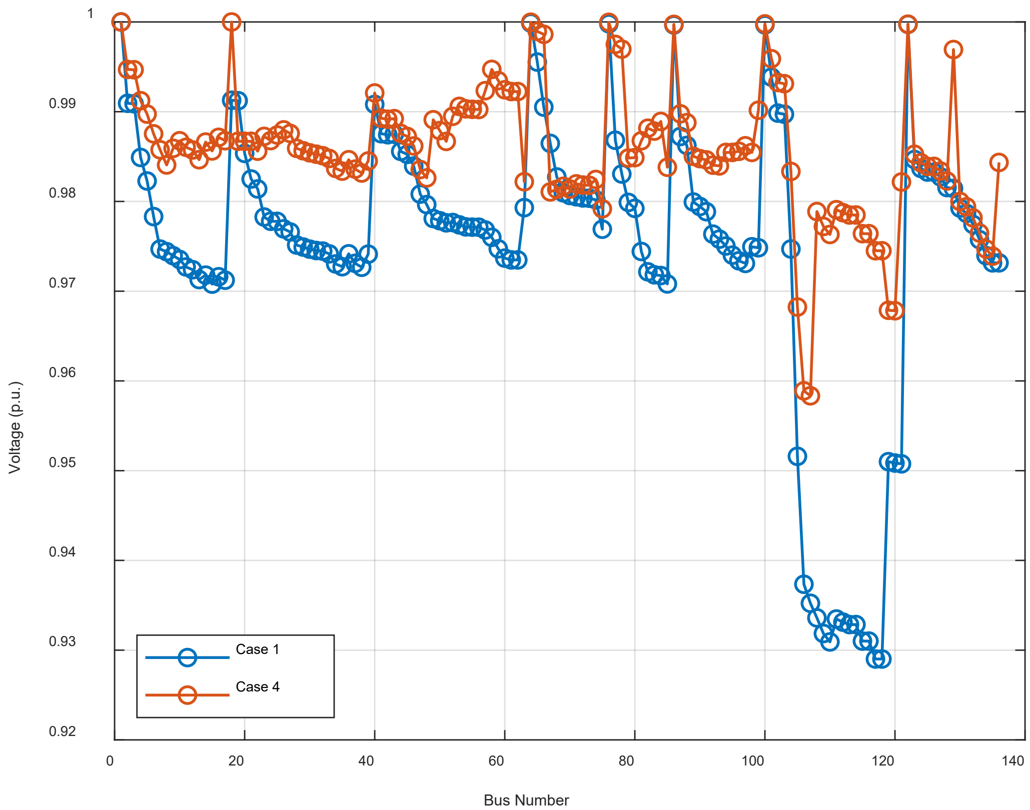

Source: Author's elaboration.

Table 12 – Simulation results before and after simultaneous network reconfiguration and installing 3 DG units using CPSO

Simulation results of 136-bus distribution network		
	Base Case	Simultaneous network reconfiguration and 3 DGs
Active power loss:	320.37 kW	163.28 kW
Reactive power loss:	702.95 kVAr	339.72 kVAr
Active power loss reduction:	_	49.03 %
Tie switches:	136, 137, 138, 139, 140, 141, 142, 143, 144, 145, 146, 147, 148, 149, 150, 151, 152, 153, 154, 155, 156	66, 18, 78, 135, 48, 93, 98, 120, 144, 145, 84, 147, 148, 149, 150, 151, 152, 107, 154, 128, 156
Optimal DG location	_	52, 57, 83
Optimal DG size P	_	2751.0, 1873.0, 2678.0 kW
Minimum voltage/(Bus):	0.9290 p.u./(117, 118)	0.9584 p.u./(107)

Source: Author's elaboration.

Figure 34 illustrates the convergence of the CPSO after simultaneous network reconfiguration and installing 3 DG units along the iterations on a 136-bus system. In Figure 34, the fitness (optimal solution) was found in about 40 iterations.

Figure 34 – Convergence of CPSO after simultaneous network reconfiguration and installing 3 DG units

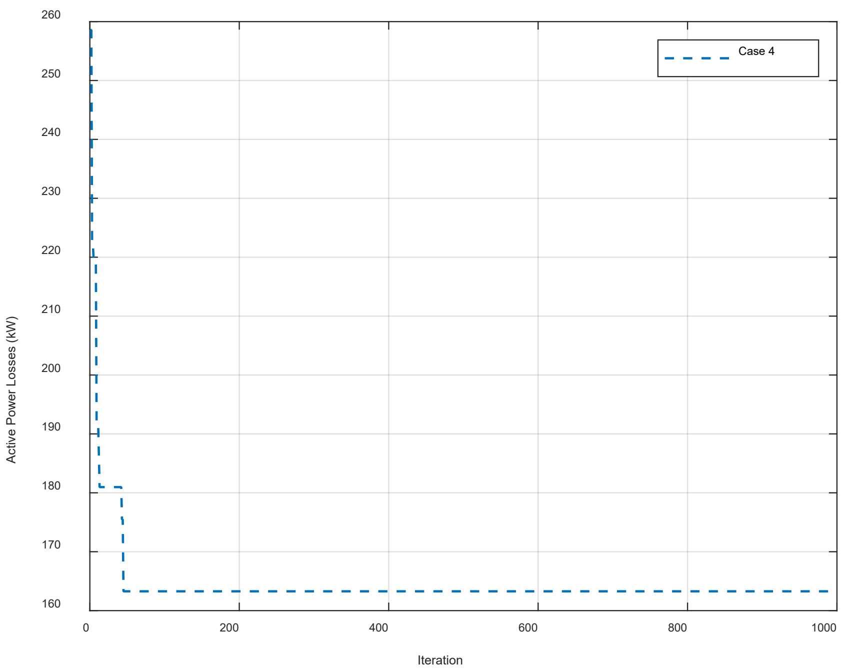

Source: Author's elaboration.

As shown in Figure 35, a comparison was made between 4 scenarios in voltage profile variations on a 136-bus system. A comparison of convergence between 3 scenarios in a 136-bus system is shown in Figure 36. For comparing the performance of the CPSO method with other methods, UVDA in Bayat *et al*. (2016), SFS in Tran *et al*. (2020), and adaptive ant colony optimization (AACO) in Swarnkar *et al*. (2011) methods are considered (see Table 13). As you can see in Table 13, the power loss and minimum voltage of Case 2 in CPSO and other methods are almost the same. In Case 3, the CPSO method minimizes the power loss more compared to the SFS, but the CPSO and SFS methods are the same regarding the minimum voltage. The SFS approach performs better than the CPSO approach in terms of power loss in Case 4 because the total capacity of DGs in SFS is 11166 kW, which is about 70 % of the total active power demand of the network, whereas the total capacity of DGs in CPSO is 7302 kW, which is about 40 % of the total active power demand of the network. However, the minimum voltage of Case 4 is almost similar in CPSO and SFS. As a result, CPSO generally performs better than SFS.

Figure 35 – Comparison of voltage profile variations in 4 scenarios

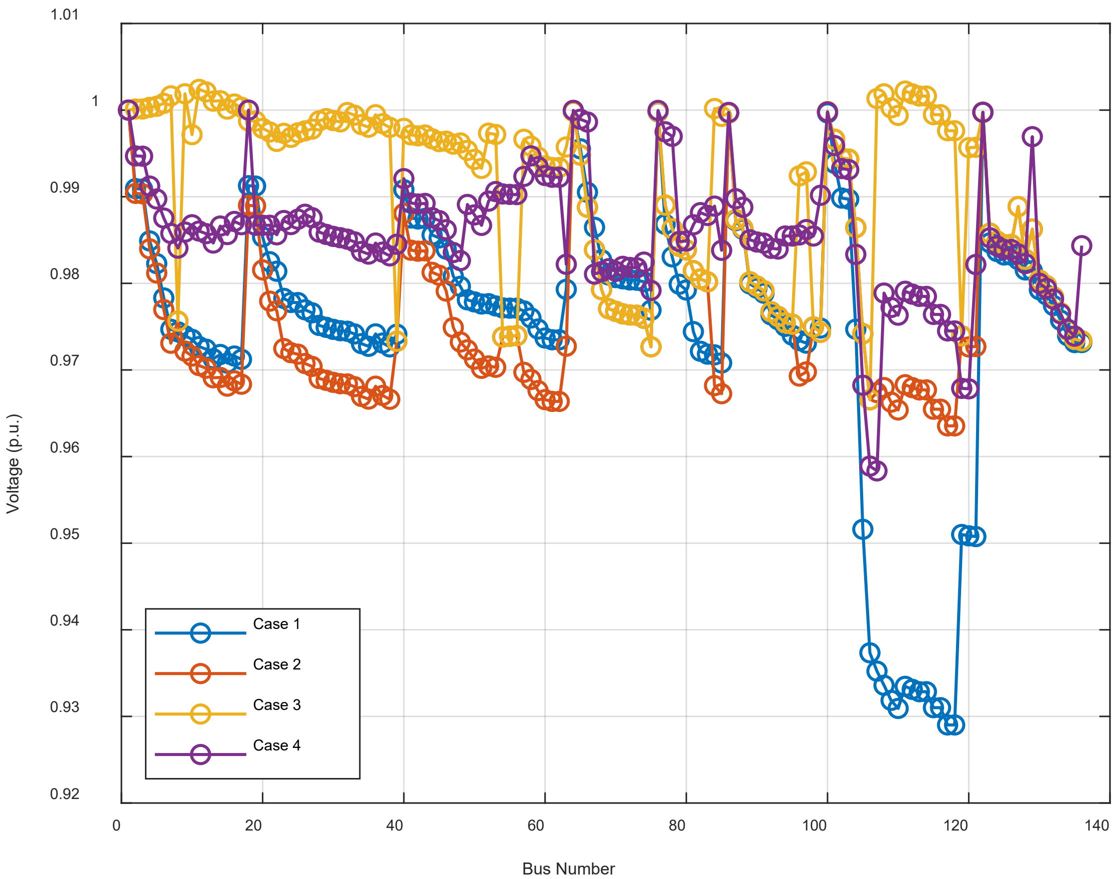

Source: Author's elaboration.

Figure 36 – Comparison of convergence in 3 scenarios

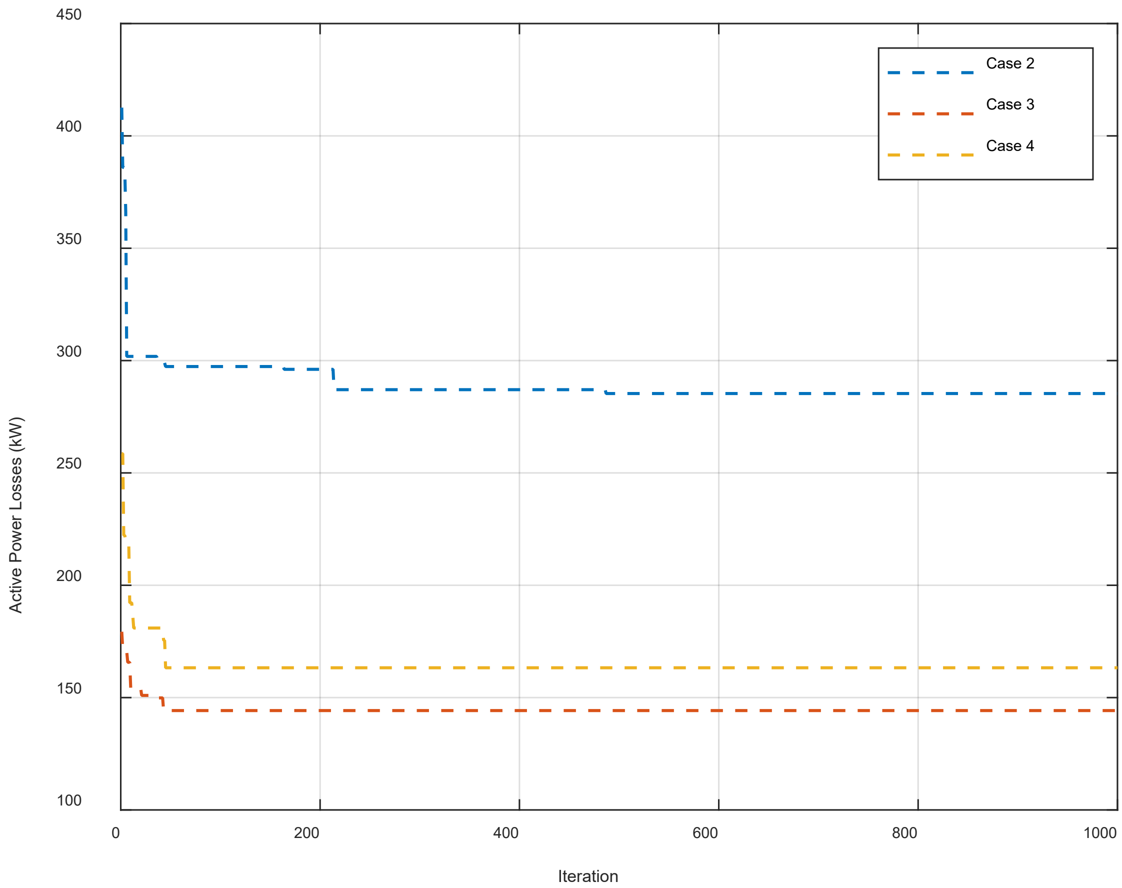

Source: Author's elaboration.

Table 13 – Summary of the results for the 136-bus network

Case	Item	UVDA (Bayat *et al.*, 2016)	SFS (Tran *et al.*, 2020)	AACO (Swarnkar *et al.*, 2011)	CPSO
1	Tie switches	–	–	–	136-137-138-139-140-141-142-143-144-145-146-147-148-149-150-151-152-153-154-155-156
	P_L (kW)	–	–	–	320.37
	Q_L (kVAr)	–	–	–	702.95
	V_{min} (p.u.)	–	–	–	0.9290
	Time (s)	–	–	–	1.4

2	**Tie switches**	7-35-51-90-96-106-118-126-135-137-138-141-142-144-145-146-147-148-150-151-155	7-58-62-84-90-98-106-118-126-128-135-137-138-139-141-144-145-147-148-150-151	7-35- 51-90-95-106-118-126-135-137-138-141-142-144-145-146-147-148-150-151-155	7-9-83-38-51-95-53-119-144-145-146-147-148-149-150-151-152-106-126-128-156
	P_L **(kW)**	280.18	278.9	279.75	285.34
	Q_L **(kVAr)**	–	–	–	621.55
	P_L **reduction (%)**	12.55	13.03	12.68	10.93
	$V_{\min}$ **(p.u.)**	0.9589	0.9616	0.9602	0.9635
	Time (s)	–	–	–	235380.8
3	**Tie switches**	–	7-58-62-84-90-98-106-118-126-128-135-137-138-139-141-144-145-147-148-150-151	–	7-9-83-38-51-95-53-119-144-145-146-147-148-149-150-151-152-106-126-128-156
	P_{DG} **(kW)/(Bus)**	– – –	2490.7/(28) 2233.4/(48) 1844.2/(106)	– – –	2505.0/(10) 2494.0/(31) 2516.0/(110)
	P_L **(kW)**	–	160.45	–	144.23
	Q_L **(kVAr)**	–	–	–	300.62
	P_L **reduction (%)**	–	49.97	–	54.98
	$V_{\min}$ **(p.u.)**	–	0.9728	–	0.9666
	Time (s)	–	–	–	123541
4	**Tie switches**	–	35-61-73-81-89-92-95-98-104-110-130-135-137-141-144-145-146-148-150-154-155	–	66-18-78-135-48-93-98-120-144-145-84-147-148-149-150-151-152-107-154-128-156

	P_{DG} (kW)/(Bus)	– – –	3445.3/(14) 4690.2/(48) 3030.5/(106)	– – –	2751.0/(52) 1873.0/(57) 2678.0/(83)
	P_L (kW)	–	118.73	–	163.28
	Q_L (kVAr)	–	–	–	339.72
	P_L reduction (%)	–	62.98	–	49.03
	$V_{\min}$ (p.u.)	–	0.9662	–	0.9584
	Time (s)	–	–	–	244338

Source: Author's elaboration.

4.4 415-BUS TEST SYSTEM

The 415-bus system is presented in Bernal-Agustin (1998). It has 414 load buses, one substation bus and 473 feeders. The voltage at the substation bus is 10.00 kV and the base power of the system is 100 MVA. The total active and reactive power demands are 27372.40 kW and 13237.00 kVAr, respectively. The maximum size of each DG unit is 4562.06 kW.

Figure 37 illustrates the 415-bus system with 59 tie switches 1, 5, 15, 16, 26, 31, 53, 54, 55, 75, 82, 94, 96, 97, 106, 107, 119, 136, 138, 154, 155, 156, 168, 169, 177, 179, 194, 195, 201, 207, 211, 214, 219, 241, 256, 258, 282, 297, 302, 314, 321, 354, 359, 362, 364, 385, 388, 395, 396, 404, 407, 423, 424, 426, 431, 436, 445, 446 and 449 that are initially open and illustrated by dashed lines. The complete data of this system are presented in Appendix D.

Figure 37 – Schematic of the studied network of 415-bus

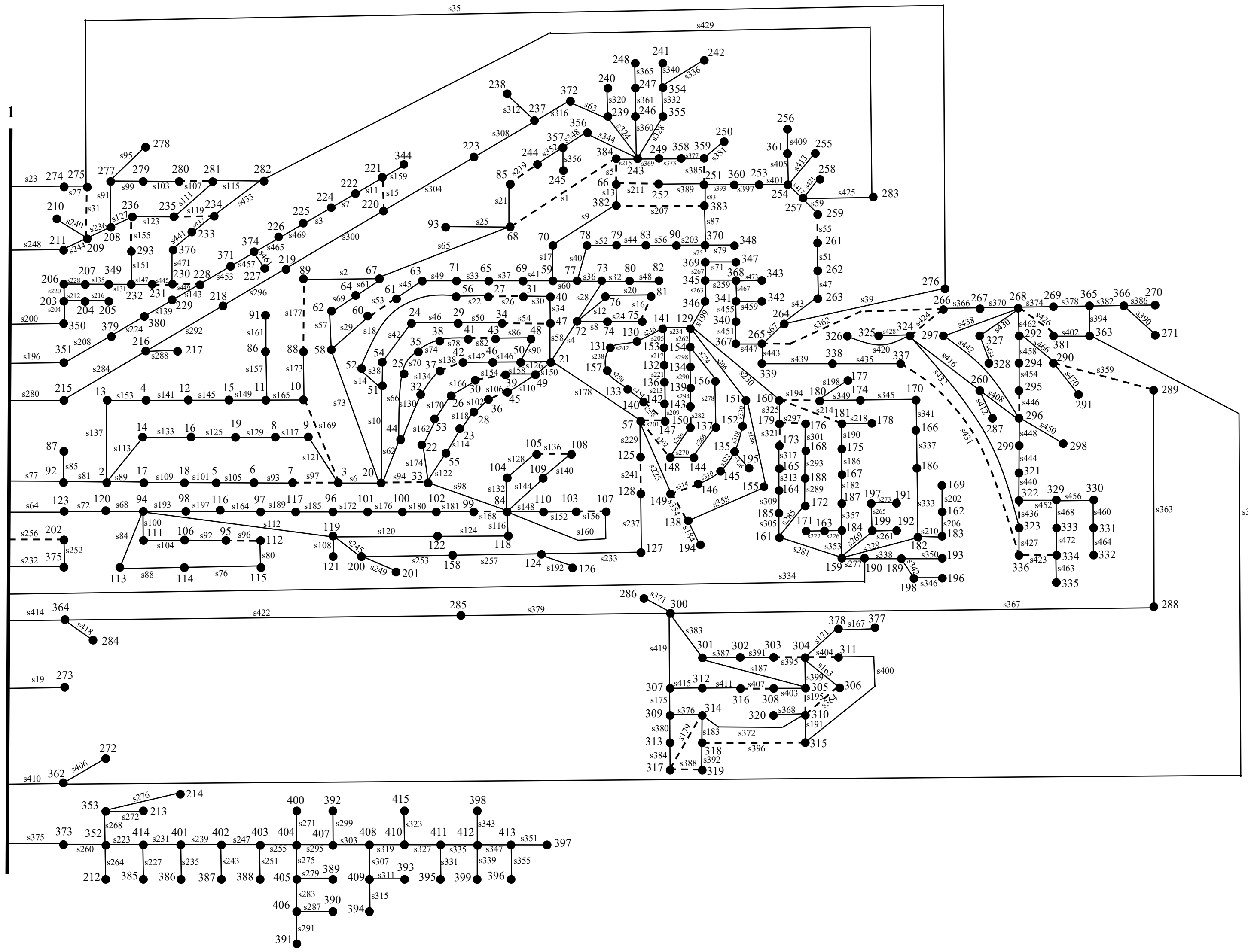

Source: Mahdavi (2023).

4.4.1 Distribution network reconfiguration using chaotic particle swarm optimization (CPSO) algorithm

Figure 38 illustrates voltage profile variations before and after network reconfiguration on a 415-bus system. As shown in Figure 38 and Table 14, the power loss was 708.94 kW and minimum voltage was 0.9300 per-unit in base case. The power loss was reduced to 650.43 kW, thus having a reduction of 8.25 % compared to the base case. The minimum voltage was improved to 0.9440 per-unit after network reconfiguration. The tie switches which were opened after network reconfiguration, were 1, 5, 11, 12, 13, 30, 31, 45, 50, 55, 60, 61, 86, 87, 93, 94, 99, 104, 111, 131, 134, 144, 148, 150, 155, 166, 169, 172, 178, 179, 182, 195, 201, 213, 252, 263, 278, 298, 310, 321, 325, 344, 358, 362, 385, 391, 392, 396, 399, 402, 403, 404, 424, 431, 436, 437, 446, 466, and 472.

Figure 38 – Voltage profile variations before and after network reconfiguration

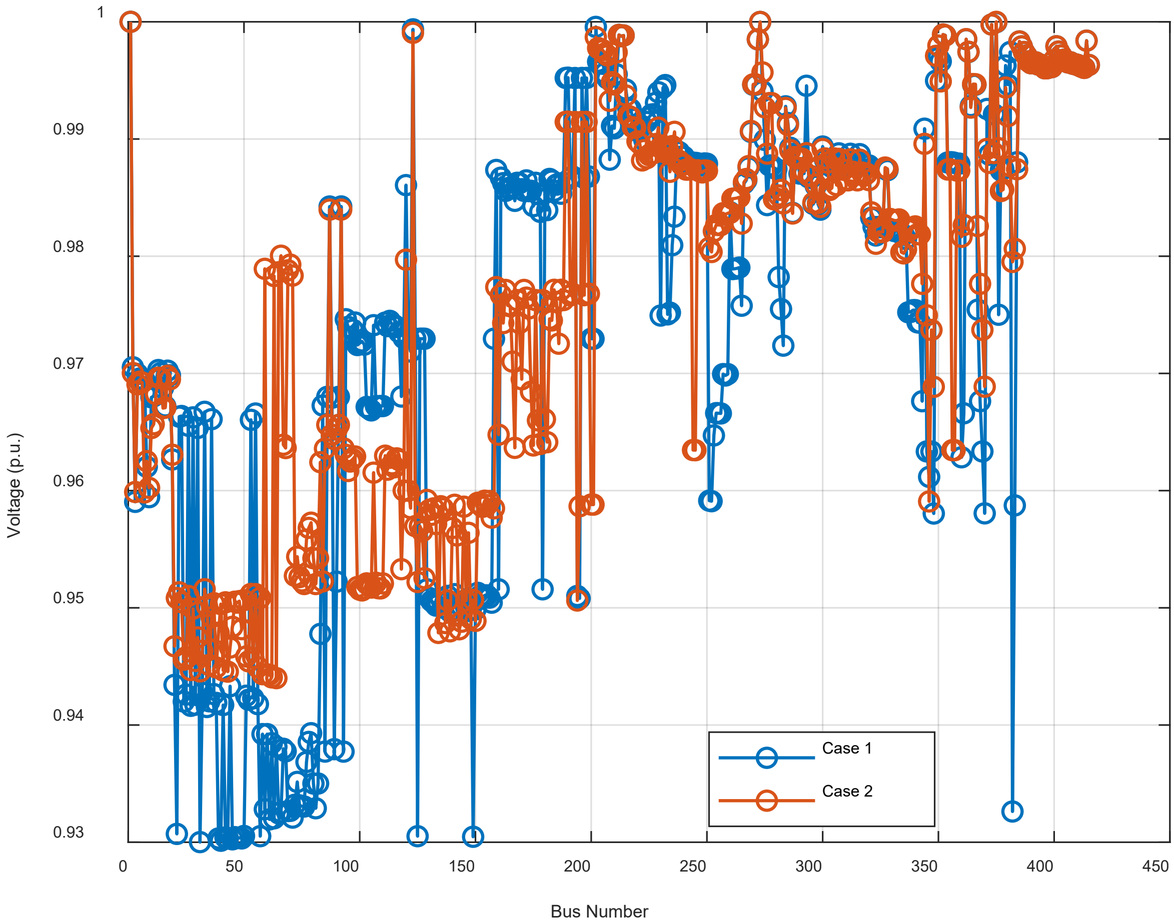

Source: Author's elaboration.

Table 14 – Simulation results before and after network reconfiguration using CPSO

Simulation results of 415-bus distribution network		
	Base Case	Network Reconfiguration
Active power loss:	708.94 kW	650.43 kW
Reactive power loss:	538.48 kVAr	548.31 kVAr
Active power loss reduction:	–	8.25 %
Tie switches:	1, 5, 15, 16, 26, 31, 53, 54, 55, 75, 82, 94, 96, 97, 106, 107, 119, 136, 138,	1, 5, 11, 12, 13, 30, 31, 45, 50, 55, 60, 61, 86, 87, 93, 94, 99, 104, 111, 131,

	154, 155, 156, 168, 169, 177, 179, 194, 195, 201, 207, 211, 214, 219, 241, 256, 258, 282, 297, 302, 314, 321, 354, 359, 362, 364, 385, 388, 395, 396, 404, 407, 423, 424, 426, 431, 436, 445, 446, 449	134, 144, 148, 150, 155, 166, 169, 172, 178, 179, 182, 195, 201, 213, 252, 263, 278, 298, 310, 321, 325, 344, 358, 362, 385, 391, 392, 396, 399, 402, 403, 404, 424, 431, 436, 437, 446, 466, 472
Minimum voltage/(Bus):	0.9300 p.u./(31)	0.9440 p.u./(64)

Source: Author's elaboration.

Figure 39 illustrates the convergence of the CPSO after network reconfiguration along the iterations on a 415-bus system. In Figure 39, the fitness (optimal solution) was found in about 350 iterations.

Figure 39 – Convergence of CPSO after network reconfiguration

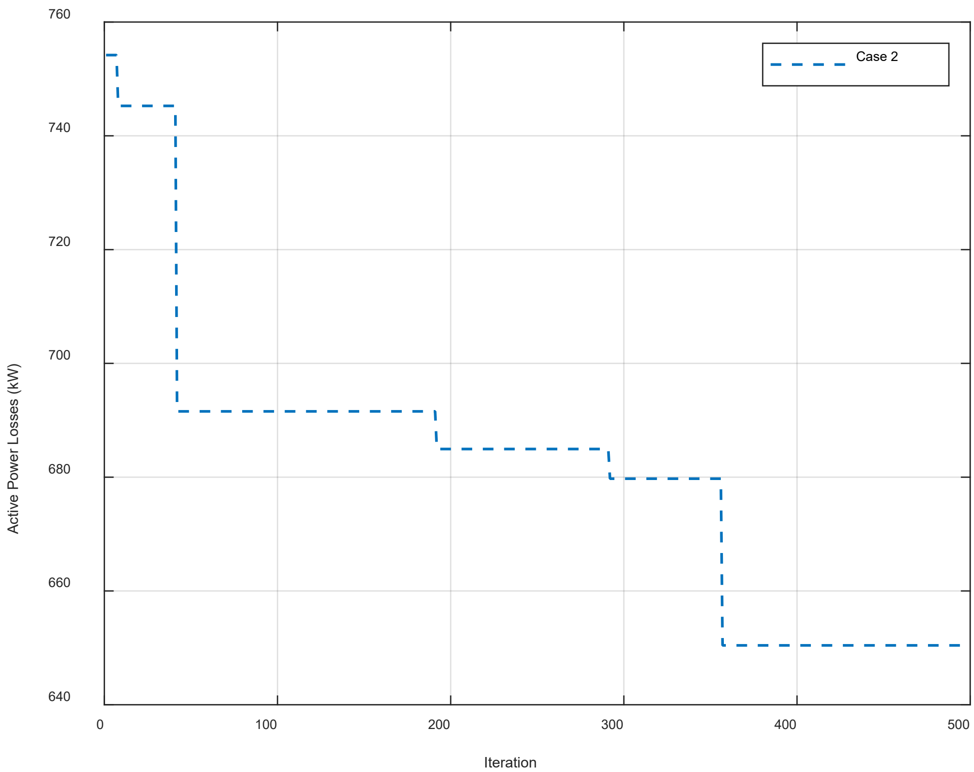

Source: Author's elaboration.

4.4.2 The optimal location and size of 3 distributed generations (DGs) after distribution network reconfiguration (according to the result of Case 2) using chaotic particle swarm optimization (CPSO) algorithm

The tie switches were determined after network reconfiguration in scenario 2 and the opened tie switches were 1, 5, 11, 12, 13, 30, 31, 45, 50, 55, 60, 61, 86, 87, 93, 94, 99, 104, 111, 131, 134, 144, 148, 150, 155, 166, 169, 172, 178, 179, 182, 195, 201, 213, 252, 263, 278, 298, 310, 321, 325, 344, 358, 362, 385, 391, 392, 396, 399, 402, 403, 404, 424, 431, 436, 437, 446, 466, and 472. We assumed that these switches were open and then the optimal location and size of DG units were specified by CPSO algorithm. We installed 3 DG units in this scenario after network reconfiguration.

Figure 40 illustrates voltage profile variations before and after network reconfiguration and installing 3 DG units on a 415-bus system. As shown in Figure 40 and Table 15, the power loss was 708.94 kW and minimum voltage was 0.9300 per-unit in base case. The power loss was reduced to 315.24 kW, thus having a reduction of 55.53 % compared to the base case. The minimum voltage was improved to 0.9502 per-unit after network reconfiguration and installing 3 DG units. Also, the optimal location and size of DGs were obtained by the CPSO algorithm and 3 DG units with the capacity of 2479.0, 4134.0, and 3061.0 kW were allocated in buses 25, 119, and 166.

Figure 40 – Voltage profile variations before and after network reconfiguration and installing 3 DG units

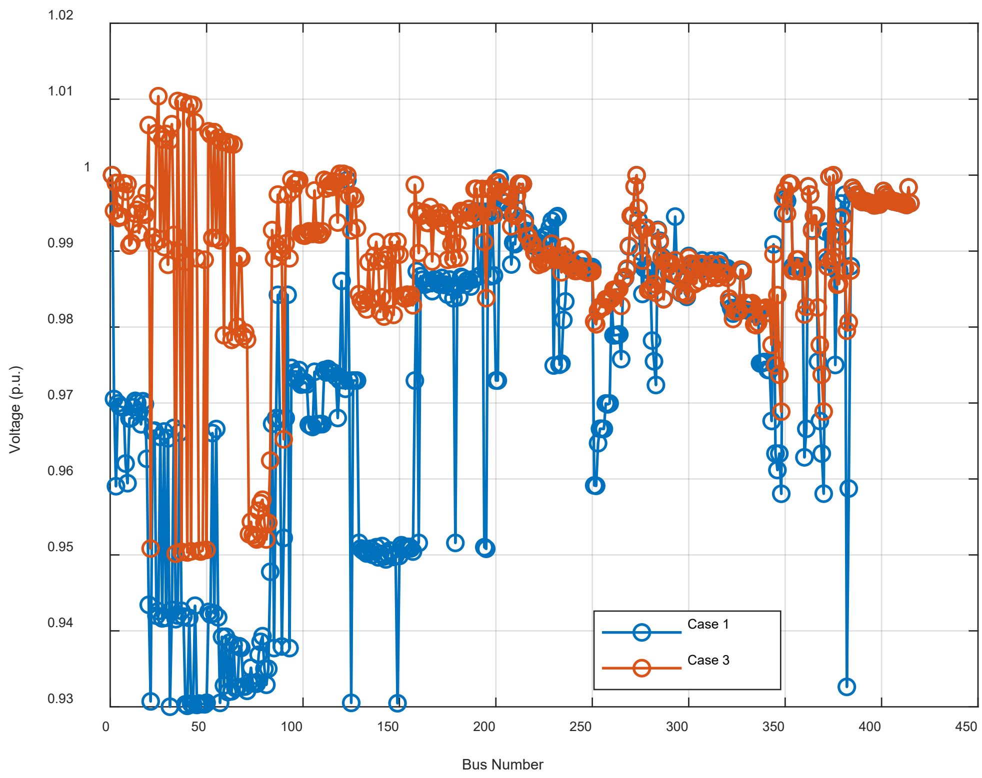

Source: Author's elaboration.

Table 15 – Simulation results before and after network reconfiguration and installing 3 DG units using CPSO

Simulation results of 415-bus distribution network		
	Base Case	3 DGs After Network Reconfiguration
Active power loss:	708.94 kW	315.24 kW
Reactive power loss:	538.48 kVAr	239.00 kVAr
Active power loss reduction:	_	55.53 %
Tie switches:	1, 5, 15, 16, 26, 31, 53, 54, 55, 75, 82, 94, 96, 97, 106, 107, 119, 136, 138, 154, 155, 156, 168, 169, 177, 179, 194, 195, 201, 207, 211, 214, 219, 241, 256, 258, 282, 297, 302, 314, 321, 354, 359, 362, 364, 385, 388, 395, 396, 404, 407, 423, 424, 426, 431, 436, 445, 446, 449	1, 5, 11, 12, 13, 30, 31, 45, 50, 55, 60, 61, 86, 87, 93, 94, 99, 104, 111, 131, 134, 144, 148, 150, 155, 166, 169, 172, 178, 179, 182, 195, 201, 213, 252, 263, 278, 298, 310, 321, 325, 344, 358, 362, 385, 391, 392, 396, 399, 402, 403, 404, 424, 431, 436, 437, 446, 466, 472
Optimal DG location	_	25, 119, 166
Optimal DG size P	_	2479.0, 4134.0, 3061.0 kW
Minimum voltage/(Bus):	0.9300 p.u./(31)	0.9502 p.u./(34)

Source: Author's elaboration.

Figure 41 illustrates the convergence of the CPSO after network reconfiguration and installing 3 DG units along the iterations on a 415-bus system. In Figure 41, the fitness (optimal solution) was found in about 100 iterations.

Figure 41 – Convergence of CPSO after network reconfiguration and installing 3 DG units

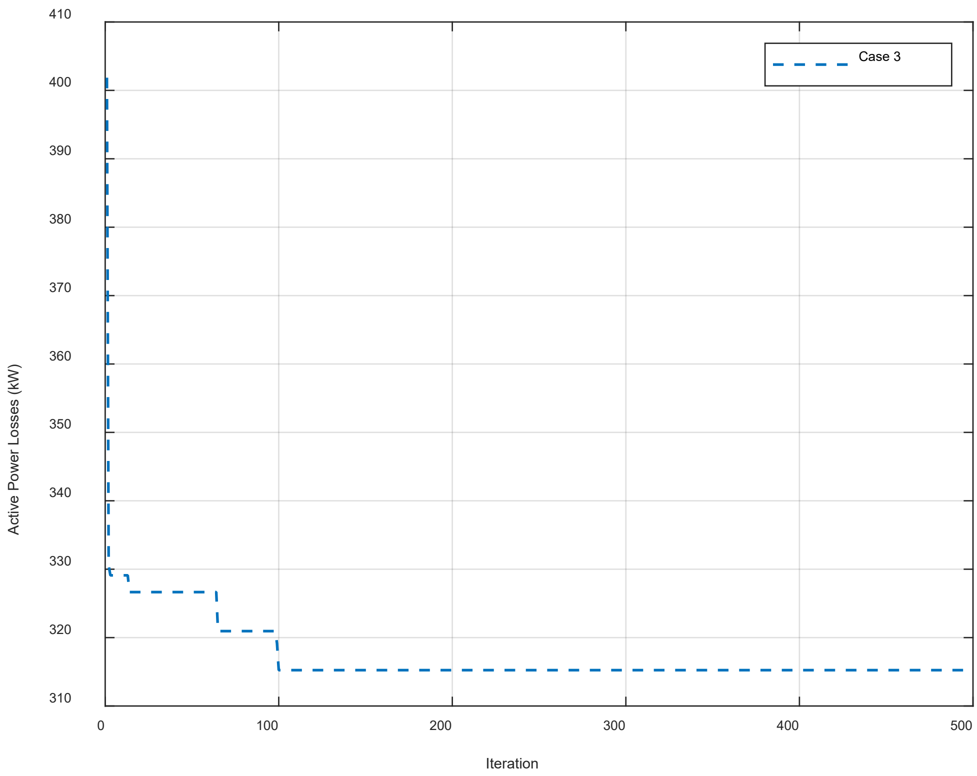

Source: Author's elaboration.

4.4.3 The simultaneous distribution network reconfiguration and the optimal location and size of 3 distributed generations (DGs) using chaotic particle swarm optimization (CPSO) algorithm

Figure 42 illustrates voltage profile variations before and after simultaneous network reconfiguration and installing 3 DG units on a 415-bus system. As shown in Figure 42 and Table 16, the power loss was 708.94 kW and minimum voltage was 0.9300 per-unit in base case. The power loss was reduced to 306.47 kW, thus having a reduction of 56.77 % compared to the base case. The minimum voltage was improved to 0.9616 per-unit after simultaneous network reconfiguration and installing 3 DG units. Also, the optimal location and size of DGs were obtained by the CPSO algorithm and 3 DG units with the capacity of 2980.0, 1374.0, and 3541.0 kW were allocated in buses 119, 131, and 150. The tie switches which were opened after simultaneous network reconfiguration and installing 3 DG units, were 1, 3, 5, 10, 14, 16, 31, 33, 51, 57, 60, 62, 87, 88, 94, 103, 105, 111, 132, 146, 148, 150, 154, 155, 168, 169, 179, 183, 188, 199, 205, 211, 214, 228, 256, 274, 294, 297, 325, 330, 341, 344, 363, 364, 370, 380, 385, 395, 402, 404, 407, 419, 423, 424, 435, 436, 441, 454, and 467.

Figure 42 – Voltage profile variations before and after simultaneous network reconfiguration and installing 3 DG units

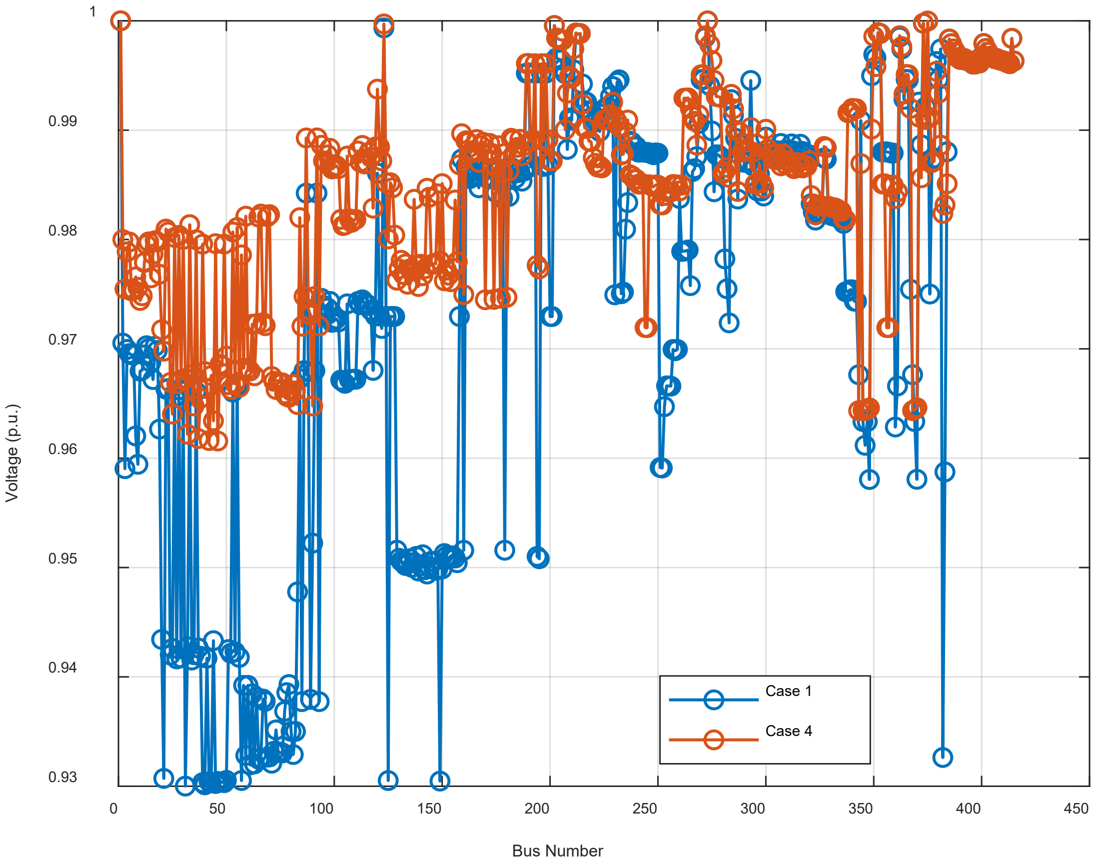

Source: Author's elaboration.

Table 16 – Simulation results before and after simultaneous network reconfiguration and installing 3 DG units using CPSO

Simulation results of 415-bus distribution network		
	Base Case	Simultaneous network reconfiguration and 3 DGs
Active power loss:	708.94 kW	306.47 kW
Reactive power loss:	538.48 kVAr	234.70 kVAr
Active power loss reduction:	_	56.77 %
Tie switches:	1, 5, 15, 16, 26, 31, 53, 54, 55, 75, 82, 94, 96, 97, 106, 107, 119, 136, 138, 154, 155, 156, 168, 169, 177,	1, 3, 5, 10, 14, 16, 31, 33, 51, 57, 60, 62, 87, 88, 94, 103, 105, 111, 132, 146, 148, 150, 154, 155, 168, 169, 179, 183, 188, 199, 205, 211, 214, 228, 256, 274, 294, 297, 325,

	179, 194, 195, 201, 207, 211, 214, 219, 241, 256, 258, 282, 297, 302, 314, 321, 354, 359, 362, 364, 385, 388, 395, 396, 404, 407, 423, 424, 426, 431, 436, 445, 446, 449	330, 341, 344, 363, 364, 370, 380, 385, 395, 402, 404, 407, 419, 423, 424, 435, 436, 441, 454, 467
Optimal DG location	_	119, 131, 150
Optimal DG size P	_	2980.0, 1374.0, 3541.0 kW
Minimum voltage/(Bus):	0.9300 p.u./(31)	0.9616 p.u./(46)

Source: Author's elaboration.

Figure 43 illustrates the convergence of the CPSO after simultaneous network reconfiguration and installing 3 DG units along the iterations on a 415-bus system. In Figure 43, the fitness (optimal solution) was found in about 220 iterations.

Figure 43 – Convergence of CPSO after simultaneous network reconfiguration and installing 3 DG units

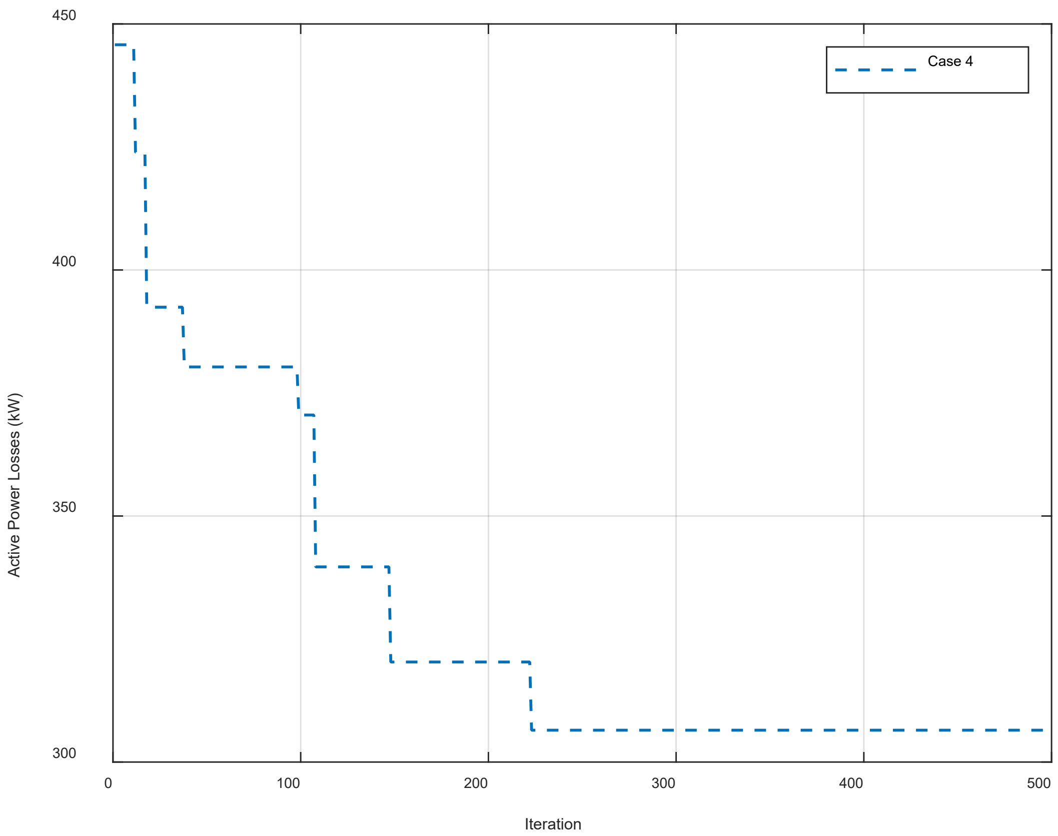

Source: Author's elaboration.

As shown in Figure 44, a comparison was made between 4 scenarios in voltage profile variations on a 415-bus system. A comparison of convergence between 3 scenarios in a 415-bus system is shown in Figure 45. Table 17 shows that the power loss reduction percentage and voltage profile improvement for Case 4 is more significant than the other cases.

Figure 44 – Comparison of voltage profile variations in 4 scenarios

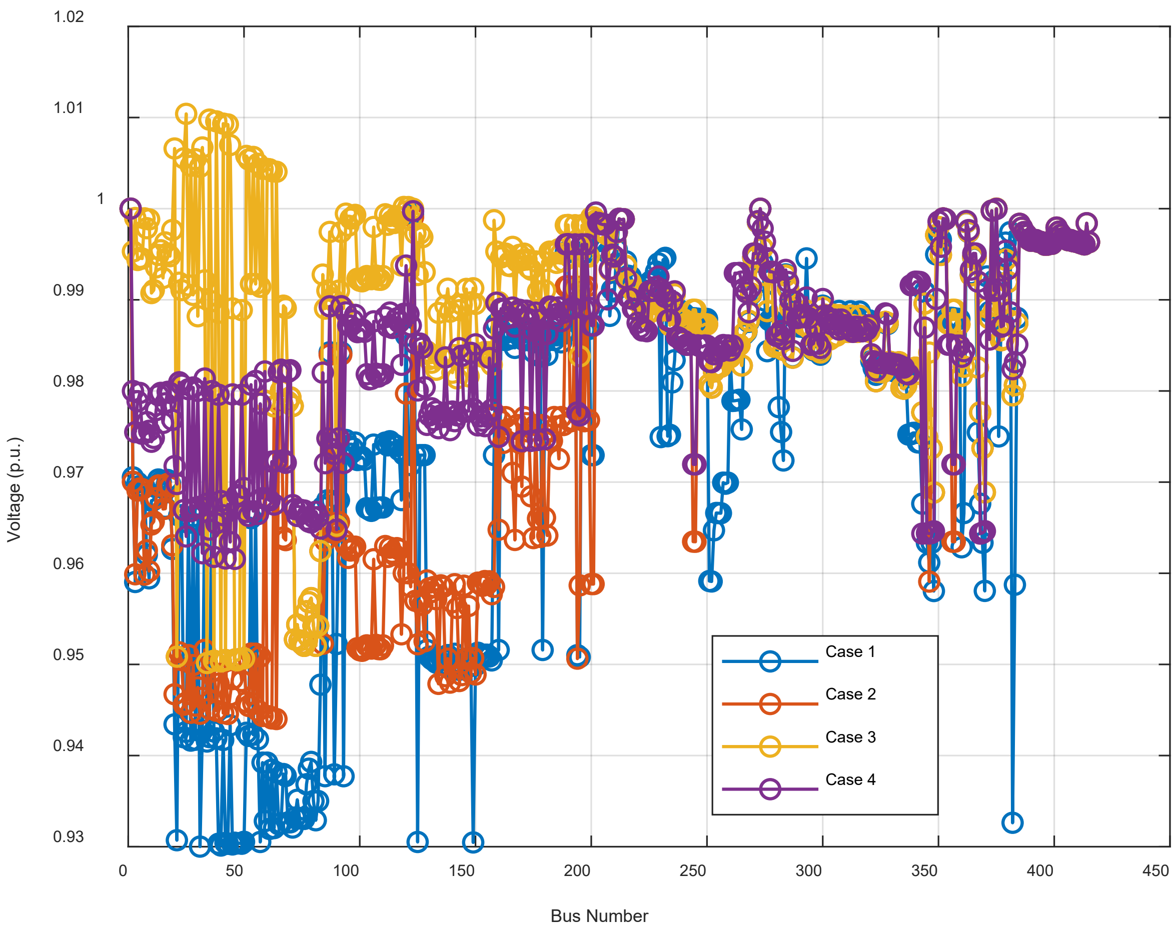

Source: Author's elaboration.

Figure 45 – Comparison of convergence in 3 scenarios

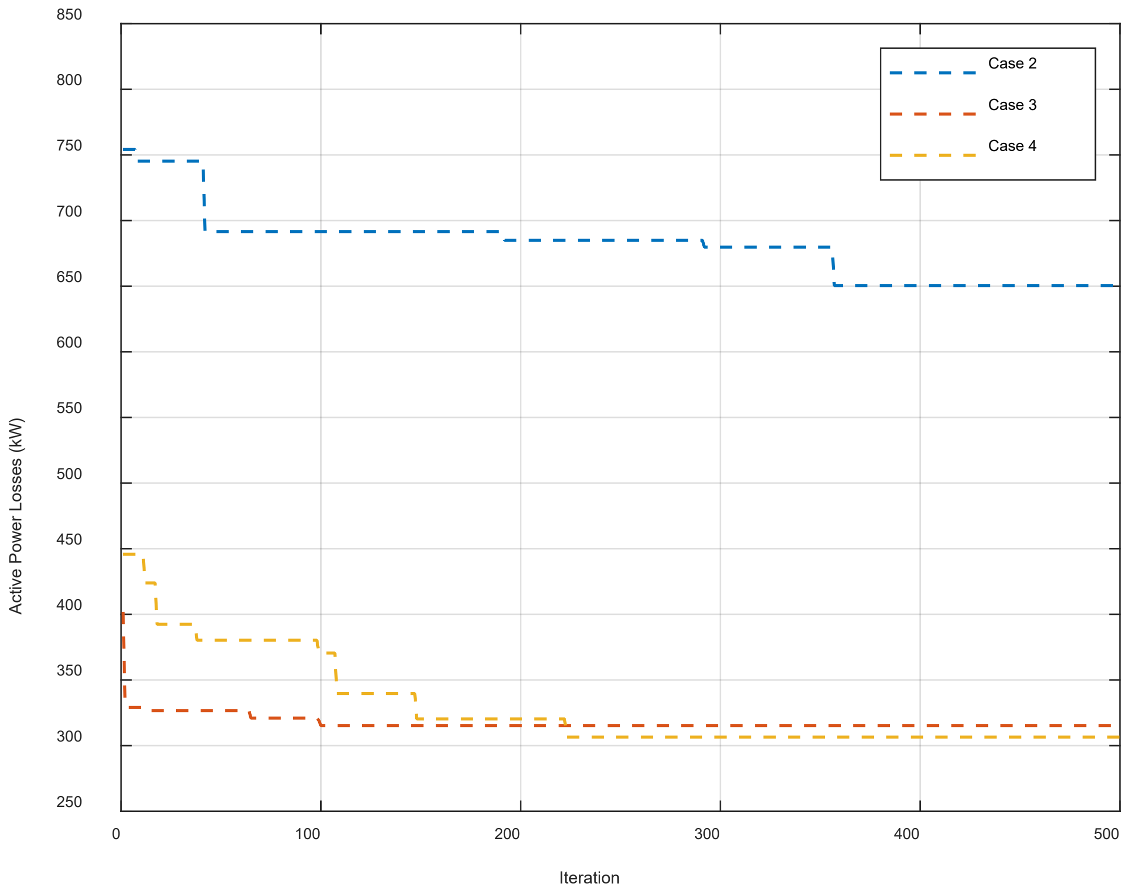

Source: Author's elaboration.

Table 17 – Summary of the results for the 415-bus network

Item	Case 1	Case 2	Case 3	Case 4
Tie switches	1-5-15-16-26-31-53-54-55-75-82-94-96-97-106-107-119-136-138-154-155-156-168-169-177-179-194-195-201-207-211-214-219-241-256-258-282-297-302-314-321-	1-5-11-12-13-30-31-45-50-55-60-61-86-87-93-94-99-104-111-131-134-144-148-150-155-166-169-172-178-179-182-195-201-213-252-263-278-298-310-321-325-344-358-	1-5-11-12-13-30-31-45-50-55-60-61-86-87-93-94-99-104-111-131-134-144-148-150-155-166-169-172-178-179-182-195-201-213-252-263-278-298-310-321-325-344-358-	1-3-5-10-14-16-31-33-51-57-60-62-87-88-94-103-105-111-132-146-148-150-154-155-168-169-179-183-188-199-205-211-214-228-256-274-294-297-325-330-341-344-

	354-359-362-364-385-388-395-396-404-407-423-424-426-431-436-445-446-449	362-385-391-392-396-399-402-403-404-424-431-436-437-446-466-472	362-385-391-392-396-399-402-403-404-424-431-436-437-446-466-472	363-364-370-380-385-395-402-404-407-419-423-424-435-436-441-454-467
P_{DG} (kW)/(Bus)	– – –	– – –	2479.0/(25) 4134.0/(119) 3061.0/(166)	2980.0/(119) 1374.0/(131) 3541.0/(150)
P_L (kW)	708.94	650.43	315.24	306.47
Q_L (kVAr)	538.48	548.31	239.00	234.70
P_L reduction (%)	–	8.25	55.53	56.77
$V_{\min}$ (p.u.)	0.9300	0.9440	0.9502	0.9616
Time (s)	21.4	1540200	1056744.2	1127495

Source: Author's elaboration.

5 CONCLUSIONS

Distribution network has important role for delivering electrical power generated by power stations to consumers, in which its power losses is more than generation and transmission systems. Using computational simulations, as expected, it appears that power loss can be significantly reduced by reconfiguring the primary distribution network and installing DG units.

Voltage levels are optimized in all simulated cases. In some cases, the initial configuration had unstable and critical voltage levels. In these scenarios, the voltage levels were increased to the considered adequate levels by implementing the reconfiguration and installing DG units by the meta-heuristic.

The optimization configurations shown to reduce power loss were effective in improving voltage levels as expected. The obtained results for those topologies show, in some cases, minimum voltage values very close to those obtained with the optimization topologies shown to improve voltage levels. Therefore, it is concluded that in those cases, the implementation of optimization topologies is more advantageous to reduce the losses, it is now able to adjust the voltage levels and provide a further reduction in the percentage of power loss.

Integrating chaotic motion with PSO allows much improvement in the searching capabilities of the PSO. Although PSO can converge quickly to good solution, yet it can easily get trapped in a local optimum. On the other hand, chaotic motion can traverse every state in a certain region and every state is visited only once. Chaos search has a very special ability to avoid being trapped in local optima. On the other hand, it often needs a large number of iterations to reach the global optimum and is not effective in large searching space. Therefore, a chaotic PSO is shown to be a good approach.

It is concluded that the developed system is based on an adequate methodology to assist energy distribution planning activities that aim to optimize the percentage of power loss and adjust the grid voltage levels using reconfiguration and DG units. It can provide viable topologies, which satisfy the radial constraints and optimize the predefined parameters.

The proposed model is tested on IEEE 33-bus and IEEE 69-bus, 136-bus, and 415-bus distribution networks considering and without considering reconfiguration and

DG units. DG units can reduce network losses by generating the power at the load points and therefore they reduce the network costs.

In future research, the impact of photovoltaics, wind turbines, sea and ocean wave power, and tidal power will be investigated, which Brazil has a great talent and capacity in extraction and exploitation of the aforementioned forces. It can also be optimized to reduce the installation of DGs in the distribution network on the issue of the location and capacity increase of DGs so that it is economically affordable for the beneficiary.

REFERENCES

ABDI, H.; DEHNAVI, E.; MOHAMMADI, F. Dynamic economic dispatch problem integrated with demand response (DEDDR) considering non-linear responsive load models. *IEEE Trans. Smart Grid*, New York, v. 7, n. 6, p. 2586-2595, 2016.

AGHAJANI, G.; GHADIMI, N. Multi-objective energy management in a microgrid. *Energy Reports*, Amsterdam, v. 4, p. 218-225, 2018.

AMIN, U.; HOSSAIN, M. J.; FERNANDEZ, E. Optimal price based control of HVAC systems in multizone office buildings for demand response. *Journal of Cleaner Production*, Amsterdam, v. 270, p. 122059, 2020.

BAYAT, A.; BAGHERI, A.; NOROOZIAN, R. Optimal siting and sizing of distributed generation accompanied by reconfiguration of distribution networks for maximum loss reduction by using a new UVDA-based heuristic method. *International Journal of Electrical Power & Energy Systems*, Oxford, v. 77, p. 360-371, 2016.

BERNAL-AGUSTIN, J. L. *Application of genetic algorithms to the optimal design of power distribution systems*. 1998. 346 f. Thesis (Doctorate in Electrical Engineering) - University of Zaragoza, Zaragoza, 1998.

BISWAS, S.; GOSWAMI, S. K.; CHATTERJEE, A. Optimum distributed generation placement with voltage sag effect minimization. *Energy Conversion and Management*, Amsterdam, v. 53, n. 1, p. 163-174, 2012.

BOMPARD, E.; CARPANETO, E.; CHICCO, G.; NAPOLI, R. Convergence of the backward/forward sweep method for the load-flow analysis of radial distribution systems. *International Journal of Electrical Power & Energy Systems*, Oxford, v. 22, n. 7, p. 521-530, 2000.

BORGES, C. L. T.; FALCÃO, D. M. Optimal distributed generation allocation for reliability, losses, and voltage improvement. *International Journal of Electrical Power & Energy Systems*, Oxford, v. 28, n. 6, p. 413-420, 2006.

BORNAPOUR, M.; HOOSHMAND, R.-A.; PARASTEGARI, M. An efficient scenario-based stochastic programming method for optimal scheduling of CHP-PEMFC, WT, PV and hydrogen storage units in micro grids. *Renewable Energy*, Amsterdam, v. 130, p. 1049-1066, 2019.

CELLI, G.; GHIANI, E.; MOCCI, S.; PILO, F. A multiobjective envolutionary algorithm for the sizing and siting of distributed generation. *IEEE Transactions on Power Systems*, New York, v. 20, n. 2, p. 750-757, 2005.

CHOUDHRY, M. A.; KHAN, H. Power loss reduction in radial distribution system with multiple distributed energy resources through efficient islanding detection. *Energy*, Paisley, v. 35, n. 12, p. 4843-4861, 2010.

DAS, D. Reconfiguration of distribution system using fuzzy multi-objective approach. *International Journal of Electrical Power & Energy Systems*, Oxford, v. 28, n. 5, p. 331-338, 2006.

DEVARAJ, D.; ROSELYN, J. P. Genetic algorithm based reactive power dispatch for voltage stability improvement. *International Journal of Electrical Power & Energy Systems*, Oxford, v. 32, n. 10, p. 1151-1156, 2010.

EDDAHECH, A.; CHTOUROU, S.; CHTOUROU, M. Hierarchical neural networks based prediction and control of dynamic reconfiguration for multilevel embedded systems. *Journal of Systems Architecture*, Amsterdam, v. 59, n. 1, p. 48-59, 2013.

EL-KHATTAM, W.; SALAMA, M. M. A. Distributed generation technologies, definitions and benefits. *Electric Power System Research*, Amsterdam, v. 71, p. 119-128, 2004.

EL-ZONKOLY, A. M. Optimal placement of multi-distributed generation units including different load models using particle swarm optimization. *Swarm and Evolutionary Computation*, Amsterdam, v. 1, n. 1, p. 50-59, 2011.

FATHABADI, H. Power distribution network reconfiguration for power loss minimization using novel dynamic fuzzy c-means (dFCM) clustering based ANN approach. *International Journal of Electrical Power & Energy Systems*, Oxford, v. 78, p. 96-107, 2016.

GHATAK, U.; MUKHERJEE, V. A fast and efficient load flow technique for unbalanced distribution system. *International Journal of Electrical Power & Energy Systems*, Oxford, v. 84, p. 99-110, 2017.

GRAINGER, J.; LEE, S. H. Optimal size and location of shunt capacitors for reduction of losses in distribution feeders. *IEEE Trans. Power App. Syst.*, New York, v. PAS-100, p. 1105–1118, 1981.

GRIES, D.; SCHNEIDER, F. B. *Fundamentals of the new artificial intelligence*. 2. ed. London: Springer, 2008. 256 p.

HAMOUDA, A.; ZEHAR, K. Improved algorithm for radial distribution networks load flow solution. *International Journal of Electrical Power & Energy Systems*, Oxford, v. 33, n. 3, p. 508-514, 2011.

HEFNY, H. A.; AZAB, S. S. Chaotic particle swarm optimization. In: *2010 The 7th International Conference on Informatics and Systems (INFOS)*. Cairo, 2010, 1-8.

KASHEM, M. A.; MOGHAVVEMI, M.; MOHAMED, A.; JASMON, G. B. Artificial neural network approach to network reconfiguration for loss minimization in distribution networks. *International Journal of Electrical Power & Energy Systems*, Oxford, v. 20, n. 4, p. 247-258, 1998a.

KASHEM, M. A.; MOGHAVVEMI, M.; MOHAMED, A.; JASMON, G. B. Loss reduction in distribution networks using new network reconfiguration algorithm. *Electric Machines and Power System*, London, v. 26, n. 8, p. 815-829, 1998b.

KIM, K. H.; LEE, Y. J.; RHEE, S. B.; LEE, S. K.; YOU, S. K. Dispersed generation placement using fuzzy- GA in distribution system. In: *Proceedings of IEEE Power Engineering Society Summer Meeting*. Chicago, 2002, vol. 3, 1148-1153.

KUSAKANA, K. Optimal energy management of a grid-connected dual-tracking photovoltaic system with battery storage: case of a microbrewery under demand response. *Energy*, Paisley, v. 212, p. 118782, 2020.

LAMONT, J. W.; OBESSIS, E. V. Emission dispatch models and algorithms for the 1990s. *IEEE Trans PWRS*, New York, v. 10, n. 2, p. 941–947, 1995.

LIU, B.; WANG, L.; JIN, Y.-H.; TANG, F.; HUANG, D.-X. Improved particle swarm optimization combined with chaos. *Chaos, Solitons & Fractals*, Amsterdam, v. 25, n. 5, p. 1261-1271, 2005.

MAHDAVI, E. *Reconfiguration of distribution networks with simultaneous allocation of distributed generation using the whale optimization algorithm*. 2023. 154 f. : il. Thesis (Doctorate in Electrical Engineering) - Universidade Estadual Paulista, Faculdade de Engenharia de Ilha Solteira, Ilha Solteira, 2023.

MANTOVANI, J. R. S.; CASARI, F.; ROMERO, R. A. Reconfiguração de sistemas de distribuição radiais utilizando o critério de queda de tensão. *Controle and Automação*, Campinas, v. 11, n. 3, p. 150-159, 2000.

MASOUM, M. A. S.; JAFARIAN, A.; LADJEVARDI, M.; FUCHS, E. F.; GRADY, W. M. Fuzzy approach for optimal placement and sizing of capacitor banks in the presence of harmonics. *IEEE Transactions on Power Delivery*, New York, v. 19, n. 2, p. 822-829, 2004.

MITHULANANTHAN, N.; THAN, O. Distributed generator placement to maximize the loadability of distribution system. *International Journal of Electrical Engineering Education*, Manchester, v. 43, n. 2, p. 107-118, 2006.

NARA, K.; HAYASHI, Y.; IKEDA, K.; ASHIZAWA, T. Application of tabu search to optimal placement of distributed generators. In: *IEEE Power Engineering Society Winter Meeting*. Columbus, 2001, vol. 2, 918-923.

NAVEEN, S.; KUMAR, K. S.; RAJALAKSHMI, K. Distribution system reconfiguration for loss minimization using modified bacterial foraging optimization algorithm. *International Journal of Electrical Power & Energy Systems*, Oxford, v. 69, p. 90-97, 2015.

NEDJAH, N.; MOURELLE, L. *Swarm intelligent systems.* 2006th. ed. (Studies in Computational Intelligence (SCI)). Berlin, Germany: Springer, 2006.

NGUYEN, T. T.; TRUONG, A. V.; PHUNG, T. A. A novel method based on adaptive cuckoo search for optimal network reconfiguration and distributed generation allocation in distribution network. *International Journal of Electrical Power & Energy Systems*, Oxford, v. 78, p. 801-815, 2016.

NIKMEHR, N.; RAVADANEGH, S. N. Optimal operation of distributed generations in micro-grids under uncertainties in load and renewable power generation using heuristic algorithm. *IET Renew. Power Gener.*, London, v. 9, n. 8, p. 982–990, 2015.

NIKNAM, T. A new approach based on ant colony optimization for daily Volt/Var control in distribution networks considering distributed generators. *Energy Conversion and Management*, Amsterdam, v. 49, n. 12, p. 3417-3424, 2008.

NIKNAM, T. A new HBMO algorithm for multiobjective daily Volt/Var control in distribution systems considering distributed generators. *Applied Energy*, Amsterdam, v. 88, n. 3, p. 778–788, 2011.

NIKNAM, T.; -BAHMAN, B. B.; OSTADI, A. A new fuzzy adaptive particle swarm optimization for daily Volt/Var control in distribution networks considering distributed generators. *Applied Energy*, Amsterdam, v. 87, n. 6, p. 1919-1928, 2010.

OLAMAEI, J.; NIKNAM, T.; GHAREHPETIAN, G. Application of particle swarm optimization for distribution feeder reconfiguration considering distributed generators. *Applied Mathematics and Computation*, New York, v. 201, n. 1-2, p. 575-586, 2008.

PEGADO, R.; ÑAUPARI, Z.; MOLINA, Y.; CASTILLO, C. Radial distribution network reconfiguration for power losses reduction based on improved selective BPSO. *Electric Power Systems Research*, Amsterdam, v. 169, p. 206-213, 2019.

RADHA, B.; KING, R. A.; RUGHOOPUTH, H. Optimal network reconfiguration of electrical distribution systems. In: *Proc. of IEEE International Conference on Industrial Technology*. Maribor, 2003, vol. 1, 66-71.

RAJ, P.; GUPTA, P.; SHARMA, D. K.; SHARMA, N. K.; YADAV, B. Advantage of kirchhoff law in electrical circuit. *Journal of Emerging Technologies and Innovative Research (JETIR)*, Ahmedabad, v. 4, n. 10, p. 177-180, 2017.

RAJARAM, R.; KUMAR, K. S.; RAJASEKAR, N. Power system reconfiguration in a radial distribution network for reducing losses and to improve voltage profile using modified plant growth simulation algorithm with distributed generation (DG). *Energy Reports*, Amsterdam, v. 1, p. 116-122, 2015.

RAMADAN, H. S.; HELMI, A. M. Optimal reconfiguration for vulnerable radial smart grids under uncertain operating conditions. *Computers & Electrical Engineering*, Kidlington, v. 93, p. 107310, 2021.

SANTOS, S. F.; FITIWI, D. Z.; CRUZ, M. R. M.; CABRITA, C. M. P.; CATALÃO, J. P. S. Impacts of optimal energy storage deployment and network reconfiguration on renewable integration level in distribution systems. *Applied Energy*, Amsterdam, v. 185, n. 1, p. 44-55, 2017.

SAVIER, J. S.; DAS, D. Loss allocation to consumers before and after reconfiguration of radial distribution networks. *International Journal of Electrical Power & Energy Systems*, Oxford, v. 33, n. 3, p. 540-549, 2011.

SHIRMOHAMMADI, D. Service restoration in distribution network via network reconfiguration. *IEEE Trancs. Power Delivery*, New York, v. 7, p. 952-958, 1992.

SHIRMOHAMMADI, D.; HONG, H. W.; SEMLYEN, A.; LUO, G. X. A compensation-based power flow method for weakly meshed distribution and transmission networks. *IEEE Transactions on Power Systems*, New York, v. 3, n. 2, p. 753-762, 1988.

SINGH, S.; SINGH, M.; KAUSHIK, S. C. Optimal power scheduling of renewable energy systems in microgrids using distributed energy storage system. *Renewable Power Generation, IET*, London, v. 10, n. 9, p. 1328-1339, 2016.

SOLIMAN, M.; ABDELAZIZ, A. Y.; EL-HASSANI, R. M. Distribution power system reconfiguration using whale optimization algorithm. *International Journal of Applied Power Engineering (IJAPE)*, Semarang, v. 9, n. 1, p. 48-57, 2020.

SONG, Y.; CHEN, Z.; YUAN, Z. New chaotic PSO-based neural network predictive control for nonlinear process. *IEEE Transactions on Neural Networks*, New York, v. 18, p. 595-601, 2007.

SWARNKAR, A.; GUPTA, N.; NIAZI, K. R. Adapted ant colony optimization for efficient reconfiguration of balanced and unbalanced distribution systems for loss minimization. *Swarm and Evolutionary Computation*, Amsterdam, v. 1, n. 3, p. 129-137, 2011. https://doi.org/10.1016/j.swevo.2011.05.004.

TABANJAT, A.; BECHERIF, M.; HISSEL, D. Reconfiguration solution for shaded PV panels using switching control. *Renewable Energy*, Amsterdam, v. 82, p. 4-13, 2015.

TENG, J. H.; CHANG, C.-Y. Backward/forward sweep- based harmonic analysis method for distribution systems. *IEEE Transactions on Power Delivery*, New York, v. 22, n. 3, p. 1665-1672, 2007.

THAKAR, S.; A.S., V.; DOOLLA, S. System reconfiguration in microgrids. *Sustainable Energy, Grids and Networks*, Amsterdam, v. 17, p. 100191, 2019.

TIRANUCHIT, A.; THOMAS, R. J. A posturing strategy against voltage instabilities in electric power systems. *IEEE Transactions on Power Systems*, New York, v. 3, n. 1, p. 87-93, 1988.

TRAN, T. T.; TRUONG, K. H.; VO, D. N. Stochastic fractal search algorithm for reconfiguration of distribution networks with distributed generations. *Ain Shams Engineering Journal*, Cairo, v. 11, n. 2, p. 389-407, 2020.

TRIFUNOVIC, J.; MIKULOVIC, J.; DJURISIC, Z.; KOSTIC, M. Reductions in electricity losses in the distribution power system in case of the mass use of compact fluorescent lamps. *Electric Power Systems Research*, Amsterdam, v. 81, n. 2, p. 465-477, 2011.

WU, Y.-K.; LEE, C.-Y.; LIU, L.-C.; TSAI, S.-H. Study of reconfiguration for the distribution system with distributed generators. *IEEE Transactions on Power Delivery*, New York, v. 25, n. 3, p. 1678-1685, 2010.

XIANG, Y.; LIU, J.; LIU, Y. Robust energy management of microgrid with uncertain renewable generation and load. *IEEE Trans. Smart Grid*, New York, v. 7, n. 2, p. 1034-1043, 2016.

YASIN, Z. M.; RAHMAN, T. K. Influence of distributed generation on distribution network performance during network reconfiguration for service restoration. In: *Proc. of the IEEE International Power and Energy Conf. PECon*. Putra Jaya, 2006, 566-570.

ZAKARIAZADEH, A.; JADID, S.; SIANO, P. Smart microgrid energy and reserve scheduling with demand response using stochastic optimization. *International Journal of Electrical Power & Energy Systems*, Oxford, v. 63, p. 523-533, 2014.

ZANGENEH, A.; JADID, S. Fuzzy multiobjective model for distributed generation expansion planning in uncertain environment. *European Transactions on Electrical Power*, Hoboken, v. 21, n. 1, p. 129-141, 2010.

APPENDIX A – 33-BUS SYSTEM DATA

The complete case study data of the 33-bus distribution system is presented in this appendix.

The data of the 33-bus system was described in Table 18 (SOLIMAN *et al*., 2020).

- Substation bus: 1;
- Base voltage: 12.66 kV;
- Base power: 100 MVA.

Table 18 – The data of 33-bus test system

Bus	P [kW]	Q [kVAr]	Branch Node	From Node	To Node	Resistance [Ω]	Reactance [Ω]
1	0	0	1	1	2	0.0922	0.047
2	100	60	2	2	3	0.493	0.2511
3	90	40	3	3	4	0.366	0.1864
4	120	80	4	4	5	0.3811	0.1941
5	60	30	4	5	6	0.819	0.707
6	60	20	6	6	7	0.1872	0.6188
7	200	100	7	7	8	0.7114	0.2351
8	200	100	8	8	9	1.03	0.74
9	60	20	9	9	10	1.044	0.74
10	60	20	10	10	11	0.1966	0.065
11	45	30	11	11	12	0.3744	0.1238
12	60	35	12	12	13	1.468	1.155
13	60	35	13	13	14	0.5416	0.7129
14	120	80	14	14	15	0.591	0.526
15	60	10	15	15	16	0.7463	0.545
16	60	20	16	16	17	1.289	1.721
17	60	20	17	17	18	0.732	0.574
18	90	40	18	2	19	0.164	0.1565
19	90	40	19	19	20	1.5042	1.3554

20	90	40	20	20	21	0.4095	0.4784
21	90	40	21	21	22	0.7089	0.9373
22	90	40	22	3	23	0.4512	0.3083
23	90	50	23	23	24	0.898	0.7091
24	420	200	24	24	25	0.896	0.7011
25	420	200	25	6	26	0.203	0.1034
26	60	25	26	26	27	0.2842	0.1447
27	60	25	27	27	28	1.059	0.9337
28	60	20	28	28	29	0.8042	0.7006
29	120	70	29	29	30	0.5075	0.2585
30	200	600	30	30	31	0.9744	0.963
31	150	70	31	31	32	0.3105	0.3619
32	210	100	32	32	33	0.341	0.5302
33	60	40	33	8	21	2	2
34	0	0	34	9	15	2	2
35	0	0	35	12	22	2	2
36	0	0	36	18	33	0.5	0.5
37	**3715**	**2300**	37	25	29	0.5	0.5

Source: Soliman *et al*. (2020).

APPENDIX B – 69-BUS SYSTEM DATA

The complete case study data of the 69-bus distribution system is presented in this appendix.

The data of the 69-bus system was described in Table 19 (SOLIMAN *et al*., 2020).

- Substation bus: 1;
- Base voltage: 12.66 kV;
- Base power: 100 MVA.

Table 19 – The data of 69-bus test system

Bus	P [kW]	Q [kVAr]	Branch Node	From Node	To Node	Resistance [Ω]	Reactance [Ω]
1	0	0	1	1	2	0.0005	0.0012
2	0	0	2	2	3	0.0005	0.0012
3	0	0	3	3	4	0.0015	0.0036
4	0	0	4	4	5	0.0251	0.0294
5	0	0	5	5	6	0.366	0.1864
6	2.6	2.2	6	6	7	0.3811	0.1941
7	40.4	30	7	7	8	0.0922	0.047
8	75	54	8	8	9	0.0493	0.0251
9	30	22	9	9	10	0.819	0.2707
10	28	19	10	10	11	0.1872	0.0619
11	145	104	11	11	12	0.7114	0.2351
12	145	104	12	12	13	1.03	0.34
13	8	5	13	13	14	1.044	0.345
14	8	5.5	14	14	15	1.058	0.3496
15	0	0	15	15	16	0.1966	0.065
16	45.5	30	16	16	17	0.3744	0.1238
17	60	35	17	17	18	0.0047	0.0016
18	60	35	18	18	19	0.3276	0.1083
19	0	0	19	19	20	0.2106	0.069

20	1	0.6	20	20	21	0.3416	0.1129
21	114	81	21	21	22	0.014	0.0046
22	5	3.5	22	22	23	0.1591	0.0526
23	0	0	23	23	24	0.3463	0.1145
24	28	20	24	24	25	0.7488	0.2475
25	0	0	25	25	26	0.3089	0.1021
26	14	10	26	26	27	0.1732	0.0572
27	14	10	27	3	28	0.0044	0.0108
28	26	18.6	28	28	29	0.064	0.1565
29	26	18.6	29	29	30	0.3978	0.1315
30	0	0	30	30	31	0.0702	0.0232
31	0	0	31	31	32	0.351	0.116
32	0	0	32	32	33	0.839	0.2816
33	14	10	33	33	34	1.708	0.5646
34	19.5	14	34	34	35	1.474	0.4873
35	6	4	35	3	36	0.0044	0.0108
36	26	18.55	36	36	37	0.064	0.1565
37	26	18.55	37	37	38	0.1053	0.123
38	0	0	38	38	39	0.0304	0.0355
39	24	17	39	39	40	0.0018	0.0021
40	24	17	40	40	41	0.7283	0.8509
41	1.2	1	41	41	42	0.31	0.3623
42	0	0	42	42	43	0.041	0.0478
43	6	4.3	43	43	44	0.0092	0.0116
44	0	0	44	44	45	0.1089	0.1373
45	39.22	26.3	45	45	46	0.0009	0.0012
46	39.22	26.3	46	4	47	0.0034	0.0084
47	0	0	47	47	48	0.0851	0.2083
48	79	56.4	48	48	49	0.2898	0.7091
49	384.7	274.5	49	49	50	0.0822	0.2011
50	384.7	274.5	50	8	51	0.0928	0.0473
51	40.5	28.3	51	51	52	0.3319	0.1114
52	3.6	2.7	52	9	53	0.174	0.0886

53	4.35	3.5	53	53	54	0.203	0.1034
54	26.4	19	54	54	55	0.2842	0.1447
55	24	17.2	55	55	56	0.2813	0.1433
56	0	0	56	56	57	1.59	0.5337
57	0	0	57	57	58	0.7837	0.263
58	0	0	58	58	59	0.3042	0.1006
59	100	72	59	59	60	0.3861	0.1172
60	0	0	60	60	61	0.5075	0.2585
61	1244	888	61	61	62	0.0974	0.0496
62	32	23	62	62	63	0.145	0.0738
63	0	0	63	63	64	0.7105	0.3619
64	227	162	64	64	65	1.041	0.5302
65	59	42	65	11	66	0.2012	0.0611
66	18	13	66	66	67	0.0047	0.0014
67	18	13	67	12	68	0.7394	0.2444
68	28	20	68	68	69	0.0047	0.0016
69	28	20	69	11	43	0.5	0.5
70	0	0	70	13	21	0.5	0.5
71	0	0	71	15	46	1	1
72	0	0	72	50	59	2	2
73	**3802**	**2694.1**	73	27	65	1	1

Source: Soliman *et al*. (2020).

APPENDIX C – 136-BUS SYSTEM DATA

The complete case study data of the 136-bus distribution system is presented in this appendix.

The data of the 136-bus system was described in Table 20 (MANTOVANI *et al.*, 2000).

- Substation bus: 136;
- Base voltage: 13.80 kV;
- Base power: 100 MVA.

Table 20 – The data of 136-bus test system

Bus	P [kW]	Q [kVAr]	Branch Node	From Node	To Node	Resistance [Ω]	Reactance [Ω]
1	0	0	1	136	1	0.33205	0.76653
2	47.78	19.009	2	1	2	0.00188	0.00433
3	42.55	16.929	3	2	3	0.22324	0.51535
4	87.02	34.622	4	3	4	0.09943	0.22953
5	311.31	123.855	5	4	5	0.15571	0.35945
6	148.869	59.228	6	5	6	0.16321	0.37677
7	238.672	94.956	7	6	7	0.11444	0.26417
8	62.3	24.786	8	6	8	0.05675	0.05666
9	124.598	49.571	9	8	9	0.52124	0.27418
10	140.175	55.768	10	8	10	0.10877	0.1086
11	116.813	46.474	11	10	11	0.39803	0.20937
12	249.203	99.145	12	10	12	0.91744	0.31469
13	291.447	115.952	13	10	13	0.11823	0.11805
14	303.72	120.835	14	13	14	0.50228	0.26421
15	215.396	85.695	15	13	15	0.05675	0.05666
16	198.586	79.007	16	15	16	0.29379	0.15454
17	0	0	17	136	17	0.33205	0.76653
18	0	0	18	17	18	0.00188	0.00433

19	0	0	19	18	19	0.22324	0.51535
20	30.13	14.729	20	19	20	0.10881	0.25118
21	230.972	112.92	21	20	21	0.71078	0.37388
22	60.26	29.458	22	20	22	0.18197	0.42008
23	230.972	112.92	23	22	23	0.30326	0.15952
24	120.507	58.915	24	22	24	0.02439	0.0563
25	0	0	25	24	25	0.04502	0.10394
26	56.98	27.857	26	25	26	0.01876	0.04331
27	364.665	178.281	27	26	27	0.11823	0.11805
28	0	0	28	27	28	0.02365	0.02361
29	124.647	60.939	29	28	29	0.18954	0.0997
30	56.98	27.857	30	29	30	0.39803	0.20937
31	0	0	31	28	31	0.05675	0.05666
32	85.47	41.787	32	31	32	0.09477	0.04985
33	0	0	33	32	33	0.41699	0.21934
34	396.735	193.96	34	33	34	0.11372	0.05982
35	0	0	35	31	35	0.07566	0.07555
36	181.152	88.563	36	35	36	0.3696	0.19442
37	242.172	118.395	37	36	37	0.26536	0.13958
38	75.32	36.821	38	35	38	0.05675	0.05666
39	0	0	39	136	39	0.33205	0.76653
40	1.25	0.531	40	39	40	0.11819	0.27283
41	6.27	2.66	41	40	41	2.96288	1.01628
42	0	0	42	40	42	0.00188	0.00433
43	117.88	49.971	43	42	43	0.06941	0.16024
44	62.67	26.566	44	43	44	0.81502	0.42872
45	172.285	73.034	45	43	45	0.06378	0.14724
46	458.556	194.388	46	45	46	0.13132	0.30315
47	262.962	111.473	47	46	47	0.06191	0.14291
48	235.761	99.942	48	47	48	0.11444	0.26417
49	0	0	49	48	49	0.28374	0.28331
50	109.215	46.298	50	49	50	0.28374	0.28331
51	0	0	51	48	51	0.04502	0.10394

52	72.81	30.865	52	51	52	0.02626	0.06063
53	258.473	109.57	53	52	53	0.06003	0.13858
54	69.17	29.322	54	53	54	0.03002	0.06929
55	21.84	9.26	55	54	55	0.02064	0.04764
56	0	0	56	52	56	0.10881	0.25118
57	20.53	8.702	57	56	57	0.25588	0.1346
58	150.548	63.819	58	57	58	0.41699	0.21934
59	220.687	93.552	59	58	59	0.50228	0.26421
60	92.38	39.163	60	59	60	0.3317	0.17448
61	0	0	61	60	61	0.20849	0.10967
62	226.693	96.098	62	47	62	0.13882	0.32047
63	0	0	63	136	63	0.0075	0.01732
64	294.016	116.974	64	63	64	0.27014	0.62362
65	83.02	33.028	65	64	65	0.3827	0.88346
66	83.02	33.028	66	65	66	0.33018	0.7622
67	103.77	41.285	67	66	67	0.3283	0.75787
68	176.408	70.184	68	67	68	0.17072	0.39409
69	83.02	33.028	69	68	69	0.55914	0.29412
70	217.917	86.698	70	68	70	0.05816	0.13425
71	23.29	9.267	71	70	71	0.7013	0.3689
72	5.08	2.019	72	71	72	1.02352	0.53839
73	72.64	28.899	73	70	73	0.06754	0.15591
74	405.99	161.5235	74	73	74	1.32352	0.45397
75	0	0	75	136	75	0.01126	0.02598
76	100.182	42.468	76	75	76	0.72976	1.68464
77	142.523	60.417	77	76	77	0.22512	0.51968
78	96.04	40.713	78	77	78	0.20824	0.48071
79	300.454	127.366	79	78	79	0.0469	0.10827
80	141.238	59.873	80	79	80	0.6195	0.61857
81	279.847	118.631	81	80	81	0.34049	0.33998
82	87.31	37.013	82	81	82	0.56862	0.29911
83	243.849	103.371	83	81	83	0.10877	0.1086
84	247.75	105.025	84	83	84	0.56862	0.29911

85	0	0	85	136	85	0.01126	0.02598
86	89.88	38.101	86	85	86	0.41835	0.96575
87	1137.28	482.108	87	86	87	0.10499	0.13641
88	458.339	194.296	88	86	88	0.43898	1.01338
89	385.197	163.29	89	88	89	0.0752	0.02579
90	0	0	90	89	90	0.07692	0.17756
91	79.61	33.747	91	90	91	0.33205	0.76653
92	87.31	37.013	92	91	92	0.08442	0.19488
93	0	0	93	92	93	0.1332	0.30748
94	74	31.37	94	93	94	0.2932	0.29276
95	232.05	98.369	95	94	95	0.21753	0.21721
96	141.819	60.119	96	95	96	0.26482	0.26443
97	0	0	97	93	97	0.10318	0.23819
98	76.45	32.408	98	97	98	0.13507	0.31181
99	0	0	99	136	99	0.00938	0.02165
100	51.32	21.756	100	99	100	0.16884	0.38976
101	59.87	25.381	101	100	101	0.11819	0.27283
102	9.07	3.843	102	101	102	2.28608	0.78414
103	2.09	0.887	103	101	103	0.45587	1.05236
104	16.735	7.094	104	103	104	0.696	1.60669
105	1506.522	638.634	105	104	105	0.45774	1.05669
106	313.023	132.694	106	105	106	0.20298	0.26373
107	79.83	33.842	107	106	107	0.21348	0.27737
108	51.32	21.756	108	107	108	0.54967	0.28914
109	0	0	109	108	109	0.54019	0.28415
110	202.435	85.815	110	107	110	0.0455	0.05911
111	60.82	25.784	111	110	111	0.47385	0.24926
112	45.62	19.338	112	111	112	0.86241	0.45364
113	0	0	113	112	113	0.56862	0.29911
114	157.07	66.584	114	108	114	0.77711	0.40878
115	0	0	115	114	115	1.08038	0.5683
116	250.148	106.041	116	109	116	1.09933	0.57827
117	0	0	117	116	117	0.47385	0.24926

118	69.81	29.593	118	104	118	0.32267	0.74488
119	32.07	13.596	119	118	119	0.14633	0.33779
120	61.08	25.894	120	119	120	0.12382	0.28583
121	0	0	121	136	121	0.01126	0.02598
122	94.62	46.26	122	121	122	0.6491	1.49842
123	49.86	24.375	123	122	123	0.04502	0.10394
124	123.164	60.214	124	123	124	0.5264	0.18056
125	78.35	38.304	125	123	125	0.02064	0.04764
126	145.475	71.121	126	125	126	0.53071	0.27917
127	21.37	10.447	127	125	127	0.09755	0.2252
128	74.79	36.564	128	127	128	0.11819	0.27283
129	227.926	111.431	129	127	129	0.13882	0.32047
130	35.61	17.411	130	129	130	0.04315	0.09961
131	249.295	121.877	131	130	131	0.09192	0.2122
132	316.722	154.842	132	131	132	0.16134	0.37244
133	333.817	163.199	133	132	133	0.37832	0.37775
134	249.295	121.877	134	133	134	0.39724	0.39664
135	0	0	135	134	135	0.2932	0.29276
136	0	0	136	7	73	0.13132	0.30315
137	0	0	137	9	24	0.26536	0.13958
138	0	0	138	15	83	0.14187	0.14166
139	0	0	139	38	135	0.08512	0.08499
140	0	0	140	25	51	0.04502	0.10394
141	0	0	141	50	96	0.14187	0.14166
142	0	0	142	55	98	0.14187	0.14166
143	0	0	143	62	120	0.0394	0.09094
144	0	0	144	66	79	0.12944	0.29882
145	0	0	145	79	131	0.01688	0.03898
146	0	0	146	84	135	0.3317	0.17448
147	0	0	147	91	104	0.14187	0.14166
148	0	0	148	90	129	0.07692	0.17756
149	0	0	149	90	103	0.07692	0.17756
150	0	0	150	92	104	0.07692	0.17756

151	0	0	151	92	132	0.07692	0.17756
152	0	0	152	96	120	0.26482	0.26443
153	0	0	153	110	47	0.49696	0.64567
154	0	0	154	126	76	0.17059	0.08973
155	0	0	155	128	77	0.05253	0.12126
156	**18313.81**	**7932.534**	156	135	98	0.2932	0.29276

Source: Mantovani *et al*. (2000).

APPENDIX D – 415-BUS SYSTEM DATA

The complete case study data of the 415-bus distribution system is presented in this appendix.

The data of the 415-bus system was described in Table 21 (BERNAL-AGUSTIN, 1998).

- Substation bus: 1;
- Base voltage: 10.00 kV;
- Base power: 100 MVA.

Table 21 – The data of 415-bus test system

Bus	P [kW]	Q [kVAr]	Branch Node	From Node	To Node	Resistance [Ω]	Reactance [Ω]
1	0.1	0	1	384	68	0.0310675	0.02142
2	0.1	0	2	89	67	0.1078225	0.07434
3	122	59	3	225	224	0.069445	0.04788
4	0.1	0	4	21	72	0.193715	0.13356
5	0.1	0	5	66	384	0.0347225	0.02394
6	114	55	6	3	20	0.610385	0.42084
7	51	25	7	224	222	0.069445	0.04788
8	83	40	8	72	74	0.02193	0.01512
9	0.1	0	9	70	382	0.0310675	0.02142
10	122	59	10	20	51	0.08772	0.06048
11	122	59	11	222	221	0.08772	0.06048
12	77	37	12	76	72	0.054825	0.0378
13	0.1	0	13	382	66	0.032895	0.02268
14	68	33	14	51	52	0.069445	0.04788
15	71	34	15	221	220	0.084065	0.05796
16	0.1	0	16	75	81	0.084065	0.05796
17	0.1	0	17	59	70	0.0537285	0.037044
18	77	37	18	52	56	0.11696	0.08064

19	30	14	19	1	273	0.0142545	0.009828
20	13	6	20	81	76	0.0529975	0.03654
21	1	0	21	68	85	0.02924	0.02016
22	194	94	22	56	27	0.09503	0.06552
23	77	37	23	1	274	0.115498	0.079632
24	77	37	24	74	75	0.105995	0.07308
25	77	37	25	68	93	0.084065	0.05796
26	122	59	26	27	31	0.10234	0.07056
27	104	51	27	274	275	0.0836995	0.057708
28	0.1	0	28	72	73	0.098685	0.06804
29	77	37	29	60	58	0.010965	0.00756
30	243	118	30	31	40	0.105995	0.07308
31	77	37	31	275	209	0.139621	0.096264
32	77	37	32	73	80	0.0731	0.0504
33	0.1	0	33	65	71	0.0712725	0.04914
34	121	58	34	40	47	0.091375	0.063
35	194	94	35	275	276	0.1158635	0.079884
36	122	59	36	73	77	0.076755	0.05292
37	77	37	37	69	65	0.0310675	0.02142
38	0.1	0	38	51	54	0.054825	0.0378
39	0.1	0	39	276	264	0.1151325	0.07938
40	96	47	40	77	78	0.05117	0.03528
41	122	59	41	59	69	0.021199	0.014616
42	70	34	42	54	24	0.0731	0.0504
43	58	28	43	263	264	0.068714	0.047376
44	0.1	0	44	79	83	0.24123	0.16632
45	122	59	45	63	61	0.10965	0.0756
46	122	59	46	24	29	0.09503	0.06552
47	122	59	47	262	263	0.0630936	0.0532656
48	86	42	48	82	80	0.0731	0.0504
49	77	37	49	71	63	0.022661	0.015624
50	0.1	0	50	29	34	0.1151325	0.07938
51	122	59	51	261	262	0.037973	0.032058

52	122	59	52	78	79	0.02193	0.01512
53	122	59	53	61	60	0.04386	0.03024
54	0.1	0	54	34	47	0.1736125	0.1197
55	42	20	55	259	261	0.0511175	0.043155
56	122	59	56	83	90	0.1209805	0.083412
57	13	6	57	58	62	0.129387	0.089208
58	77	37	58	47	21	0.084065	0.05796
59	50	24	59	257	259	0.068714	0.047376
60	0.1	0	60	77	59	0.38743	0.26712
61	60	29	61	64	67	0.0449565	0.030996
62	71	34	62	20	44	0.01462	0.01008
63	122	59	63	372	239	0.0265811	0.0224406
64	77	37	64	123	1	0.013524	0.015953
65	95	46	65	67	68	0.086258	0.059472
66	121	58	66	44	25	0.127925	0.0882
67	77	37	67	264	265	0.072369	0.049896
68	103	50	68	120	94	0.2538284	0.2584552
69	52	25	69	62	64	0.0603075	0.04158
70	57	27	70	25	35	0.127925	0.0882
71	171	83	71	369	347	0.13158	0.09072
72	121	58	72	120	123	0.294875	0.30025
73	39	19	73	58	20	0.59211	0.40824
74	119	58	74	35	38	0.08041	0.05544
75	49	24	75	369	370	0.208335	0.14364
76	0.1	0	76	114	115	0.047515	0.03276
77	50	24	77	1	92	0.388892	0.268128
78	44	21	78	38	41	0.1041675	0.07182
79	82	40	79	370	348	0.1187875	0.0819
80	132	64	80	115	112	0.040205	0.02772
81	194	94	81	92	2	0.3410115	0.235116
82	0.1	0	82	41	43	0.11696	0.08064
83	122	59	83	383	251	0.010965	0.00756
84	3	1	84	94	113	0.032895	0.02268

85	52	25	85	92	87	0.0128524	0.0108504
86	103	50	86	43	48	0.08041	0.05544
87	21	10	87	383	370	0.018275	0.0126
88	21	10	88	113	114	0.076755	0.05292
89	21	10	89	2	17	0.08772	0.06048
90	5	3	90	48	50	0.0731	0.0504
91	0.1	0	91	208	277	0.067252	0.046368
92	0.1	0	92	106	95	0.084065	0.05796
93	21	10	93	6	7	0.040205	0.02772
94	18	9	94	20	33	0.06579	0.04536
95	122	59	95	277	278	0.032895	0.02268
96	116	56	96	95	112	0.032895	0.02268
97	7	3	97	7	3	0.051901	0.035784
98	64	31	98	84	33	0.0420325	0.02898
99	49	24	99	277	279	0.048246	0.033264
100	16	8	100	94	111	0.06579	0.04536
101	77	37	101	18	5	0.1224425	0.08442
102	119	58	102	28	36	0.091375	0.063
103	71	34	103	279	280	0.034357	0.023688
104	77	37	104	111	106	0.06579	0.04536
105	194	94	105	5	6	0.0493425	0.03402
106	122	59	106	36	45	0.13158	0.09072
107	55	27	107	280	281	0.062135	0.04284
108	38	18	108	119	121	0.0102235	0.008631
109	22	10	109	17	18	0.11696	0.08064
110	0.1	0	110	49	45	0.04386	0.03024
111	77	37	111	281	235	0.0493425	0.03402
112	122	59	112	94	119	0.056028	0.066091
113	38	18	113	2	14	0.0164475	0.01134
114	122	59	114	55	23	0.076755	0.05292
115	27	13	115	281	282	0.0537285	0.037044
116	64	31	116	118	84	0.040205	0.02772
117	0.1	0	117	8	9	0.09503	0.06552

118	0.1	0	118	23	28	0.069445	0.04788
119	0.1	0	119	235	234	0.083334	0.057456
120	0.1	0	120	119	122	0.05117	0.03528
121	79	38	121	9	3	0.01462	0.01008
122	247	119	122	33	55	0.04386	0.03024
123	0.1	0	123	235	236	0.0420325	0.02898
124	0.1	0	124	122	118	0.201025	0.1386
125	0.1	0	125	16	19	0.157165	0.10836
126	0.1	0	126	21	50	0.03655	0.0252
127	0.1	0	127	208	236	0.076755	0.05292
128	0.1	0	128	104	105	0.049657	0.041922
129	77	37	129	19	8	0.02193	0.01512
130	122	59	130	32	44	0.25585	0.1764
131	62	30	131	232	349	0.075946	0.064116
132	105	51	132	84	104	0.0731	0.0504
133	122	59	133	14	16	0.098685	0.06804
134	77	37	134	37	32	0.105995	0.07308
135	77	37	135	349	207	0.032131	0.027126
136	0.1	0	136	105	108	0.06579	0.04536
137	85	41	137	2	13	0.032131	0.027126
138	8	4	138	42	37	0.0676175	0.04662
139	122	59	139	380	229	0.0411861	0.0347706
140	35	17	140	109	108	0.049657	0.041922
141	55	27	141	4	12	0.067183	0.056718
142	153	74	142	46	42	0.025585	0.01764
143	316	153	143	229	228	0.0630936	0.0532656
144	105	51	144	84	109	0.047515	0.03276
145	20	10	145	12	15	0.105156	0.088776
146	95	46	146	46	50	0.03655	0.0252
147	38	18	147	232	231	0.0968575	0.06678
148	83	40	148	110	84	0.04386	0.03024
149	50	24	149	15	11	0.1329055	0.112203
150	77	37	150	21	49	0.135235	0.09324

151	122	59	151	232	293	0.0749275	0.05166
152	102	49	152	103	110	0.076755	0.05292
153	60	29	153	13	4	0.0452755	0.038223
154	77	37	154	39	30	0.11696	0.08064
155	194	94	155	293	236	0.069445	0.04788
156	56	27	156	107	103	0.054825	0.0378
157	122	59	157	11	86	0.035052	0.029592
158	0.1	0	158	49	39	0.08772	0.06048
159	3	1	159	221	344	0.02924	0.02016
160	1	0	160	84	107	0.06579	0.04536
161	52	25	161	86	91	0.09503	0.06552
162	194	94	162	53	22	0.040205	0.02772
163	10	5	163	304	306	0.069445	0.04788
164	128	62	164	97	116	0.04386	0.03024
165	16	8	165	10	11	0.046736	0.039456
166	37	18	166	30	26	0.054825	0.0378
167	154	75	167	378	377	0.1114775	0.07686
168	0.1	0	168	84	99	0.13158	0.09072
169	0.1	0	169	3	10	0.1078225	0.07434
170	78	38	170	26	53	0.1005125	0.0693
171	0.1	0	171	304	378	0.0588455	0.040572
172	27	13	172	101	96	0.105995	0.07308
173	103	50	173	10	88	0.1095375	0.092475
174	122	59	174	22	33	0.04386	0.03024
175	72	35	175	309	307	0.098685	0.06804
176	0.1	0	176	100	101	0.05848	0.04032
177	122	59	177	88	89	0.08041	0.05544
178	194	94	178	21	57	0.215645	0.14868
179	0.1	0	179	314	317	0.0815065	0.056196
180	77	37	180	102	100	0.054825	0.0378
181	82	40	181	99	102	0.05117	0.03528
182	53	26	182	187	167	0.084709	0.071514
183	122	59	183	314	318	0.072369	0.049896

184	64	31	184	138	194	0.0127925	0.00882
185	86	42	185	96	117	0.0785825	0.05418
186	82	40	186	167	175	0.090551	0.076446
187	0.1	0	187	301	305	0.04386	0.03024
188	167	81	188	155	151	0.069445	0.04788
189	0.1	0	189	117	97	0.040205	0.02772
190	0.1	0	190	175	181	0.084709	0.071514
191	131	64	191	310	315	0.061404	0.042336
192	21	10	192	126	124	0.02924	0.02016
193	21	10	193	98	94	0.040205	0.02772
194	21	10	194	160	180	0.04386	0.03024
195	21	10	195	310	305	0.082603	0.056952
196	0.1	0	196	1	351	0.22661	0.15624
197	0.1	0	197	116	98	0.062135	0.04284
198	0.1	0	198	180	177	0.054825	0.0378
199	0.1	0	199	129	346	0.261698	0.180432
200	0.1	0	200	1	350	0.22661	0.15624
201	52	25	201	57	147	0.157165	0.10836
202	202	98	202	169	162	0.076755	0.05292
203	202	98	203	90	370	0.157896	0.108864
204	73	35	204	350	203	0.023392	0.016128
205	81	39	205	153	141	0.073025	0.06165
206	115	56	206	162	183	0.084065	0.05796
207	118	57	207	382	383	0.1502205	0.103572
208	318	154	208	351	379	0.023392	0.016128
209	161	78	209	147	142	0.105995	0.07308
210	126	61	210	183	182	0.032895	0.02268
211	59	29	211	66	252	0.192984	0.133056
212	24	12	212	203	204	0.0511175	0.043155
213	24	12	213	142	136	0.08041	0.05544
214	5	2	214	160	181	0.091375	0.063
215	126	61	215	384	243	0.227341	0.156744
216	56	27	216	204	205	0.062135	0.04284

217	62	30	217	132	153	0.08772	0.06048
218	0.1	0	218	181	178	0.05848	0.04032
219	32	15	219	85	244	0.1399865	0.096516
220	158	77	220	203	206	0.1034034	0.0872964
221	126	61	221	136	132	0.149855	0.10332
222	202	98	222	171	163	0.064262	0.054252
223	41	20	223	352	414	0.0705415	0.048636
224	81	39	224	379	380	0.1034034	0.0872964
225	126	61	225	57	149	0.069445	0.04788
226	202	98	226	163	184	0.075946	0.064116
227	18	9	227	414	385	0.0720035	0.049644
228	202	98	228	206	207	0.0598805	0.050553
229	106	51	229	57	125	0.091375	0.063
230	175	85	230	160	129	0.227838	0.192348
231	174	84	231	414	401	0.0727345	0.050148
232	113	55	232	1	375	0.010965	0.00756
233	202	98	233	127	124	0.02924	0.02016
234	0.1	0	234	129	141	0.032131	0.027126
235	202	98	235	401	386	0.059211	0.040824
236	403	195	236	208	209	0.0383775	0.02646
237	202	98	237	128	127	0.27047	0.18648
238	126	61	238	131	157	0.03655	0.0252
239	0.1	0	239	401	402	0.070907	0.048888
240	29	14	240	209	210	0.11696	0.08064
241	9	4	241	125	128	0.02193	0.01512
242	5	2	242	130	131	0.054825	0.0378
243	0.1	0	243	402	387	0.0566525	0.03906
244	18	9	244	209	211	0.0559215	0.038556
245	45	22	245	200	119	0.076755	0.05292
246	32	16	246	141	130	0.046736	0.039456
247	61	30	247	402	403	0.0595765	0.041076
248	81	39	248	211	1	0.056287	0.038808
249	126	61	249	200	201	0.00731	0.00504

250	23	11	250	157	133	0.113305	0.07812
251	14	7	251	403	388	0.083334	0.057456
252	18	9	252	375	202	0.149855	0.10332
253	126	61	253	158	200	0.02193	0.01512
254	5	3	254	133	140	0.105995	0.07308
255	26	13	255	403	404	0.0683485	0.047124
256	18	9	256	202	1	0.48246	0.33264
257	126	61	257	124	158	0.10234	0.07056
258	81	39	258	140	147	0.15351	0.10584
259	0.1	0	259	368	345	0.1151325	0.07938
260	126	61	260	373	352	0.1041675	0.07182
261	41	20	261	199	192	0.01462	0.01008
262	0.1	0	262	129	154	0.035052	0.029592
263	28	14	263	345	346	0.05848	0.04032
264	30	14	264	352	212	0.1136705	0.078372
265	81	39	265	199	197	0.069445	0.04788
266	202	98	266	137	144	0.09503	0.06552
267	318	154	267	345	369	0.0529975	0.03654
268	176	85	268	352	353	0.2138175	0.14742
269	126	61	269	159	199	0.27047	0.18648
270	6	3	270	144	148	0.09503	0.06552
271	31	15	271	400	404	0.047515	0.03276
272	60	29	272	353	213	0.201025	0.1386
273	56	27	273	197	191	0.010965	0.00756
274	126	61	274	154	156	0.032131	0.027126
275	118	57	275	404	405	0.040205	0.02772
276	126	61	276	353	214	0.0500735	0.034524
277	202	98	277	159	190	0.2359	0.2402
278	10	5	278	156	137	0.084065	0.05796
279	126	61	279	405	389	0.0588455	0.040572
280	202	98	280	1	215	0.3475905	0.239652
281	318	154	281	159	161	0.084065	0.05796
282	82	40	282	143	150	0.098685	0.06804

283	126	61	283	405	406	0.071638	0.049392
284	22	10	284	215	216	0.105995	0.07308
285	13	6	285	161	172	0.08772	0.06048
286	71	34	286	150	148	0.02193	0.01512
287	101	49	287	406	390	0.045322	0.031248
288	113	54	288	216	217	0.099314	0.083844
289	126	61	289	172	188	0.091375	0.063
290	0.1	0	290	134	139	0.119761	0.101106
291	34	17	291	406	391	0.0731	0.0504
292	83	40	292	216	218	0.06579	0.04536
293	59	29	293	188	168	0.091375	0.063
294	126	61	294	139	143	0.062135	0.04284
295	145	70	295	404	407	0.083334	0.057456
296	202	98	296	218	219	0.002924	0.002016
297	50	24	297	176	179	0.06579	0.04536
298	41	20	298	154	134	0.078867	0.066582
299	202	98	299	407	392	0.0785825	0.05418
300	77	37	300	219	220	0.08041	0.05544
301	161	78	301	168	176	0.113305	0.07812
302	477	231	302	148	57	0.1462	0.1008
303	68	33	303	407	408	0.048977	0.033768
304	14	7	304	220	223	0.0709803	0.0599238
305	4	2	305	161	185	0.13158	0.09072
306	0.1	0	306	129	151	0.032895	0.02268
307	66	32	307	408	409	0.0668865	0.046116
308	0.1	0	308	223	237	0.081788	0.069048
309	60	29	309	185	164	0.091375	0.063
310	95	46	310	145	146	0.032895	0.02268
311	0.1	0	311	409	393	0.073831	0.050904
312	19	9	312	237	238	0.0622173	0.0525258
313	67	32	313	164	165	0.032895	0.02268
314	18	9	314	146	149	0.054825	0.0378
315	33	16	315	409	394	0.0690795	0.047628

316	21	10	316	237	372	0.0537464	0.0453744
317	33	16	317	165	173	0.13889	0.09576
318	42	20	318	152	135	0.076755	0.05292
319	52	25	319	408	410	0.0551905	0.038052
320	43	21	320	239	240	0.005842	0.004932
321	126	61	321	173	179	0.113305	0.07812
322	107	52	322	135	145	0.142545	0.09828
323	202	98	323	410	415	0.06579	0.04536
324	126	61	324	239	243	0.0835406	0.0705276
325	24	12	325	179	160	0.069445	0.04788
326	101	49	326	135	195	0.0091375	0.0063
327	81	39	327	410	411	0.064328	0.044352
328	155	75	328	243	355	0.0054825	0.00378
329	23	11	329	159	182	0.054096	0.063812
330	31	15	330	151	152	0.054825	0.0378
331	126	61	331	411	395	0.0595765	0.041076
332	13	6	332	355	354	0.127925	0.0882
333	56	27	333	182	186	0.0483	0.056975
334	120	58	334	1	190	0.14154	0.14412
335	126	61	335	411	412	0.0676175	0.04662
336	403	195	336	354	242	0.018275	0.0126
337	81	39	337	186	166	0.037744	0.038432
338	177	86	338	190	189	0.0731	0.0504
339	151	73	339	412	399	0.0566525	0.03906
340	9	4	340	354	241	0.0731	0.0504
341	29	14	341	166	170	0.037744	0.038432
342	14	7	342	189	198	0.10965	0.0756
343	23	11	343	412	398	0.071638	0.049392
344	45	22	344	243	356	0.0091375	0.0063
345	0.1	0	345	170	174	0.02921	0.02466
346	36	17	346	198	196	0.03655	0.0252
347	5	2	347	412	413	0.0873545	0.060228
348	9	4	348	356	357	0.05117	0.03528

349	80	39	349	174	180	0.063693	0.064854
350	0.1	0	350	189	193	0.023392	0.016128
351	0.1	0	351	413	397	0.0705415	0.048636
352	0.1	0	352	357	244	0.0127925	0.00882
353	0.1	0	353	159	184	0.22661	0.15624
354	0.1	0	354	149	138	0.127925	0.0882
355	0.1	0	355	413	396	0.069445	0.04788
356	0.1	0	356	357	245	0.0054825	0.00378
357	0.1	0	357	184	187	0.035052	0.029592
358	0.1	0	358	138	155	0.105995	0.07308
359	0.1	0	359	290	289	0.062866	0.043344
360	0.1	0	360	243	246	0.0365125	0.030825
361	0.1	0	361	246	247	0.052632	0.036288
362	0.1	0	362	265	266	0.1078225	0.07434
363	0.1	0	363	289	288	0.046784	0.032256
364	0.1	0	364	306	310	0.126463	0.087192
365	0.1	0	365	247	248	0.0727345	0.050148
366	0.1	0	366	266	267	0.099416	0.068544
367	0.1	0	367	288	300	0.1867705	0.128772
368	0.1	0	368	310	320	0.0127925	0.00882
369	0.1	0	369	243	249	0.0487807	0.0411822
370	0.1	0	370	267	268	0.156434	0.107856
371	0.1	0	371	300	286	0.10965	0.0756
372	0.1	0	372	310	314	0.072369	0.049896
373	0.1	0	373	249	358	0.043129	0.029736
374	0.1	0	374	268	269	0.0549647	0.0559666
375	0.1	0	375	1	373	0.027778	0.019152
376	0.1	0	376	314	309	0.0698105	0.048132
377	86	41	377	358	359	0.0054825	0.00378
378	86	41	378	269	365	0.07077	0.07206
379	0.1	0	379	300	285	0.081141	0.055944
380	0.1	0	380	309	313	0.0785825	0.05418
381	0.1	0	381	359	250	0.0201025	0.01386

382	0.1	0	382	365	366	0.025585	0.01764
383	0.1	0	383	300	301	0.0932025	0.06426
384	0.1	0	384	313	317	0.0683485	0.047124
385	68	33	385	359	251	0.1407175	0.09702
386	15	7	386	366	270	0.1005125	0.0693
387	56	27	387	301	302	0.055556	0.038304
388	12	6	388	317	319	0.123539	0.085176
389	50	24	389	251	252	0.1882325	0.12978
390	115	56	390	366	271	0.0164475	0.01134
391	14	7	391	302	303	0.045322	0.031248
392	5	2	392	319	318	0.066521	0.045864
393	19	9	393	251	360	0.098685	0.06804
394	34	17	394	365	363	0.0483595	0.049241
395	10	5	395	303	304	0.195177	0.134568
396	40	19	396	318	315	0.069445	0.04788
397	28	14	397	360	253	0.049708	0.034272
398	14	7	398	363	362	0.018872	0.019216
399	17	8	399	304	305	0.208335	0.14364
400	41	20	400	315	311	0.083334	0.057456
401	0.1	0	401	253	254	0.0458597	0.0387162
402	0.1	0	402	363	381	0.26316	0.18144
403	0.1	0	403	305	308	0.050439	0.034776
404	0.1	0	404	311	304	0.105264	0.072576
405	0.1	0	405	254	361	0.0588455	0.040572
406	0.1	0	406	362	272	0.0164475	0.01134
407	0.1	0	407	308	316	0.2218585	0.152964
408	0.1	0	408	296	260	0.0478805	0.033012
409	0.1	0	409	361	256	0.040205	0.02772
410	0.1	0	410	362	1	0.02415	0.0284875
411	0.1	0	411	316	312	0.105264	0.072576
412	0.1	0	412	260	287	0.035819	0.024696
413	0.1	0	413	254	255	0.0274125	0.0189
414	0.1	0	414	1	364	0.28509	0.19656

415	19	9	415	312	307	0.072369	0.049896
416	0	0	416	260	324	0.1078225	0.07434
417	0	0	417	254	257	0.078867	0.066582
418	0	0	418	364	284	0.1041675	0.07182
419	0	0	419	307	300	0.078217	0.053928
420	0	0	420	324	326	0.0054825	0.00378
421	0	0	421	257	258	0.105995	0.07308
422	0	0	422	364	285	0.05848	0.04032
423	0	0	423	334	336	0.0712725	0.04914
424	0	0	424	324	266	0.103802	0.071568
425	0	0	425	257	283	0.0537464	0.0453744
426	0	0	426	381	268	0.3095785	0.213444
427	0	0	427	336	323	0.054825	0.0378
428	0	0	428	324	325	0.048246	0.033264
429	0	0	429	283	282	0.0663067	0.0559782
430	0	0	430	268	327	0.0383775	0.02646
431	0	0	431	336	337	0.0646935	0.044604
432	0	0	432	324	323	0.08772	0.06048
433	0	0	433	282	234	0.055499	0.046854
434	0	0	434	327	328	0.054825	0.0378
435	0	0	435	337	338	0.02924	0.02016
436	0	0	436	323	322	0.0676175	0.04662
437	0	0	437	234	233	0.0277495	0.023427
438	0	0	438	268	297	0.050439	0.034776
439	0	0	439	338	339	0.0420325	0.02898
440	0	0	440	322	321	0.09503	0.06552
441	0	0	441	233	376	0.011684	0.009864
442	0	0	442	297	296	0.050439	0.034776
443	0	0	443	339	265	0.067983	0.046872
444	0	0	444	321	299	0.070176	0.048384
445	0	0	445	230	231	0.0455676	0.0384696
446	0	0	446	296	295	0.0741965	0.051156
447	0	0	447	265	367	0.008772	0.006048

448	0	0	448	299	296	0.038012	0.026208
449	0	0	449	230	228	0.026289	0.022194
450	0	0	450	296	298	0.0376465	0.025956
451	0	0	451	367	340	0.0010965	0.000756
452	0	0	452	322	329	0.031433	0.021672
453	0	0	453	228	371	0.046736	0.039456
454	0	0	454	295	294	0.022661	0.015624
455	0	0	455	340	341	0.0274125	0.0189
456	0	0	456	329	330	0.0266815	0.018396
457	0	0	457	371	374	0.0394335	0.033291
458	0	0	458	294	292	0.0917405	0.063252
459	0	0	459	341	342	0.113305	0.07812
460	0	0	460	330	331	0.041667	0.028728
461	0	0	461	374	227	0.003655	0.00252
462	0	0	462	268	292	0.098685	0.06804
463	0	0	463	334	335	0.0559215	0.038556
464	0	0	464	331	332	0.0274125	0.0189
465	0	0	465	374	226	0.0023368	0.0019728
466	0	0	466	292	290	0.016813	0.011592
467	0	0	467	341	368	0.179095	0.12348
468	0	0	468	329	333	0.05848	0.04032
469	0	0	469	226	225	0.0274125	0.0189
470	0	0	470	290	291	0.0054825	0.00378
471	0	0	471	376	230	0.0277495	0.023427
472	0	0	472	333	334	0.041667	0.028728
473	**27372.4**	**13237**	473	368	343	0.0091375	0.0063

Source: Bernal-Agustin (1998).